MOLECULAR EVOLUTION IN ASTROPHYSICAL ENVIRONMENTS

by

William Bruce Latter

A Dissertation Submitted to the Faculty of the

DEPARTMENT OF ASTRONOMY

In Partial Fulfillment of the Requirements

For the Degree of

DOCTOR OF PHILOSOPHY

In the Graduate College

THE UNIVERSITY OF ARIZONA

1 9 8 9

Order Number 9010483

Molecular evolution in astrophysical envir ıments

Latter, William Bruce, Ph.D.

The University of Arizona, 1989

U·M·I
300 N. Zeeb Rd.
Ann Arbor, MI 48106

MOLECULAR EVOLUTION IN ASTROPHYSICAL ENVIRONMENTS

by

William Bruce Latter

A Dissertation Submitted to the Faculty of the

DEPARTMENT OF ASTRONOMY

In Partial Fulfillment of the Requirements

For the Degree of

DOCTOR OF PHILOSOPHY

In the Graduate College

THE UNIVERSITY OF ARIZONA

1 9 8 9

THE UNIVERSITY OF ARIZONA
GRADUATE COLLEGE

As members of the Final Examination Committee, we certify that we have read the dissertation prepared by William B. Latter

entitled MOLECULAR EVOLUTION IN ASTROPHYSICAL ENVIRONMENTS

and recommend that it be accepted as fulfilling the dissertation requirement for the Degree of Doctor of Philosophy.

John H. Black	1989 September 22 Date
Gary D. Schmidt	9/22/89 Date
Ramesh Narayan	9/22/89 Date
George H. Rieke	9/22/89 Date
Craig J. Hogan	9/22/89 Date

Final approval and acceptance of this dissertation is contingent upon the candidate's submission of the final copy of the dissertation to the Graduate College.

I hereby certify that I have read this dissertation prepared under my direction and recommend that it be accepted as fulfilling the dissertation requirement.

Dissertation Director	1989 September 26 Date

STATEMENT BY AUTHOR

This dissertation has been submitted in partial fulfillment of requirements for an advanced degree at The University of Arizona and is deposited in the University Library to be made available to borrowers under rules of the Library.

Brief quotations from this dissertation are allowable without special permission, provided that accurate acknowledgment of source is made. Requests for permission for extended quotation from or reproduction of this manuscript in whole or in part may be granted by the head of the major department or the Dean of the Graduate College when in his or her judgment the proposed use of the material is in the interests of scholarship. In all other instances, however, permission must be obtained from the author.

SIGNED: 

ACKNOWLEDGEMENTS

As I sat down to write these acknowledgements, I looked back over the now more than eleven years which have led up to the completion of this dissertation. Much of that time is lost in the haze of a semi-controlled insanity. It is clear, however, that there is one person to whom the hand of gratitude should be extended, or, perhaps more appropriately, the finger of blame pointed. I thank Heywood Sobel for turning my rambling interests into a passion for astrophysics. It has been worth it, I think.

Most importantly, I would like to thank my dissertation advisor, mentor, and friend, John Black. He has always been a crucial source of ideas, criticisms, and support when I needed it most. For some reason he thought it worthwhile to teach me some molecular astrophysics. I hope he has not suffered greatly from the attempt. Hang loose, dude.

For helping to keep me in one piece during my life as a graduate student, I thank EdO and Dr. B., Roc and Elaine, "Drs." Kem Cook, Mike and Doris, Gary and Pam Schmidt, Mike Margulis, Phil "Mega-dude" Maloney, Dennis and Jane, Mark, Richard, Hans-Walter, Pig, James, Joe and Penny, John Hill, Rexbo, Doug, Karen, Chris and Connie, Davy "What a Hick", Todd "Mr. Mile", Diana, Grace, Joe and Karen, and especially those who started with me at Steward: Steve Pompea, Buell Jannuzi, and Erica Ellingson.

I thank my collaborators and teachers who have enlightened me to things important and otherwise. They include Gary Schmidt, Harley "Let's have elevator races" Thronson, Marcia and George Rieke, Ray White, Mike Jura, Mirek Plavec, Jim Liebert, John McGraw, Charlie Lada, Craig Hogan, Simon White, Rob Kennicutt, Ramesh Narayan, Craig Foltz, and Chris Impey.

A very special mention and thank you must go to a person who has been many things to me, a fishing buddy, a friend, and a confidant. Best of all, he is my big brother. It is to him, and his family, that this work is dedicated. The ordeal which he must endure makes the production of this dissertation seem trival. When you're feeling better, Rick, we'll talk about what's in this thing.

For rest of my family, Rob, Dad, and especially my mother, there are not thanks enough. They never once doubted me, or hestitated to offer assistance when needed. Most of all, I thank them for their encouragement. Thanks to *all* of the Engler Family, especially Mary and Jerry, and Arnold and Mary.

Over the last few years, it has become brutally clear to my wife that I am growing older, but not up. The fact is, she wouldn't have it any other way. For the adventures we have shared and the motivation she gives me, I thank Diane most of all. We have been lost in the night, raced over the desert, trod a distant avenue of champions, and, even though there are lots of mangos in Paris, there is *still* so much to be done.

TABLE OF CONTENTS

TABLE OF CONTENTS – *Continued*

TABLE OF CONTENTS – *Continued*

LIST OF ILLUSTRATIONS

LIST OF TABLES

ABSTRACT

Molecular formation and destruction processes are explored in rapidly evolving, non-equilibrium astrophysical environments. First, a semi-classical calculation is made for the rate coefficients of excited atom radiative association to form molecular hydrogen and of the process $C^+ + O \rightarrow CO^+ + h\nu$. The latter process may be important to the formation of CO in the core of Supernova 1987A. It is shown that the excited atom process may have been important to the formation of H_2 during the early part of the epoch of recombination in the early Universe.

The equations of ionization balance and molecular formation and destruction have been integrated through the epoch of recombination. Other processes are examined in detail. These include heating and cooling of the primordial plasma, damping of fluctuations prior to decoupling, and the possibility of a radiation-driven instability at the onset of recombination.

A calculation is presented of the time-dependent chemical evolution in the rapidly expanding outer envelope of SN 1987A. Various cooling rates and hydrogen abundances in the envelope have been examined. It is found that large molecular abundances, in particular CO, form rapidly, while hydrogen remains mostly in its atomic forms.

Near-infrared observations of the proto-planetary nebula CRL 618 are presented and discussed. Images acquired in the H and K bandpasses are

consistent with a bipolar axis highly inclined to the plane of the sky. From the spectrum, a visual extinction of $A_v = 5.3$ magnitudes to the molecular hydrogen emitting lobes is found. It is shown by comparision with spectral models that the near-infrared H_2 spectrum exhibits emission from thermally excited molecules at $T_{ex} \sim 2000$ K. A component of fluorescent emission may also be present.

The suggestion is explored that large molecules, in particular polycyclic aromatic hydrocarbons (PAHs), are formed in stellar winds. It is asserted that the primary source of interstellar PAHs is mass-losing asymptotic giant branch carbon stars. It is apparent that the known numbers of the most extreme mass-losing carbon stars are able to produce PAHs in sufficient quantities to maintain an interstellar medium well mixed in such molecules at the inferred abundance.

CHAPTER 1

INTRODUCTION

Orion, the mighty hunter of the night, holds in his scabbard not a sword, but a brightly shining wonder. He journeys across the sky carrying with him a glowing cloud of gas and dust illuminated by the light of newborn stars, known as the Orion Nebula. Astronomers have long pondered the nature of this vast, diffuse object. Recently, we have come to know many of the secrets held by the Orion Nebula. A key to this understanding has been the examination of electromagnetic radiation emitted by atoms and molecules. Like the manner in which the complex, yet cyclic composition of a Bach fugue reveals hidden mysteries, the harmonic predictability in the spectra of atoms and molecules reveals clues to the nature of the Universe.

The detailed study of atomic and molecular processes is central to our grasp of the diverse conditions found within interstellar and circumstellar space. Most of our current understanding of the structure of the Universe has come from observations of the various types of radiation emitted and absorbed by its microscopic constituents. Detailed analysis and theoretical modeling have resulted in knowledge of such varied properties as the interstellar radiation field, cosmic elemental abundances, masses of giant molecular clouds, the pro-

cess of star formation and star death, and indeed even the temperature of the microwave background at various epochs (*i.e.* Meyer *et al.* 1986). Theoretical analysis plays a key role in the study of material between and around the stars, since conditions known to exist there cannot be easily reproduced in terrestrial laboratories. The kinds of theoretical tools brought into play are as varied as the conditions to be studied. Often *ab initio* determinations of transition probabilities, energy levels, and other fundamental atomic and molecular properties are all that is available. Chemical modeling provides knowledge of molecular formation rates and dissociation processes, and leads ultimately to a deeper understanding of the environment.

Until the advent of precise radio wave astronomy in the mid 1960's, the study of molecules in the interstellar medium (ISM) was limited to absorption line analysis of diffuse regions. The presence of an interstellar medium was demonstrated by narrow Ca II (this notation refers to the spectrum of Ca^+) absorption lines which remained stationary with respect to the shifting photospheric lines of the spectroscopic binary δ Orionis (Hartmann 1904). The earliest detections of molecular absorption lines were of CH, CH^+, and CN in the spectra of background stars (Adams 1941, 1943; McKellar 1940; Douglas and Herzberg 1941). A major achievement of astronomy at millimeter and far-infrared wavelengths has been the identification of a rich variety of molecules, ranging from simple diatomics to long-chain thirteen-atom molecules (see Table I.1).

TABLE I.1

IDENTIFIED INTERSTELLAR AND CIRCUMSTELLAR MOLECULES

Two-Atom Molecules:	
H_2	molecular hydrogen
C_2	diatomic carbon
CH	methylidyne
CH^+	methylidyne ion
CN	cyanogen
CO	carbon monoxide
CS	carbon monosulfide
OH	hydroxyl
HCl	hydrogen chloride
NO	nitric oxide
NS	nitrogen sulfide
SiC	silicon carbide
SiO	silicon monoxide
SiS	silicon sulfide
SO	sulfur monoxide
MgO	magnesium monoxide†
PN	
NaCl	sodium chloride*
AlCl	aluminum chloride*
KCl	potassium chloride*
AlF	aluminum fluoride*†
Three-Atom Molecules:	
H_2D^+	
C_2H	ethynyl
HCN	hydrogen cyanide
HNC	hydrogen isocyanide
HCO	formyl
HCO^+	formyl ion
N_2H^+	protonated nitrogen
HNO	nitroxyl
H_2O	water
HCS^+	thioformyl ion
H_2S	hydrogen sulfide
OCS	carbonyl sulfide
SO_2	sulfur dioxide

TABLE I.1 – *Continued*

SiC_2	silicon dicarbide (silacyclopropyne)*
C_2S	
C_3	triatomic carbon*
Four-Atom Molecules:	
C_2H_2	acetylene
C_3H	propynylidyne
H_2CO	formaldehyde
NH_3	ammonia
HNCO	isocyanic acid
$HOCO^+$	protonated carbon dioxide
$HCNH^+$	protonated hydrogen cyanide
HNCS	isothiocyanic acid
C_3N	cyanoethynyl
C_3O	tricarbon monoxide
H_2CS	thioformaldehyde
H_3O^+	hydronium ion†
C_3S	
Five-Atom Molecules:	
C_4H	butadiynyl
C_3H_2	cyclopropenylidene
HCOOH	formic acid
CH_2CO	ketene
HC_3N	cyanoacetylene
CH_2CN	cyanomethyl
NH_2CN	cyanamide
CH_2NH	methanimine
CH_4	methane*
SiH_4	silane*
C_5	*
C_4Si	*
Six-Atom Molecules:	
C_5H	pentynylidyne
CH_3OH	methanol
CH_3CN	methyl cyanide
CH_3SH	methyl mercaptan
NH_2CHO	formamide

TABLE I.1 – *Continued*

Seven-Atom Molecules:		
	C_6H	
	CH_2CHCN	vinyl cyanide
	CH_3C_2H	methylacetylene
	CH_3CHO	acetaldehyde
	CH_3NH_2	methylamine
	HC_5N	cyanodiacetylene
Eight-Atom Molecules:		
	$HCOOCH_3$	methyl formate
	CH_3C_3N	methylcyanoacetylene
Nine-Atom Molecules:		
	CH_3C_4H	methyldiacetylene
	CH_3CH_3O	dimethyl ether
	CH_3CH_2CN	ethyl cyanide
	CH_3CH_2OH	ethanol
	HC_7N	cyanohexatriyne
Ten-Atom Molecules:		
	CH_3CH_3CO	acetone
Eleven-Atom Molecules:		
	HC_9N	cyano-octa-tetra-yne
Thirteen-Atom Molecules:		
	$HC_{11}N$	cyano-deca-penta-yne

*Detected in circumstellar envelopes only.

†Tentative.

Reported but doubtful, unconfirmed, or rejected: CO^+, CS^+, HOC^+, NaOH, NH_2CH_2COOH, CH_2CH_2O.

This table kindly supplied by J. H. Black, 1989 July 22.

Molecules are found in many regions of interest: diffuse interstellar clouds, the cores of star formation regions, stellar atmospheres and circumstellar envelopes, even in the shocked material of supernova shells and ionization fronts. The temperatures and total densities of these regions range from 10 to a few $\times$ 10^4 K and $10^2 - 10^8$ cm^{-3}. This diversity is characteristic of the field of astrochemistry. The primary goal of astrochemistry is understanding the existence of molecules and their abundances in differing environments. Such will be a goal of this dissertation. First, we present a brief summary of the interstellar medium and simple molecular processes.

1.1 THE INTERSTELLAR MEDIUM

The presence of obscuring material in interstellar space has been known for over two hundred years. Herschel noticed "dark holes," or regions that were apparently devoid of stars (Herschel 1784). It was not until 1889 that Barnard correctly identified these regions as clouds of intervening matter (see Barnard 1919, 1927). Trumpler (1930) showed that this material was more pervasive and is the source of the reddening of starlight. With the advent of optical spectroscopy and millimeter-wave astronomy, it was found that these regions contained not only large particles, or dust grains, but also a great deal of atomic and molecular gas. Regions once thought to be empty were found to be abundant in interstellar matter. The prediction by van de Hulst (1945) of the observability of the 21 cm spin-flip hyperfine transition in atomic hydrogen came to fruition in 1951 with the detection by Ewen and Purcell (1951). Since that time atomic hydrogen has been observed throughout the cosmos and has become a valuable tool in the study of the structure of the Universe.

The contents of the interstellar medium within the Galaxy is usually separated into several categories. Regions composed primarily of atoms and atomic ions can be described as follows. H II regions surround hot, young stars and have total densities of $n \sim 10 - 10^4$ cm^{-3} and temperatures on the order of 10,000 K. The hot coronal gas occupies a substantial fraction of the total volume of the interstellar medium with $T \approx 10^6$ K and $n \approx 3 \times 10^{-3}$

cm^{-3}. A warm intercloud medium also exists and has $T \approx$ 10,000 K and $n \approx$ 0.1 cm^{-3} (McKee and Ostriker 1977; Kulkarni and Heiles 1987; Jura 1987a). Few molecules are found within these harsh environments.

The molecular component of the interstellar medium is often divided into such categories as diffuse clouds, giant molecular clouds (GMC's), dark clouds, and circumstellar envelopes. Interstellar clouds can be arbitrarily classified according to the role of photoprocesses within them: important (diffuse cloud), moderately significant (GMC), and totally shielded (dark cloud). Reviews of galactic molecular clouds may be found in Goldsmith (1987) and Myers (1987).

Diffuse clouds are thin, patchy regions with column densities of gas and dust sufficient to produce no more than 1 or 2 magnitudes of visual extinction. Frequently seen at high galactic latitudes, these structures are most often observed in absorption against background stars. The atomic species with ionization potentials $<$ 13.6 eV are largely ionized, the others being shielded from the ambient stellar UV radiation field by the large abundance of hydrogen. Diffuse clouds are found to have a temperatures of about 100 K and densities $n \approx$ 100 cm^{-3}. As much as 2/3 of the hydrogen can be in the form of H_2. Detailed models of diffuse clouds have recently been presented by van Dishoeck and Black (1986, 1989) and Viala (1986).

Giant molecular clouds are typified by moderate to high optical depths due to dust. These fairly dense regions are characterized by temperature $T \approx$ 40 K, density $n \lesssim 10^4$ cm^{-3}, total mass $M_{total} \lesssim 10^5$ $M_\odot$, and cloud radius

$r \approx 10$ pc. Generally associated into giant molecular cloud complexes, GMC's can also be found in fairly isolated regions (It should be noted that often no distinction is made between GMC's and GMC complexes). GMC complexes are the largest, most massive structures known within the Galaxy. These objects are found to have diameters of 40 – 100 pc and masses of $\sim 10^6\ M_\odot$. Temperatures, weighted by the distribution of observable consitutuents and averaged over the entire complex, are cold with $T \approx 10$ K.

Dark clouds are also found in complexes or in isolation. These are regions characterized by extremely large optical depths in the visible and UV. Hydrogen is almost entirely in the form of H_2. The only effective ionization and destruction process is cosmic ray impact with a typical rate of $R_{cr} \approx 5 \times 10^{-17} n(H_2)$ cm^{-3} s^{-1} (van Dishoeck and Black 1986). Densities are found to be $n \approx 10^4$ cm^{-3}, with masses of $M = 10 - 10^3\ M_\odot$, and $r \approx 4$ pc. Dark clouds are extremely rich in exotic molecules and are believed to be prime sites of star formation. Although localized cores in dark clouds are quiescent, with velocity dispersions comparable to thermal values at $T \approx 10$ K, high velocity gas can be found in the vicinities of recently formed stars (see, *e.g.*, Margulis 1987). Dark clouds may also be found associated with GMC's.

Many cool evolved stars endure an episode of vigorous mass loss through a strong stellar wind. This produces an extensive circumstellar envelope, sometimes rich in exotic molecules and sometimes able to support natural masers. The structure and molecular content of such a circumstellar envelope are governed both by the conditions and abundances of the stellar photosphere and

by the limiting effect of photodissociation by background ultraviolet starlight from the outside. Objects with $[C]/[O] \gtrsim 1$ are considered carbon-rich and display a chemistry dominated by carbon. Oxygen-rich stars ($[C]/[O] \lesssim 1$) possess a molecular content favoring oxygen species. The temperatures of circumstellar shells range from about 100 to $\gtrsim$ 1000 K with optical depths in the visual and infrared ranging from < 1 to $\gg 1$. These regions are ideal for the study of dust formation processes and chemistry at much higher temperatures than usually found in the ambient interstellar medium. Supernova remnants (SNR's) and planetary nebulae (PN) are rapidly evolving and transient objects associated with the death of a star. Throughout at least part of their life, the chemical processes in SNR's and PN are dominated by high temperature (shock) physics and photoprocesses. Molecules have even been observed in the core of the hot, young supernova SN 1987A (see Chapter 4).

A major focus of this dissertation is the study of chemistry in rapidly evolving systems. Among these are mass-losing stars, young planetary nebulae, novae, and supernovae, all of which are important contributors to the overall chemical evolution of the interstellar medium. In addition, supernovae influence the large scale kinematics of the Galaxy and may aid in triggering star formation (Jura 1987a, 1987b). The perpetual cycling of star formation and star death make the ISM a continuously evolving environment.

1.2 MOLECULE FORMATION AND DESTRUCTION

Among the most important molecular formation processes in the interstellar and circumstellar medium are radiative association, charge transfer, grain surface chemistry, and, in some environments, three-body reactions. Other important gas phase reactions may include neutral exchanges

$$A + BC \rightarrow AB + C, \tag{I.1}$$

associative detachment with a negative ion

$$A^- + B \rightarrow AB + e^-, \tag{I.2}$$

and ion-molecule reactions

$$A^+ + BC \rightarrow AB^+ + C. \tag{I.3}$$

The low temperatures found to exist in much of the general interstellar medium influence the chemistry to a large degree. Only exothermic processes, which release energy during a reaction, are important in the cold regions. Endothermic reactions require energy input in order to take place and are likely only within high-temperature environments such as shocks. In general, the rate coefficients for endothermic reactions have an exponential temperature dependence of the form $\exp(-E_{th}/kT)$, where E_{th} is the minimum energy required for the reaction to take place (the energy threshold at which the total cross section becomes non-zero) and k is the Boltzmann constant ($k = 1.380658 \times 10^{-16}$ erg K^{-1}).

a) *Ion-Molecule Reactions*

Ion-molecule reactions (reaction I.3) lead to formation of polyatomic molecules ranging from familiar substances such as water (H_2O) to the exotic radical butadiynyl (C_4H). Much of the chemistry of dark clouds is driven by cosmic ray ionization of H_2 followed by the reaction of H_2^+ with H_2, which produces H_3^+, a vital component in the formation of many other molecular species (Herbst 1987). A number of quantum mechanical techniques have been developed for finding rate coefficients and branching ratios. Rate coefficients are usually determined to be of the same order ($\sim 10^{-9}$ cm^3 s^{-1}) with little temperature dependence. A classical Langevin (or orbital) model reveals the essential physics of these processes. During a close encounter, the charged ion induces a dipole moment in the neutral even if it is a non-polar molecule. The interaction potential energy is then

$$V(r) = -\left(\frac{\alpha e^2}{2r^4}\right), \tag{I.4}$$

where α is the polarizability of the neutral (Rapp and Francis 1962). Thus, determination of the rate coefficient is simply an orbital problem with a r^{-5} interaction force. The critical impact parameter beyond which a reaction will not occur is found to be

$$b_{crit} = \left(\frac{4\alpha e^2}{\mu v^2}\right)^{\frac{1}{4}}, \tag{I.5}$$

where μ is the reduced mass ($\mu^{-1} = m_1^{-1} + m_2^{-1}$, where m_i is the mass of the interacting species) and v is the relative velocity of the reactants. In this

treatment, the Langevin rate coefficient is given by $k = \langle \sigma_{crit} v \rangle$ or

$$k = 2\pi e \left(\frac{\alpha}{\mu}\right)^{\frac{1}{2}} = 1.4 \times 10^{-9} \left(\frac{\alpha}{\text{Å}^3} \frac{2.71 \text{ amu}}{\mu}\right)^{\frac{1}{2}} \text{ cm}^3 \text{ s}^{-1}. \quad \text{(I.6)}$$

This simple analysis breaks down and underestimates the rate coefficient if the neutral is a polar molecule possessing a permanent dipole moment (see Herbst 1987). A rate for associative detachment (reaction I.2) can also be approximated within this model.

b) *Radiative Association*

The process of radiative association is represented by the expression

$$\text{A} + \text{B} \rightleftarrows \text{AB}^* \rightarrow \text{AB} + h\nu \quad \text{(I.7)}$$

where A and B can be atoms, molecules, or ions. The creation of a photon conserves energy and momentum in such a two-body gas phase reaction. We will look in some detail at this process in the next chapter.

c) *Charge Transfer*

Charge transfer reactions

$$\text{A} + \text{B}^+ \rightarrow \text{A}^+ + \text{B} \quad \text{(I.8)}$$

are most efficient when there is a near resonance in the ionization potentials of two colliding particles and the Franck-Condon principle is satisfied. The processes may have a large impact on the ionization balance of a system. Rates can often be estimated semi-classically in the Landau-Zenar formulation and

can approach the Langevin value (Butler and Dalgarno 1980). An especially important charge transfer reaction is

$$O + H^+ \rightarrow O^+ + H \tag{I.9}$$

which starts a series of chemical reactions requiring the presence of O^+ (see, *e.g.*, Black and Dalgarno 1977). Indeed, charge transfer processes may have dominated the chemistry in the core of SN 1987A (see Chapter 4 and references therein).

d) *Three-Body Reactions*

An alternative to molecule formation by the interaction of two particles is that of molecule formation by a three-body encounter of the type

$$A + B + M \rightarrow AB + M. \tag{I.10}$$

The third body, M, may be any available particle which can carry off the energy liberated in the molecular formation process. However, it should be clear by the slow collision rate ($\sim 10^{-11} n_{tot}$ cm^{-3} s^{-1}) in the general ISM, that interaction with a third body during a two body collision is highly unlikely. Thus, except in the dense environment of stellar atmospheres or the terminal stages of protostellar collapse, three-body processes are negligible in the general interstellar medium.

e) *Grain Surface Chemistry*

Molecule formation on the surfaces of grains has proven to be an important process anywhere there is dust (Hollenbach and Salpeter 1971, Martin 1978, Hunter and Watson 1978, Leonas and Pjarnpuu 1981, and Duley and Williams 1984). The process

$$A + B : g \rightarrow AB + g \tag{I.11}$$

occurs when an atom sticks to the surface of a grain and migrates until it encounters another atom or molecule with which it can form a bond, assisted by an attractive potential well on the solid surface. The grain then is able to absorb part of the energy released upon the formation of the molecule through lattice vibrations. Excess energy may go into liberating the molecule from the grain surface. The most abundant molecule found in interstellar clouds, molecular hydrogen (H_2), is believed to form primarily by this process (see Appendix A). It is important to note that rates of grain surface processes decrease rapidly with increasing grain temperature, becoming negligible when the grain temperature greatly exceeds typical evaporation temperatures, *e.g.*, $T_{grain} \gtrsim 40$ - 50 K (Hollenbach and Salpeter 1971).

f) *Molecular Destruction Processes*

The three primary ways of destroying an interstellar molecule, aside from synthetic processes which form another molecule, are by photodissociation

$$AB + h\nu \rightarrow A + B, \tag{I.12}$$

photoionization to a dissociating state

$$\begin{aligned} AB + h\nu &\rightarrow AB^+ + e^- \\ &\rightarrow A + B^+, \end{aligned} \tag{I.13}$$

and, for molecular ions, dissociative recombination

$$AB^+ + e^- \rightarrow A + B. \tag{I.14}$$

In regions where photoprocesses are weak, bombardment by cosmic rays can be an important source of ionization and dissociation, witness the cosmic ray destruction of molecular hydrogen

$$\begin{aligned} H_2 + \text{C.R.} &\rightarrow H^+ + H + e^- \\ &\rightarrow H_2^+ + e^- \\ &\rightarrow H + H \\ &\rightarrow H^+ + H^-. \end{aligned} \tag{I.15}$$

Photoionization of a molecule can result in a stable molecular ion, or, if no stable state exists, in dissociation into atomic or molecular components. A rate for photodissociation can be calculated from

$$\Gamma_{pd} = \int_{\nu_o}^{\infty} \int_{\Omega} \frac{\sigma_{pd}(\nu) I(\nu)}{h\nu} d\Omega d\nu \quad \text{s}^{-1} \tag{I.16}$$

where I is the intensity of the ambient radiation field in ergs cm^{-2} s^{-1} Hz^{-1} sr^{-1}, σ_{pd} is the cross section for photodissociation in cm^{-2}, ν_o is the frequency threshold for photodissociation, Ω is the solid angle subtended by the radiation source, and h is Planck's constant ($h = 6.6260755 \times 10^{-27}$ erg s). In practice, the threshold wavelength for photodissociation will be limited to greater than

912 Å by the huge abundance of interstellar hydrogen. Dissociating radiation is attenuated by extinction by dust and, at some wavelengths, by absorption by gaseous atoms and molecules. When extinction is important, the rate will vary with depth to first order as

$$\Gamma_{pd} = \Gamma_o \exp(-\beta A_V) \quad s^{-1}, \tag{I.17}$$

where Γ_o is the unattenuated dissociation rate, A_V is the visual extinction in magnitudes and $\beta \approx 1 - 5$ for many small molecules (see, *e.g.*, Black and Dalgarno 1977; van Dishoeck 1989a).

A number of recent reviews of chemical processes in astrophysics include Duley and Williams (1984), Herbst (1987), Black (1988), and van Dishoeck (1989a, 1989b). Chemical abundances have been discussed by Charfman (1980), Betz (1987), Federman (1987), and Irvine, Goldsmith, and Hjalmarson (1987).

1.3 IN SUMMARY

The interstellar medium is a complex chemical environment, one which will not reveal its secrets easily. Unlike terrestrial chemists, we cannot manipulate the system we are studying in order to gain a better understanding. We must combine often difficult observations with theory to bootstrap ourselves to greater knowledge. It is therefore important that we not only understand the conditions under which certain types of observable emission occur, but also understand in detail how and where molecules form. Such knowledge may be gained in part through the modeling of molecular formation and destruction processes in a variety of environments.

In this dissertation we will examine molecular processes in rapidly evolving, non-equilibrium systems. In the next chapter, we will discuss the process of radiative association in detail. A semi-classical calculation is used to determine the radiative rate coefficient for the formation of two common molecular species through unusual routes. In Chapter 3 the techniques of time-dependent chemical modeling will be applied in a detailed examination of the chemical evolution in the early Universe. Chapter 4 explores the molecular processes in the expanding envelope of Supernova 1987A. Then an examination of newly acquired near-infrared observations of the proto-planetary nebula CRL 618 will be made. Models of the thermal and fluorescent emission of molecular hydrogen arising in this source will be presented. Finally, the impact which evolved

carbon stars may have on the evolution of large molecules in the Galaxy will be discussed. Through this study, it is hoped that a greater understanding of certain detailed chemical processes will be gained. On a larger scale, some of what is learned may be applied to better our insight into the chemical evolution of the Universe and of the Galaxy in which we live.

CHAPTER 2

RADIATIVE ASSOCIATION

2.1 INTRODUCTION

At densities typical of the general interstellar medium, molecule formation by radiative association,

$$A + B \rightleftarrows AB^* \rightarrow AB + h\nu, \tag{II.1}$$

may compete with other processes in the gas phase. As a result, the determination of rate coefficients for radiative association is important to the accurate analysis of molecule formation and destruction processes in astrophysics. In conventional usage, the rate of a reaction per unit volume per unit time is given by $kn(A)n(B)$ cm^{-3} s^{-1}, where k is the rate coefficient in cm^3 s^{-1} and $n(A)$ and $n(B)$ are number densities of species A and B in cm^{-3}.

In a classical treatment, the colliding particles, which can be atoms, molecules, or ions, approach along a potential energy curve of the resultant molecule. This curve can be a repulsive (unbound) state or, as is required for rapid low temperature association, that of a bound state. Stabilization of the separated pair into a bound molecule will occur if the system radiates a

photon of energy $h\nu \geq E_{coll}$ (E_{coll} = total center of mass energy of the colliding pair), such that energy and angular momentum of the system are conserved. The resulting molecule will then be in a lower lying bound state, and the colliding particles can no longer separate to infinity. This process is, in general, inefficient since the collision time (of the order of a molecular vibrational period , 10^{-13} s) must be weighted against the inverse of the radiative lifetime (the transition probability) of the stabilizing transition. The radiative lifetime can range from $\approx$ 1 ns for allowed electronic transitions in the ultraviolet to $10^{-3} - 10^{-2}$ s for intrinsically weak vibrational transitions (van Dishoeck 1989a). The rate of radiative association will be enhanced if the emission of a stablizing photon is due to a strong electronic transition. The first accurate semi-classical calculations of radiative association rate coefficents were done by Bates (1951a). An example of such a calculation for the formation of H_2 and CO^+ will be presented in this chapter.

The usual selection rules for a transition resulting in radiative association must be followed. For electronic transitions these are as follows. Symmetry does not change

$$s \leftrightarrow s, \qquad a \leftrightarrow a, \qquad s \not\leftrightarrow a. \tag{II.2}$$

Positive terms combine only with negative and, for homonuclear molecules, even states combine only with odd

$$\begin{aligned} &+ \leftrightarrow -, \qquad + \not\leftrightarrow +, \qquad - \not\leftrightarrow -, \\ &g \leftrightarrow u, \qquad g \not\leftrightarrow g, \qquad u \not\leftrightarrow u. \end{aligned} \tag{II.3}$$

In addition, we have that

$$\Delta S = 0, \qquad \Delta\Lambda = 0, \ \pm 1, \tag{II.4}$$

and

$$\Sigma^+ \leftrightarrow \Sigma^+, \qquad \Sigma^- \leftrightarrow \Sigma^-, \tag{II.5}$$

but Σ^+ states *cannot* combine with Σ^- states. Additional selection rules for more general transitions may be found in the work of Herzberg (1950).

Due to the shapes of the interaction potentials, many radiative association coefficients are strongly temperature dependent. This is especially true if a potential barrier (activation energy) must be overcome. Frequently, it is found that

$$k_{ra} = \mathrm{A}T^{\frac{1}{2}} \exp(-q/kT). \tag{II.6}$$

A and q are constants. If laboratory experiments are possible (which is rarely the case for radiative association), they are typically required to be performed at temperatures where the exponential factor has little effect. However, in the ISM this factor can have a dramatic influence. As a result, theoretical calculations of rate coefficients at interstellar temperatures are important even in cases where empirical data may be available.

In this chapter, we discuss the semi-classical determination of a radiative rate coefficient for the excited atom process

$$\mathrm{H\,(n = 2) + H\,(n = 1) \rightarrow H_2} + h\nu, \tag{II.7}$$

where n is the principal quantum number of the separated hydrogen atoms. Ground state radiative association to form molecular hydrogen directly is ex-

tremely slow due to the lack of allowed stablizing transitions (see Appendix A). The standard gas phase routes

$$H + H^+ \rightarrow H_2^+ + h\nu \tag{II.8}$$

$$H_2^+ + H \rightarrow H_2 + H^+, \tag{II.9}$$

and

$$H + e^- \rightarrow H^- + h\nu \tag{II.10}$$

$$H^- + H \rightarrow H_2 + e^- \tag{II.11}$$

will dominate over reaction (II.7) for most interstellar environments (see Table III.1 in Appendix B). However, conditions may arise where the population of n=2 hydrogen is large enough for reaction (II.7) to be an important source of molecular hydrogen. We consider some possible applications of reaction (II.7) and discuss its influence in some specific cases.

In addition, we will examine the radiative association process

$$C^+ + O \rightarrow CO^+ + h\nu. \tag{II.12}$$

It has been pointed out by Lepp, Dalgarno, and McCray (1988) that reaction (II.12) may be an important source of CO^+ in Supernova 1987A (see Chapter 4). We calculate the rate coefficient of this process in order to assess its importance relative to other processes which may be taking place in the supernova.

2.2 METHOD OF CALCULATION

We use the semi-classical method of Bates (1951a). Such an approach is valid in the case of massive reactants or strong stabilizing transitions. It ignores the possible low temperature effects of tunneling and shape resonances. In the Bates approximation, the radiative rate coefficient is given by

$$k = 2\pi \iint bv\omega(v) P dv db \quad \text{cm}^3 \text{ s}^{-1}, \tag{II.13}$$

where b is the impact parameter, v is the relative velocity, and $\omega(v)$ is the particle velocity distribution function. The probability of a molecule being formed is given by

$$P = g \int A(r) dt. \tag{II.14}$$

$A(r)$ is the Einstein transition probability expressed as a function of internuclear separation and g is a statistical weight factor to be defined later. The integration in equation (II.14) is taken over the time within which a stabilizing transition can occur. The standard laws of motion give the center of mass energy to be $E_{coll} = \frac{1}{2}\mu\dot{r}^2 + \frac{1}{2}\frac{l^2}{\mu r^2} + U'(r)$, or

$$dt = dr \left[v^2 - \frac{b^2 v^2}{r^2} - \frac{2U'(r)}{\mu} \right]^{-\frac{1}{2}} \quad \text{s}, \tag{II.15}$$

where μ is the reduced mass of the reactants ($\mu^{-1} = m_1^{-1} + m_2^{-1}$) and $U'(r)$ is the upper state molecular potential. For a Maxwellian distribution of particle

velocities, the rate coefficient (II.13) now becomes

$$k = g\sqrt{\pi}\left(\frac{2\mu}{kT}\right)^{\frac{3}{2}}\iiint A(r)v^2 b\exp\left(-\frac{\mu v^2}{2kT}\right)\times \left[1-\frac{b^2}{r^2}-\frac{2U'(r)}{\mu v^2}\right]^{-\frac{1}{2}} dvdbdr \quad \text{cm}^3\ \text{s}^{-1}. \tag{II.16}$$

If integration over the impact parameter is carried out first, then

$$k = g\sqrt{\pi}\left(\frac{2\mu}{kT}\right)^{\frac{3}{2}}\iint A(r)\, r^2 v^2 \exp\left(-\frac{\mu v^2}{2kT}\right)\times \left[\left(1-\frac{2U'(r)}{\mu v^2}\right)^{\frac{1}{2}}-\left(1-\frac{2U'(r)}{\mu v^2}-\frac{b_m^2}{r^2}\right)^{\frac{1}{2}}\right] dvdr \ \text{cm}^3\ \text{s}^{-1}, \tag{II.17}$$

where b_m is the greatest value of the impact parameter for a specific internuclear separation r and relative velocity v. The factor g is the ratio of the statistical weight of the initial molecular state to the statistical weights of all possible molecular states that dissociate to the same separated-atom states

$$g = \frac{g'(\Lambda', S')}{\sum\limits_{states} g_i(\Lambda_i, S_i)}, \qquad g_i(\Lambda_i, S_i) = (2S_i+1)(2-\delta_{0,\Lambda_i}). \tag{II.18}$$

Substituting the dimensionless variable $\epsilon = \mu v^2/2kT$, we find

$$k = 8\sqrt{\pi}g\iint A(r)r^2 e^{-\epsilon}\left[\xi^{\frac{1}{2}}-\left(\xi-\epsilon\frac{b_m^2}{r^2}\right)^{\frac{1}{2}}\right] d\epsilon dr, \tag{II.19}$$

where

$$\xi = \epsilon - \frac{U'(r)}{kT}. \tag{II.20}$$

The transition probability is given by its usual form (see Larsson 1983)

$$A(r) = \frac{64\pi^4\Theta}{3h^4c^3}|R(r)|^2\left[U'(r)-U''(r)\right]^3 \ \text{s}^{-1}. \tag{II.21}$$

Here $\langle\psi'_e|M_e(r)|\psi''_e\rangle$ is the electronic transition moment $R(r)$, $M_e(r)$ is the dipole transition moment function, $U''(r)$ is the ground, or lower state potential curve, and Θ is given by

$$\Theta = \frac{2 - \delta_{0,\Lambda'+\Lambda''}}{2 - \delta_{0,\Lambda'}}. \tag{II.22}$$

It is important to note that if $U'(r)$ is positive everywhere, or falls off as, or more slowly than r^{-2}, then the second term in brackets of equation (II.19) is identically zero. This follows from equation (II.15), since at $r = b_m$, $\frac{dr}{dt} = 0$ by the laws of motion. However, in the most general case, $U'(r)$ falls off faster than r^{-2}. Indeed, for most bound molecular potentials this will be true. As a result, an explicit value of b_m must be found in the domain of r and ϵ where this term is non-zero (see Bates 1951a for a more detailed discussion). That value occurs where $b^2 = f(r) = r^2\,[1 - U'(r)/\epsilon kT]$ has a minimum. Thus, b_m is found at r such that $\frac{df}{dr} = 0$ for each ϵ.

The integrations in equation (II.19) were performed numerically with limits on r from the classical turning point r' to ∞ (see below, however). The lower bound on ϵ is zero where $U'(r)$ is negative and $U'(r)/kT$ where $U'(r)$ is positive. The upper bound on ϵ is $[U'(r) - U''(r)]/kT$.

As a test of the integration routine, the calculation of Bates (1951a) for reaction (II.8) was duplicated. In this case, the upper state potential curve is repulsive everywhere. Thus, the second term in equation (II.19) can be neglected. The upper state ($^2\Sigma_u^+$) and ground state ($X^2\Sigma_g^+$) potential curves are shown in Figure II.1 (Bates 1953). The transition dipole moment is from

Bates (1951b). The results were found to be identical with those of the earlier work to the precision given.

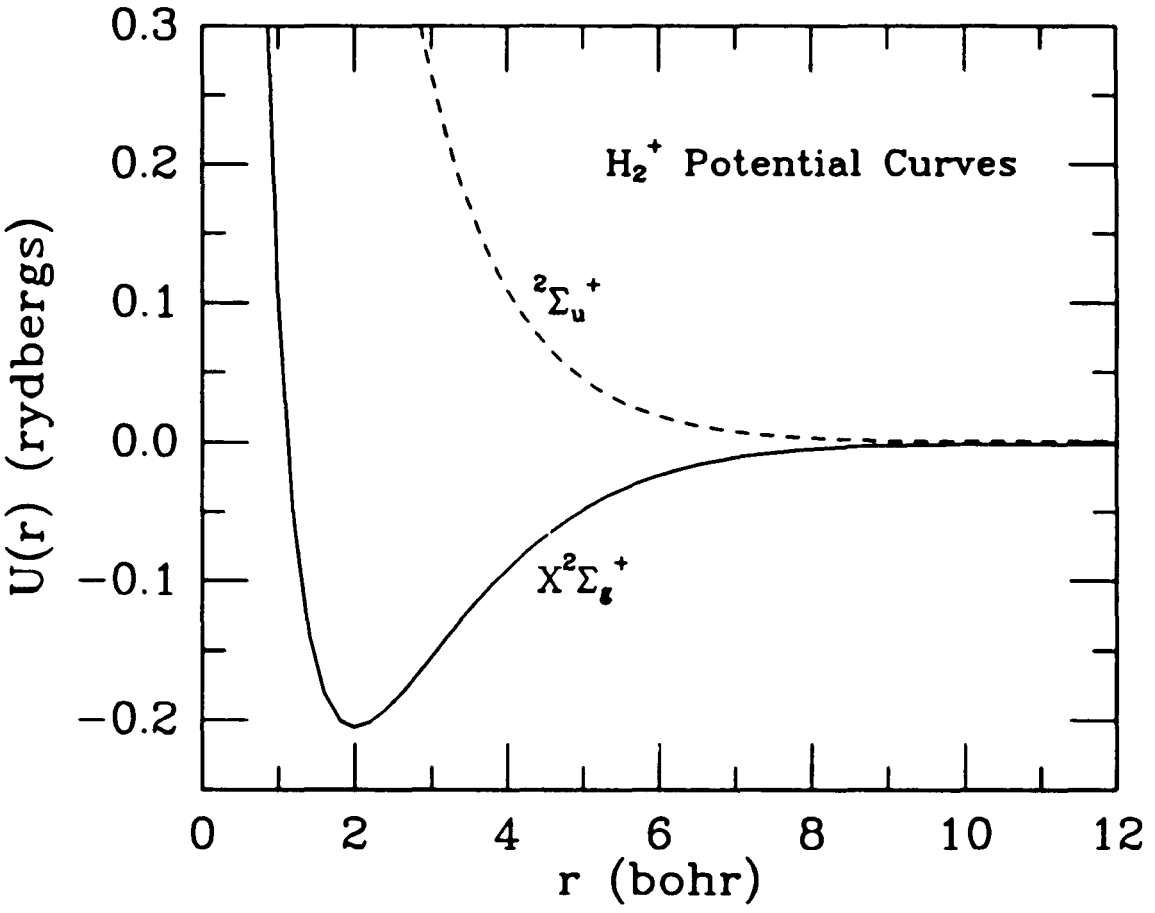

Figure II.1: Potential curves of the molecular hydrogen ion (H_2^+) taken from Bates (1953). Note that the upper $^2\Sigma_u^+$ potential is positive everywhere and is, therefore, unbound. Radiative association of H and H^+ to form H_2^+ takes place through an electronic transition from the upper state to the bound $X^2\Sigma_g^+$ ground electronic state.

2.3 RESULTS FOR H_2

As an illustration, we will make an initial order-of-magnitude estimate for the rate of reaction (II.7). The radiative rate coefficient can be expressed as the collision rate (σv cm^3 s^{-1}) weighted by the probability that a stabilizing transition can occur during the encounter. That probability is $P = A\delta t$ (equation II.14), where $\delta t = d/v$ is the collision time and d is the distance over which an interaction can take place ($\approx$ 1 Å). Taking the temperature to be $\approx$ 500 K, we find $P \approx 3.3 \times 10^{-5}$ ($A \approx 10^9$ s^{-1}) and a collision rate of $\approx 4.0 \times 10^{-10}$ cm^3 s^{-1}. Thus, the radiative rate coefficient should be of the order $k \sim 1.3 \times 10^{-14}$ cm^3 s^{-1}. The relatively large value for this rate coefficient is due to the strength of the stabilizing transition. In general, however, the n=2 population will be low and this process will be ineffective.

There are three potential curves with allowed transitions to the $X^1\Sigma_g^+$ ground state of H_2 which correlate with atomic hydrogen in n=2 and n=1. The potential curves of $B^1\Sigma_u^+$ and $C^1\Pi_u$ correlate with H($2p$) and H($1s$). The potential curve of $B'^1\Sigma_u^+$ correlates with H($2s$) and H($1s$). The potentials used are taken from Stephens and Dalgarno (1972), Stephens and Dalgarno (1974), Kołos (1975), Kołos (1976), Kołos and Wolniewicz (1975), Kołos and Rychlewski (1976), Kołos, Szalewicz, and Monkhorst (1986), and Kwok, Dalgarno, and Posen (1985). These potential curves are pictured in Figure II.2. The transition moments are from Ford *et al.* (1975), Dressler and Wolniewicz

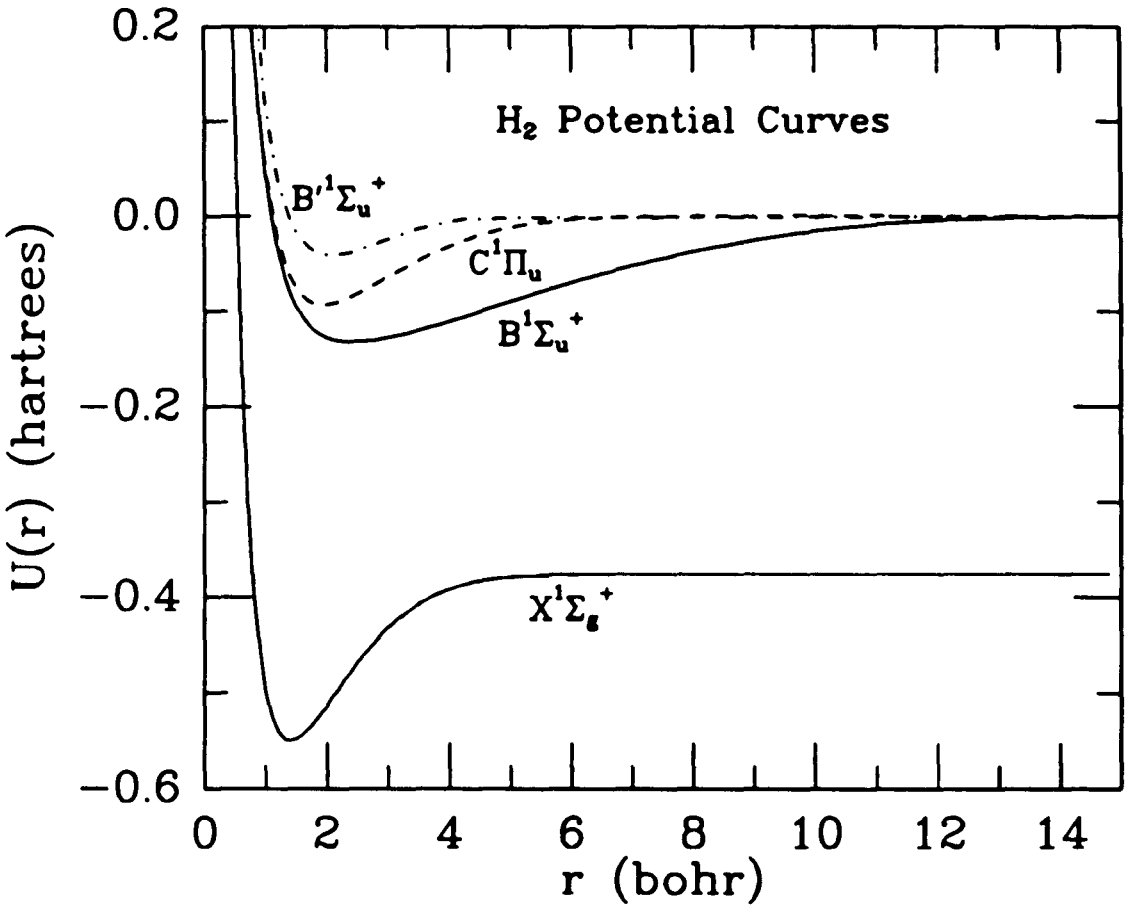

Figure II.2: Molecular hydrogen potential energy curves which are the primary routes for the excited atom radiative association process to form molecular hydrogen (reaction II.7). The $B'^1\Sigma_u^+$ state correlates with H($2s$) and H($1s$) at large internuclear separations. The potential curves of the $B^1\Sigma_u^+$ and $C^1\Pi_u$ states correlate with H($2p$) and H($1s$).

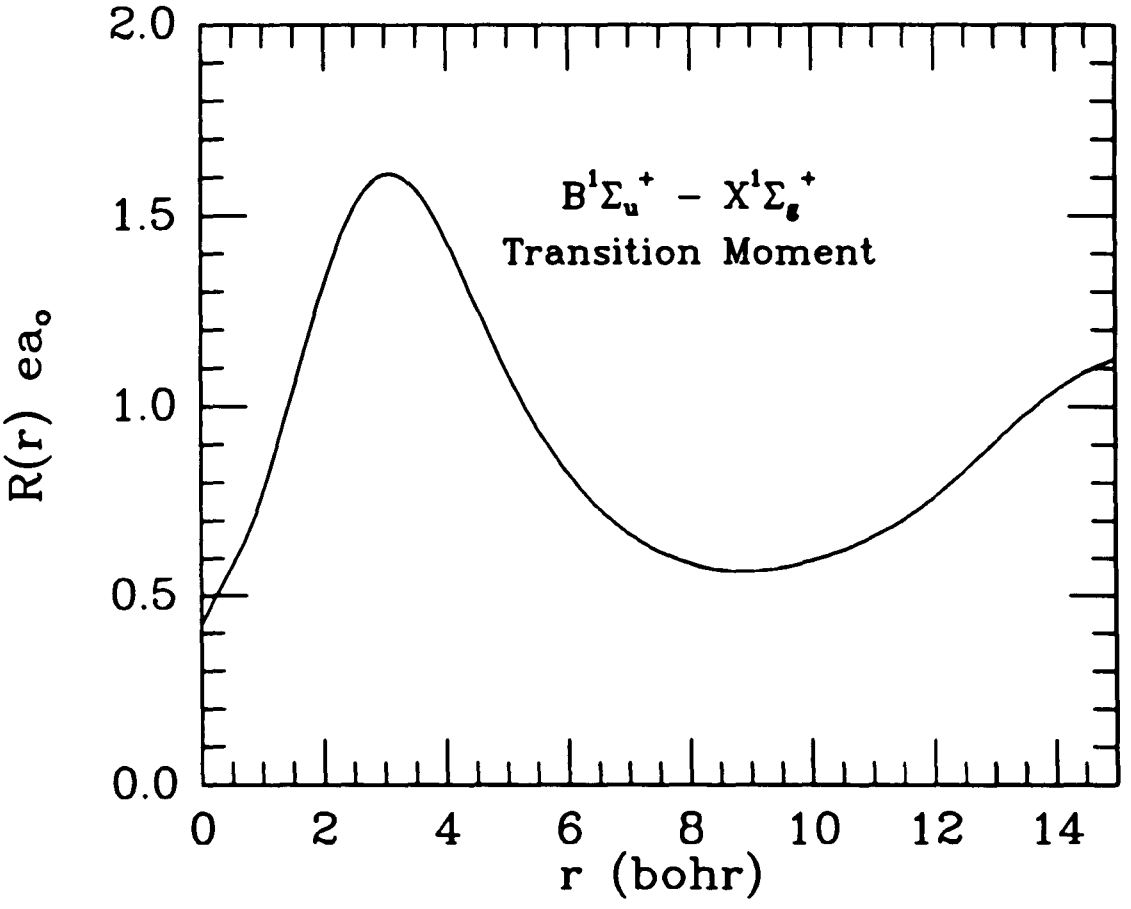

Figure II.3: Electronic transition moment function for the $B^1\Sigma_u^+ \leftrightarrow X^1\Sigma_g^+$ transition of H_2 as a function of internuclear separation (Dressler and Wolniewicz 1985).

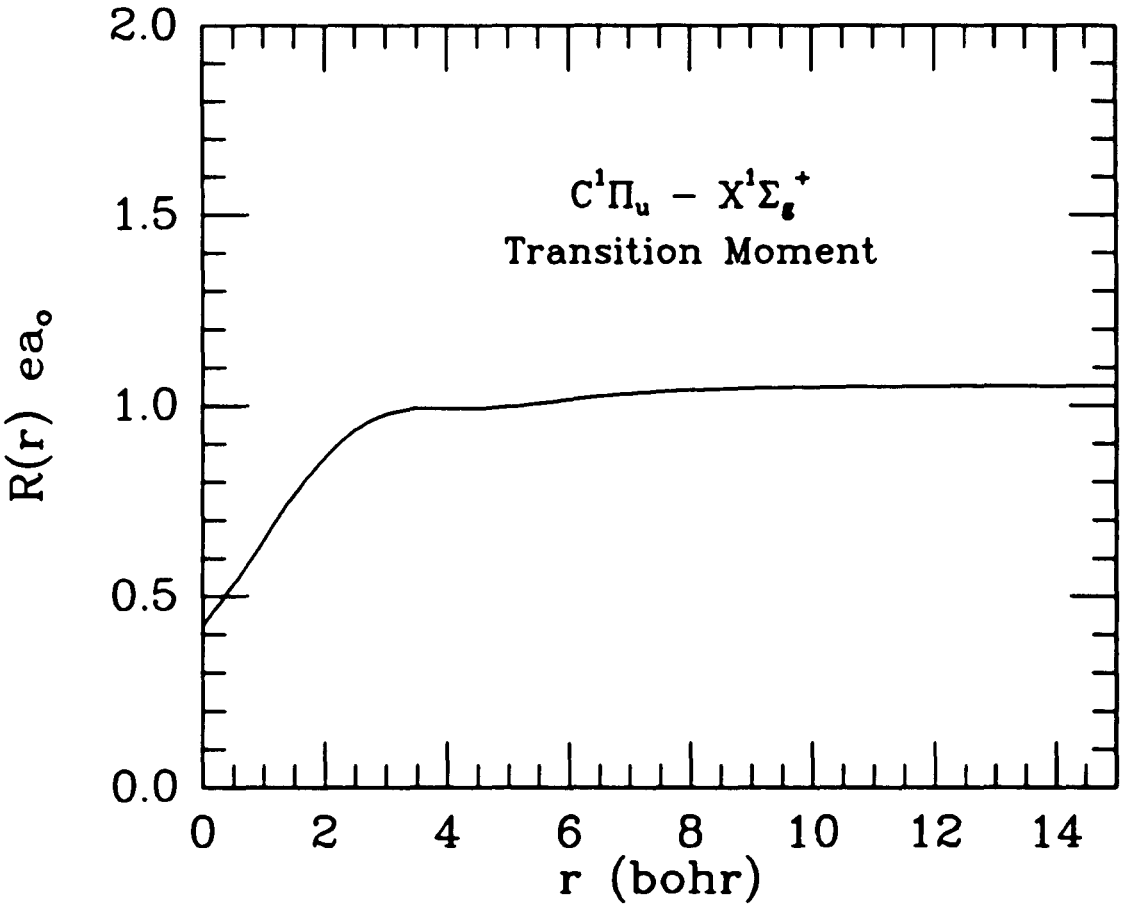

Figure II.4: Electronic transition moment function for the $C^1\Pi_u \leftrightarrow X^1\Sigma_g^+$ transition of H_2 as a function of internuclear separation (Dressler and Wolniewicz 1985).

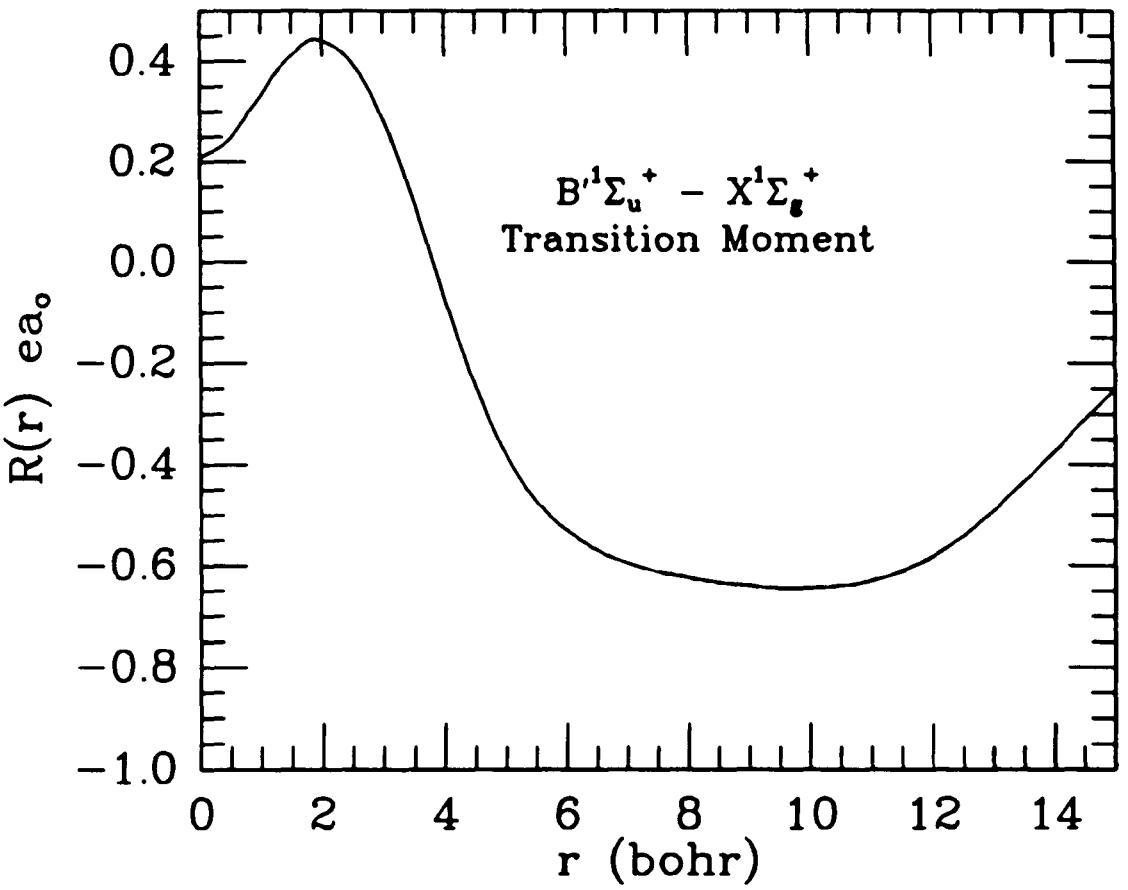

Figure II.5: Electronic transition moment function for the $B'^1\Sigma_u^+ \leftrightarrow X^1\Sigma_g^+$ transition of H_2 as a function of internuclear separation (Ford *et al.* 1975).

(1985), and Kwok *et al.* (1985) (see Figures II.3 - II.5). The statistical weight factors are $g = 1/24$ for $B^1\Sigma_u^+ \rightarrow X^1\Sigma_g^+$, $g = 2/24$ for $C^1\Pi_u \rightarrow X^1\Sigma_g^+$, $g = 1/8$ for $B'^1\Sigma_u^+ \rightarrow X^1\Sigma_g^+$, and $\Theta = 1$ (*cf.* Sharp 1971).

Since the transition probabilities for the $B^1\Sigma_u^+ \rightarrow X^1\Sigma_g^+$ and $C^1\Pi_u \rightarrow X^1\Sigma_g^+$ transitions do not tend to zero as r goes to infinity, but go to the separated atom values for the Lα transition, a maximum value of internuclear separation for which association is probable must be determined. In a quantal calculation, such a maximum internuclear separation would be estimated by evaluation of an integral to determine the degree of overlap in the molecular wavefunctions. However, since a semi-classical calculation is likely to be uncertain by factors of at least two, the detailed evaluation of an overlap integral is unjustified. A maximum value of r at which association may occur can be found in terms of a probability in the following way. We must first note that the highest bound vibration - rotation level in the ground electronic state of H_2 is v = 14, J = 4. If tunneling is ignored (implicit in the Bates method), the maximum value of r at which a bound state can be formed is 6.140 bohr when J = 0. This is just the classical turning point of the v = 14, J = 0 level in the $X^1\Sigma_g^+$ ground state of H_2. If J = 4, bound states will result out to $r = 9.058$ bohr. Classically, the rotation rate of the resultant molecule will depend on the impact parameter of the collision. If the impact parameter is zero, then J = 0. If the impact parameter is large, then J will go to 4.

It is clear that for $r \leq 6.140$ bohr, the probability that a transition can go to a bound state is unity. Likewise, for $r > 9.058$ bohr all transitions

will lead to an unbound molecule. In the range $6.014 < r \leq 9.058$ bohr, there appear to be three functional forms for the probability which are physically realistic: a) constant and about 0.5, b) linear with $P = 1.0$ at $r = 6.140$ bohr and $P = 0.0$ at $r = 9.058$ bohr, and c) an exponential. Inspection of the potential curve for the ground electronic state (Figure II.2) reveals that the potential in the range $6.014 < r < 9.058$ bohr is nearly constant. Thus, the change in internuclear separation of the classical turning point for v=14 will increase approximately linearly with J (or impact parameter). The probability of a bound state forming is largest near $r = 6.140$ bohr, since the range of impact parameter over which such a result can occur increases as r decreases toward 6.140 bohr. The converse is true as r approaches $r = 9.058$ bohr. Thus, the case b probability function (a linear function) will provide an adequate representation. Therefore, the integration in equation (II.19) over r is carried out to $r_m = 9.058$ bohr. A linear probability function is applied over $6.140 < r \leq 9.058$ bohr, limiting the range of internuclear separation over which a stablizing transition can take place. For this type of semi-classical calculation, that range would otherwise be unbounded.

Our results for transitions from each of the three upper states are shown in Table II.1. The rate coefficients are presented as $k_{2p} = k(B^1\Sigma_u^+) + k(C^1\Pi_u)$ and $k_{2s} = k(B'^1\Sigma_u^+)$. For a thermalized population in the hydrogen $2s$ and $2p$ states, the total rate coefficient is $k_{H^*} = (3k_{2p} + k_{2s})/4$. The excited atom formation rate is then $R(H^*) = k_{H^*} n(H_{n=2}) n(H_{1s})$ cm^{-3} s^{-1}.

TABLE II.1

RADIATIVE ASSOCIATION

$$H(n=2) + H(n=1) \rightarrow H_2 + h\nu$$

Temperature (K)	$k_{2s}(T) \times 10^{-14}$ cm^3 s^{-1}
50	2.7
100	2.2
500	1.4
1000	1.2
2500	1.2
5000	1.1
10000	1.1
30000	1.0

Temperature (K)	$k_{2p}(T) \times 10^{-14}$ cm^3 s^{-1}
50	0.93
100	1.2
500	2.7
1000	3.4
2500	4.1
5000	4.3
10000	4.2
30000	3.6

2.4 RESULTS FOR CO^+

The most likely stabilizing transition for reaction (II.12) is $A^2\Pi \rightarrow X^2\Sigma^+$. The $X^2\Sigma^+$ and $A^2\Pi$ states both correlate with ground-state C^+ and O at large internuclear separations, and they cross at $r = 5.3$ and 2.8 bohr, based on potential curves derived from the data of Krupenie (1966), Chambaud *et al.* (1980), and Coxon and Foster (1982) (see Figure II.6). This means that both $A^2\Pi \rightarrow X^2\Sigma^+$ and $X^2\Sigma^+ \rightarrow A^2\Pi$ stabilizing transitions can occur. The statistical weight factors are $g = 4/54$ and $\Theta = 1$ for the $A^2\Pi \rightarrow X^2\Sigma^+$ transition and $g = 2/54$ and $\Theta = 2$ for $X^2\Sigma^+ \rightarrow A^2\Pi$. It is found that the contribution to the total association rate from the $X^2\Sigma^+ \rightarrow A^2\Pi$ transition is small. The results are shown in Table II.2. These values are well fit by the function

$$k_{\Pi.12} \approx 5 \times 10^{-19}[\ln(T) - 1.91] \text{ cm}^3 \text{ s}^{-1} \quad (50 \leq T \leq 5000 \text{ K}). \qquad \text{(II.23)}$$

The relatively low value of $k_{\Pi.12}$ is a consquence of a small transition moment over the relevant range of r (Rosmus and Werner 1982) and of the small statistical weight of approach along the $X^2\Sigma^+$ and $A^2\Pi$ potentials among the large manifold of states that correlate with $C^+(^2P)$ and $O(^3P)$. The transition moment rapidly goes to zero as $r \rightarrow \infty$ (see Figure II.7). Therefore, there is no ambiguity in determining a maximum r for which a stabilizing transition can occur.

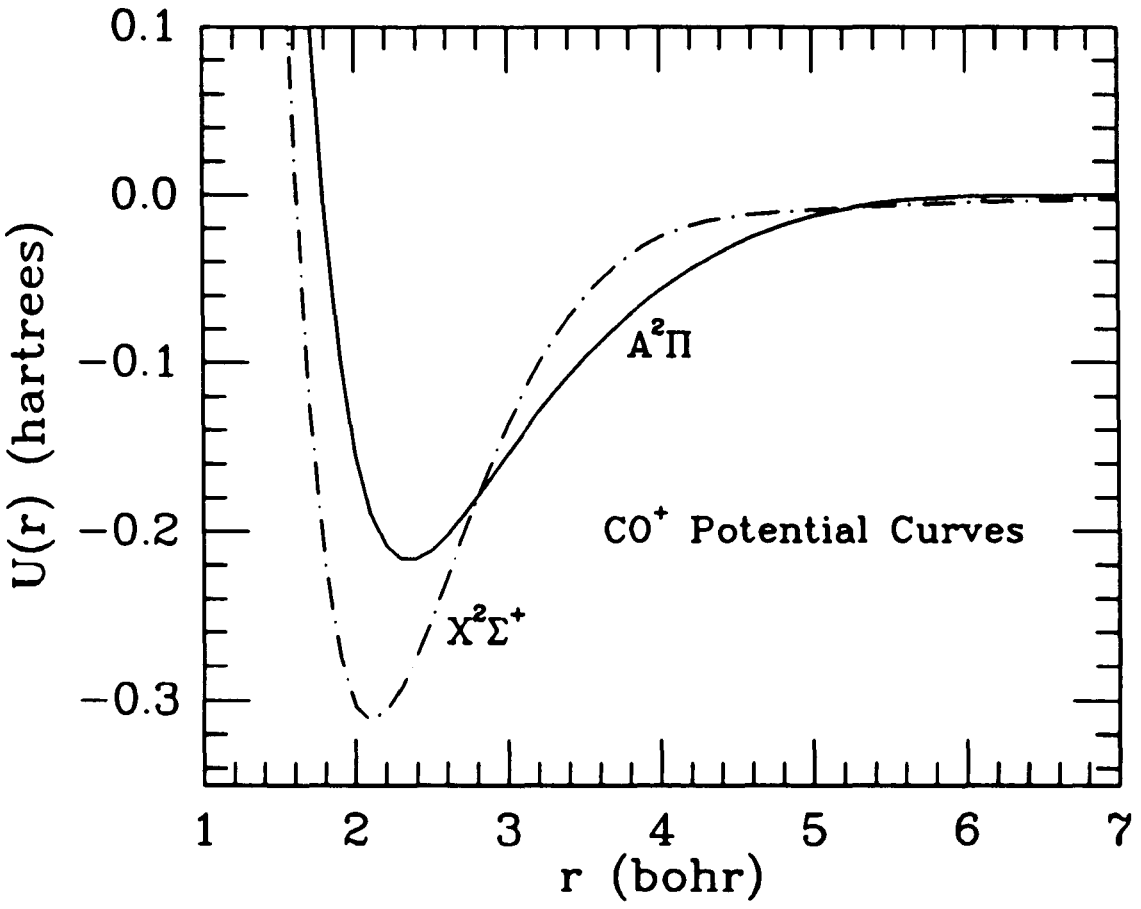

Figure II.6: Potential curves for the $X^2\Sigma^+$ and $A^2\Pi$ electronic states of CO^+. An electronic transition between these states is the fastest route for radiative association of ground state C^+ and O (see text). Note crossings of the potential curves at 2.8 and 5.3 bohr.

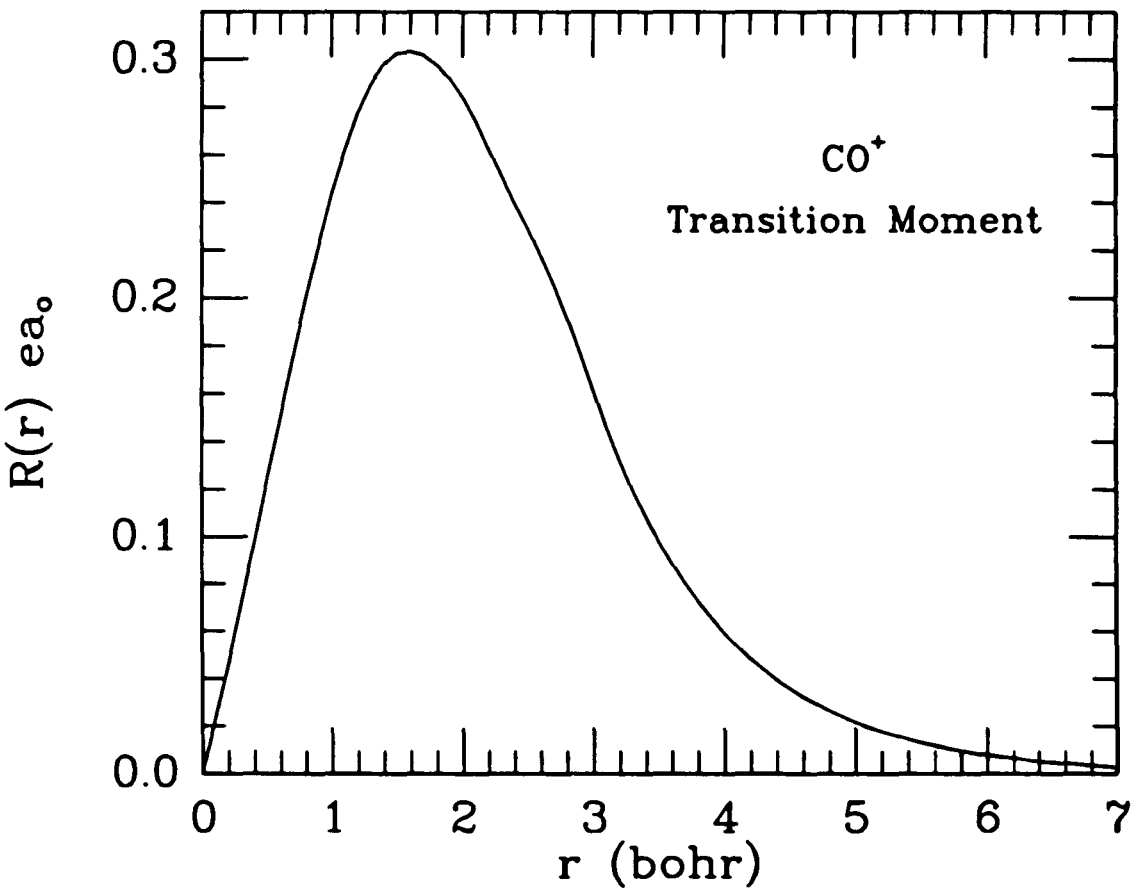

Figure II.7: Electronic transition moment function for $A^2\Pi \leftrightarrow X^2\Sigma^+$ transition of CO^+ as a function of internuclear separation (Rosmus and Werner 1982).

TABLE II.2

RADIATIVE ASSOCIATION

$C^+ + O \rightarrow CO^+ + h\nu$†

Temperature (K)	$k(T) \times 10^{-18}$ cm^3 s^{-1}
50	0.94
100	1.3
500	2.0
1000	2.4
2500	2.9
5000	3.1
10000	3.0
30000	2.0

†For the electronic transition $A^2\Pi \rightarrow X^2\Sigma^+$.

Our results for $k_{II,12}$ differ by factors of $\sim$ 0.7 to 1.6 from the values computed recently by Dalgarno, Du, and You (1989), who adopted somewhat different potential curves and transition moment functions. We consider this to be adequate agreement for this type of approximation. However, a value for the rate coefficient found by Petuchowski *et al.* (1989) is greater than that found here by several orders of magnitude. Petuchowski *et al.* inferred their rate coefficient from that of three-body association, a method for which a number of uncertainties exist (see Dalgarno *et al.* 1989).

2.5 DISCUSSION

The formation rate of CO^+ by direct radiative association (reaction II.12) is slow. Therefore it will not compete with other processes in the formation of carbon monoxide (CO), except in regions of extremely low hydrogen content relative to C and O. The most obvious environments of this type are the interiors of supernovae. A detailed discussion of how CO may be formed in the ejecta of a supernova will be presented in Chapter 4. Other astrophysical applications for reaction (II.12) are likely to be rare.

The excited atom radiative association process to form molecular hydrogen (reaction II.7) may have more general astrophysical applications. In what follows, we will examine the relative importance of this process compared to other gas phase routes to form H_2 in a number of typical environments. Since this reaction requires the presence of a significant n = 2 population, it clearly will not be important throughout most of the general interstellar medium. Rates for the H^- and H_2^+ processes (reactions II.8 - II.11) as well as the principal destruction routes are presented in Table III.1 (Appendix B).

In local thermodynamic equilibrium (LTE), a system can be defined by one unique temperature. In addition, the ionization fraction and level populations are determined by the Saha and Boltzmann equations, respectively. Of course, it is not in general necessary to consider individual processes in LTE. Nonetheless, it may be instructive to know what reactions are dominant under

various conditions. For a gas in LTE, which consists only of hydrogen, it is straightforward to show that the rate of H_2 formation by reaction (II.7), $R(H^*)$ cm^{-3} s^{-1}, compared to the associative detachment process (reactions II.10 – 11), $R(H^-)$ cm^{-3} s^{-1}, is

$$n_{H^\circ}^{\frac{1}{2}} Q^{-\frac{3}{2}}(H) \frac{R(H^*)}{R(H^-)} = \begin{cases} 14.2, & T = 4000 \text{ K} \\ 1.9 \times 10^2, & T = 5000 \text{ K} \\ 6.2 \times 10^3, & T = 7500 \text{ K} \\ 3.8 \times 10^4, & T = 10000 \text{ K}. \end{cases} \tag{II.24}$$

$Q(H)$ is the atomic hydrogen partition function which is dependent on the total density n and temperature (see Chapter 3). Compared to reaction (II.9), we find

$$n_{H^\circ}^{\frac{1}{2}} Q^{-\frac{3}{2}}(H) Q(H_2^+) \frac{R(H^*)}{R(H_2^+)} = \begin{cases} 2.6 \times 10^3, & T = 4000 \text{ K} \\ 1.0 \times 10^5, & T = 5000 \text{ K} \\ 1.4 \times 10^7, & T = 7500 \text{ K} \\ 1.8 \times 10^8, & T = 10000 \text{ K}. \end{cases} \tag{II.25}$$

Here $Q(H_2^+)$ is the H_2^+ partition function

$$\begin{aligned} Q(H_2^+) &= \sum_{n,v,J,N} g_n(N,J) \exp\left[-E(n,v,J,N)/kT\right] \\ g_n(N,J) &= (2S_n + 1)(2 - \delta_{0,\Lambda_n})(2J_n + 1). \end{aligned} \tag{II.26}$$

A convenient expression for calculating this and a number of other diatomic molecule partition functions can be found in Sauval and Tatum (1984). For $T = 5000$, $Q(H_2^+) = 340.9$ and for $T = 7500$, $Q(H_2^+) = 1011.6$. Thus, in LTE conditions, excited atom radiative association is an important process at high temperatures and relatively low densities. As will be discussed in Chapter 3, this was found in an explicit calculation to be the case during the onset of the epoch of recombination in the early Universe. At that time, the Universe was approximately in thermodynamic equilibrium. However, the n = 2 population was enhanced over the TE value. The conditions in the early Universe appear

well suited for the excited atom radiative association process and was the primary motivation for determining the rate coefficient.

It is clear that the excited atom association process cannot compete with the other gas phase processes in a cool diffuse cloud. However, it is of interest to note how the gas phase processes in a "typical" diffuse cloud ($T \approx 100$, $n_e \approx 2 \times 10^{-4} n_{\rm H}$ cm^{-3}, $n_{\rm H} \approx 300$ cm^{-3}; van Dishoeck and Black 1986) compare. The required excitation temperature of H(n=2) is found to be $T_{ex} \sim 8500$ K for reaction (II.7) to be faster than the dominant H^- process, and $T_{ex} \sim 5000$ K for it to compete with the H_2^+ process. While this greatly exceeds the kinetic temperature of the gas, such an excitation temperature may be possible in regions of extreme Lα trapping. For example, a diffuse H II region, such as that described by Draine and Salpeter (1978), is a Strömgren sphere surrounding an O7 V star with $n = 0.5$ cm^{-3} and $T = 8000$ K. The excitation temperature due to Lα pumping is $T_{ex} \sim 3500$ K in the surrounding H I region. Using the parameters of Black and van Dishoeck (1987) for the planetary nebula NGC 7027, it can be shown that $T_{ex} \sim 5200$ K in the nebula. In this case, the density and ionization are sufficiently high that the required excitation temperature for excited atom association to be competitive is in excess of 14000 K.

Another object in which the excited atom radiative association process may be important in a different way is in the bipolar nebula surrounding the star HD 44179 (the Red Rectangle). The nebular spectrum of this object displays dramatic molecular band-like emission at about 5500 - 7500 Å (Schmidt,

Cohen, and Margon 1980). These features have defied identification. It has been asserted that the emission may be due to large molecules, or polycyclic aromatic hydrocarbons (Wdowiak 1987). Another possiblity is fluorescence produced by reaction (II.7) occuring through the $EF^1\Sigma_g^+ \rightarrow B^1\Sigma_u^+$ channel. While slower than the other routes already discussed ($k_{EF} \approx 3 \times 10^{-16}$ cm^3 s^{-1} at $T = 1000$ K), it will produce an optical spectrum. Preliminary analysis shows that this process could account for at least some of the emitted flux. However, a detailed calculation of the spectrum is required.

While this discussion has not been an exhaustive search for a present day application of the excited atom radiative association process (It is not the Holy Grail after all!), it should have made clear that regions can be envisaged where this reaction can play an important role. The most likely appear to be regions surrounding quasars, active galactic nuclei, or other environments in which Lα trapping may be large. At the present time, observations of molecules in these regions are difficult at best. Thus, our understanding of the physical conditions in which molecules are forming is tenuous. Until detailed studies have been carried out, and accurate observations are possible, there will remain large uncertainties in assessing the importance of this process in these hard to reach galaxies. As techniques improve for modeling chemical processes in rapidly evolving, high temperature environments, an application may appear closer to home. In time-dependent situations, the n = 2 population could be elevated for a brief period resulting in a burst of molecular hydrogen formation. Important transient effects may ensue. Indeed, the conditions in the Universe

may always conspire in ways which will make reaction (II.7) unimportant. This somehow seems unlikely.

CHAPTER 3

THE EPOCH OF RECOMBINATION

3.1 INTRODUCTION

We live in an expanding universe. This has been well established since Hubble (1929) demonstrated the rapid recession of distant galaxies. Indeed, the idea of universal expansion was modeled by Friedmann (1924) and Lemaître (1927) just prior to Hubble's discovery. When Penzias and Wilson (1965) discovered the 3 K microwave background radiation, the strongest evidence for the origin of the Universe as a hot fireball was found. Any modern theory of cosmology must explain the observed expansion and the presence, blackbody character, and isotropy of the microwave background radiation. While not fully satisfying to some (*i.e.* Burbidge 1971; Layzer 1968; Layzer and Hively 1972), we will accept the "standard hot big bang" model as described by Harrison (1973) and Zel'dovich and Novikov (1983) as the correct description for the evolution of the Universe.

In this chapter, the discussion will be restricted to a short period in the evolution of the Universe referred to as the *epoch of recombination.* The ther-

mal history of the Universe can be briefly described in the following way. At an age of about 10^{-4} s and a temperature of $\sim 10^{12}$ K, the Universe emerges from a singularity into the *lepton era*. At this time, the Universe is primarily composed of protons, leptons, and antileptons. The lepton era is a period of rapid muon and electron pair annihilation. At a temperature of $\sim 10^{10}$ K and an age of about 2 s, the Universe evolves into the *radiation dominated era*. This is the period in which the radiation energy density exceeds that of the matter. Early in the radiation era the conditions are such that primordial nucleosynthesis can begin (Peebles 1966; Fowler, Wagoner, and Hoyle 1967; Wagoner 1973; Yang *et al.* 1984). After this relatively short period of nucleosynthesis ceases, the Universe remains radiation dominated. Radiation and matter are in intimate contact through elastic scattering of energetic photons by electrons. This lasts until a temperature of about 7000 – 5000 K (an age of $10^{11} - 10^{12}$ s) is reached, roughly the recombination temperature of atomic hydrogen. At this time, the photoionization rates of He and H become small compared to the rates of recombination,

$$He^{++} + e^- \rightarrow He^+ + h\nu$$

$$He^+ + e^- \rightarrow He + h\nu$$

$$H^+ + e^- \rightarrow H + h\nu,$$

signaling the onset of the *epoch of recombination*. He^{++}, He^+, and H^+ recombine in the sequence of their decreasing ionization potentials. The matter rapidly changes state from an ionized plasma to a primarily neutral gas. Simple molecules are now able to survive. When the number of free electrons has decreased sufficiently, momentum transfer due to Thomson scattering becomes

small. The radiation and matter decouple and begin to evolve at different temperatures. At about this time, the rest-mass density of the gas becomes greater than the energy density of the radiation (Weinberg 1972). The Universe enters the *matter dominated era*. As the Universe evolves into the present epoch, galaxy clusters, galaxies, and stars form out of gravitationally unstable fluctuations in an otherwise isotropic Universe.

Recombination of the primeval plasma as it expands and cools has been examined by Peebles (1968), Sunyaev (1968), Zel'dovich, Kurt, and Sunyaev (1969), Jones and Wyse (1985), and most recently by Krolik (1989). Molecule formation around this epoch was first discussed by Saslaw and Zipoy (1967) and Peebles and Dicke (1968). Models of molecular abundances and cooling have been studied by Lepp and Shull (1984). Dalgarno and Lepp (1987) have recently reviewed the subject. It is of interest to examine in detail the molecular evolution which may have taken place during and after the recombination epoch. Molecular hydrogen can be an efficient radiative coolant for temperatures below 10^4 K through the collisional excitation of vibrational and rotational transitions. It is important to determine the impact such cooling may have had on the early Universe. For example, radiative cooling by H_2 may have influenced the decoupling of the matter from the radiation field. In addition, such cooling was crucial to the formation of the first generation of stars by allowing continued collapse of Jeans unstable clouds. As will be discussed later, a system of primordial elemental composition cannot radiate

away the gravitational energy of collapse for temperatures much less than 10^4 K without the presence of molecular coolants.

In this chapter, the atomic and molecular processes which may have taken place around the epoch of recombination will be examined. First, the equations of ionization balance and molecular formation and destruction will be integrated through the recombination epoch. This will be followed by a more detailed examination of various processes including heating and cooling of the primordial plasma, damping of fluctuations prior to decoupling, and the possibility of a radiation driven instability at the onset of recombination. In the following section, the adopted computational method will be described.

3.2 METHOD OF CALCULATION

a) *The Cosmological Model*

The cosmological model which will be used is the standard Friedmann cosmology. The presentation of Harrison (1973) will be followed. In a Friedmann model, the state of the Universe at any proper time can be characterized by a radiation temperature, T_{rad}, and a mean density, ρ. In terms of the critical density required to close the Universe, the present mean density is $\rho_o = \rho_c \Omega$, where

$$\rho_c = \frac{3H_o^2}{8\pi G} \tag{III.1}$$

and H_o is the current value of the Hubble parameter. If the presence of non-baryonic "dark" matter is accepted, then ρ_o can be expressed in terms of $\Omega = \Omega_{tot} = \Omega_{baryon} + \Omega_{dark}$. There are strong arguments for believing that as much as 90% of the matter present in the Universe today is unseen (Blumenthal *et al.* 1984; Aaronson and Olszewski 1988). A general expression which describes the evolution of a Friedmann universe is

$$H^2 = \frac{8\pi G}{3}\left[\rho - \rho_c(\Omega - 1)(1+z)^2\right]. \tag{III.2}$$

The Universe will be closed, open, or flat if the sign of the second term in brackets, or curvature term, is positive, negative, or zero, respectively. Following convention, the density parameter will be expressed as $\hat{\Omega} = \Omega\left(\frac{H_o}{50}\right)^2$, where H_o is in units of km s^{-1} Mpc^{-1} (Note: The reference value of $H_o = 50$ has

been chosen strictly out of convenience. The actual value is probably closer to 100; Aaronson and Mould 1983; Aaronson *et al.* 1986). Therefore, the present mean mass density is $\rho_o = 4.697 \times 10^{-30}\hat{\Omega}$ gm cm^{-3}. If it is assumed that all the mass present in the Universe is in the form of nucleons, then $n_o = \frac{\rho_o}{m_p} = 2.808 \times 10^{-6}\hat{\Omega}$ cm^{-3}. The present radiation temperature is taken to be $T_{rad} = 2.7$ K (Meyer and Jura 1985). At the recombination epoch, the contribution to the total density by muons can be neglected, thus

$$\rho = \rho_m + \kappa\rho_\gamma \quad \text{gm cm}^{-3}, \tag{III.3}$$

where ρ_m is the mean density due to massive particles, ρ_γ is the mean density due to photons, and κ is a correction factor that adjusts for the neutrino background. This factor will be taken to be $\kappa = \kappa_o = 1.45$, thus accounting for all currently known neutrino types (see Weinberg 1972, Harrison 1973, and Börner 1988). In equivalent mass units, the photon density is given by

$$\rho_\gamma = \frac{1}{c^2}\left(\frac{4\sigma}{c}\right)T_{rad}^4 \quad \text{gm cm}^{-3}. \tag{III.4}$$

In terms of the redshift z, it is straightforward to show that

$$\begin{aligned} \rho_m &\propto (1+z)^3 \\ \rho_\gamma &\propto (1+z)^4. \end{aligned} \tag{III.5}$$

The densities of matter and radiation are equal at $\rho_{eq} = \rho_m = \rho_\gamma$ which corresponds to a redshift of $1 + z_{eq} = \frac{\rho_{mo}}{\rho_{\gamma o}} = 1.050 \times 10^4\hat{\Omega}$. Thus,

$$\rho_{eq} = \frac{\rho_{mo}^4}{\rho_{\gamma o}^3} = 5.438 \times 10^{-18}\hat{\Omega}^4 \quad \text{gm cm}^{-3}. \tag{III.6}$$

Now, the total density around the epoch of recombination is given by

$$\rho = \rho_{eq}(R^{-3} + \kappa_o R^{-4}) \quad \text{gm cm}^{-3}, \tag{III.7}$$

where $R = \frac{1+z_{eq}}{1+z}$. From expressions (III.4) and (III.5) it is easy to arrive at the useful relationship

$$RT_{rad} = 2.835 \times 10^4 \hat{\Omega}. \qquad \text{(III.8)}$$

As long as the mean free path for Thomson scattering remains less than the size scale of the Universe $T_{rad} = T_{mat}$, otherwise the radiation and matter decouple. Since $n_\gamma/n_m \approx 10^8$, the transfer of momentum to the matter will not significantly alter the blackbody character of the radiation spectrum (Peebles 1968; Zel'dovich *et al.* 1969). After decoupling $T_{rad} \propto R^{-1}$ and, if adiabatic cooling of the matter dominates, $T_{mat} \propto R^{-2}$. The equilibrium which prevailed during the early period of nucleosynthesis determined the composition of baryonic matter. The model used is that of Wagoner (1973) for which the primordial elemental abundances are a function of Ω only. In most of the models presented here, the elemental abundances will be fixed at stated values in order to explore the effects of other parameters.

b) *The Ionization Fraction*

Prior to recombination the ionized plazma which made up the early Universe was in thermodynamic equilibrium. In such a state the system can be described by one unique temperature. In the case of the primordial Universe prior to decoupling, the optical depth for Thomson scattering $\tau_T \gg 1$, meaning that the radiation field strongly dominated the system. Thus, the equilibrium temperature must have been T_{rad}. In thermal equilibrium, the

ionization fraction of hydrogen is described by the Saha equation

$$\frac{n_e n_{H^+}}{n_H} = \left(\frac{2\pi m_e k T_{rad}}{h^2}\right)^{\frac{3}{2}} \frac{2}{\mathrm{Q(H)}} \exp\left(-\frac{h\nu_o}{kT_{rad}}\right), \qquad \text{(III.9)}$$

where $h\nu_o$ is the ionization potential from the $1s$ ground level and Q(H) is the partition function for neutral hydrogen. As the recombination began the optical depth for absorption of ionizing and Lyman series photons became large, effectively inhibiting recombinations directly to the ground state. Therefore, the $2p$ and $2s$ levels of atomic hydrogen became overpopulated with respect to the $1s$ ground level. However, populations in excited states continued to be described by thermal equilibrium with the radiation field such that the Boltzmann equation was satisfied with respect to the $2s$ level,

$$\frac{n_{n,l}}{n_{2s}} = (2l+1)\exp\left(-\frac{\Delta E_{n,2}}{kT_{rad}}\right), \qquad \text{(III.10)}$$

where $\Delta E_{n,2}$ is the energy difference between the nth and 2nd levels (Peebles 1968). The recombination rate was governed by the rate at which Lα photons escaped the nearly endless cycle of resonance scattering. Since the Universe is a closed system, this could only have been accomplished by redshift due to expansion or by collisional transfer from $2p$ to $2s$ followed by two-photon emission from the metastable $2s$ level. Two-photon decay dominated over the cosmological expansion. This relatively slow process maintained the system in a suprathermal ionization state. Peebles (1968) derived the net rate of recombination to be given by

$$-\frac{d}{dt}\left(\frac{n_e}{n_H}\right) = \left[\frac{\alpha_B n_e^2}{n_H} - \beta_B \frac{n_{1s}}{n_H}\exp\left(-\frac{\Delta E_{1,2}}{kT_{rad}}\right)\right] C, \qquad \text{(III.11)}$$

where

$$C = \frac{1 + KA_{2s,1s}n_{1s}}{\left[1 + K(A_{2s,1s} + \beta_B)n_{1s}\right]}, \tag{III.12}$$

and

$$K = \frac{\lambda_{L\alpha}^3}{8\pi} R \left(\frac{dR}{dt}\right)^{-1}. \tag{III.13}$$

$A_{2s,1s}$ is the decay rate by two-photon emission, α_B is the case B recombination coefficient (Osterbrock 1974), and it has been assumed that $n_e \approx n_p$. Note that $n_{2s}K^{-1}$ is the rate at which Lα photons are redshifted out of the line (Zel'dovich *et al.* 1969). If the population in excited levels is negligible, then

$$\beta_B = \alpha_B \exp\left(-\frac{E_2}{kT_{rad}}\right)\left[\frac{2\pi m_e kT_{rad}}{h^2}\right]^{\frac{3}{2}}, \tag{III.14}$$

where E_2 is the binding energy of the $n = 2$ level If there are significant numbers in excited levels, then the atomic partition function Q(H) must be explicitly included. Inspection reveals that the factor C is effectively a correction which retards the recombination rate from that given by a strict Saha value. Equation (III.11) determines the ionization fraction throughout most of this calculation. Refinements to equation (III.11) as developed by Jones and Wyse (1985) and Krolik (1989), while important to a detailed understanding of the recombination, will not be significant for much of this work. However, the formulation of Jones and Wyse has been incorporated for some models in order to assess quantities such as the precise moment of decoupling.

It is desirable to rewrite equation (III.11) such that the system is characterized by T_{rad} rather than time. In order to accomplish this, we note

that the Hubble time is $\tau = 1/\mathrm{H} = R/\dot{R}$, or

$$\tau = \left(\frac{3}{8\pi G\rho}\right)^{\frac{1}{2}} = \left(\frac{3}{8\pi G\rho_{eq}}\right)^{\frac{1}{2}} \frac{R^2}{(\kappa_\circ + R)^{\frac{1}{2}}}, \tag{III.15}$$

assuming that the curvature term in the Friedmann equation (III.2) is negligible. Using (III.8) and (III.15), we can show that

$$\begin{aligned} -\frac{dx_e}{dT_{rad}} = &\left(\frac{dT_{rad}}{dt}\right)^{-1} \alpha_B C \\ &\times \left[n x_e^2 - 2.4145 \times 10^{15}(1 - x_e) T_{rad}^{\frac{3}{2}} \exp\left(-\frac{157809.09}{T_{rad}}\right)\right], \end{aligned} \tag{III.16}$$

where $x_e = n_e/n_H$ is the ionization fraction and

$$\left(\frac{dT_{rad}}{dt}\right)^{-1} = -4.610 \times 10^{20} T_{rad}^{-3} \left[\frac{3R + 4\kappa_\circ}{2(\kappa_\circ + R)^{\frac{3}{2}}}\right]. \tag{III.17}$$

Equation (III.16) can now be solved using standard techniques.

The recombination of He and D are also followed. He^+ and He have metastable states which could, in principle, have caused a similar retardation of recombination as that described for H if the optical depths for ionizing and resonance line photons in He^+ and He greatly exceeded unity. The details of helium recombination in the early Universe have not previously been worked out. However, as will be discussed later, there is motivation for such an investigation. Owing to the much lower abundance of helium, and since the Universe is approximately in thermal equilibrium during the He recombination epoch, these effects are expected to be negligible for the present calculation. Therefore, prior to decoupling, the recombination of minor species will be calculated assuming thermal equilibrium. When T_{mat} no longer equals T_{rad}, a

detailed statistical balance among microscopic processes becomes the appropriate description for the evolution of the matter.

c) *The Cooling Function*

In order to assess the contribution to cooling of the material in the early Universe by molecules, an explicit calculation of the cooling rate is made. The most important heating and cooling processes have been included. If Γ and Λ are heating and cooling functions in erg cm^{-3} s^{-1}, then the kinetic energy balance is expressed by

$$\frac{3}{2}nk\frac{dT_{mat}}{dt} - kT_{mat}\frac{dn}{dt} = \Gamma - \Lambda \quad \text{erg cm}^{-3}\ \text{s}^{-1}. \tag{III.18}$$

The first term on the left is the rate of change in thermal energy and the second term is a measure of the work being done by the expansion. If there are no sources of heating or cooling (*i.e.* $\Gamma - \Lambda = 0$), then the rate of change in kinetic temperature is determined by the rate of expansion. This is just adiabatic cooling.

The rate of energy transfer from the radiation field to the matter by Thomson scattering is

$$\begin{aligned}\Gamma_T - \Lambda_T &= \frac{4\sigma_T k n_e a T_{rad}^4}{m_e c}(T_{rad} - T_{mat}) \\ &= 1.018 \times 10^{-37} n_e T_{rad}^4 (T_{rad} - T_{mat}) \quad \text{erg cm}^{-3}\ \text{s}^{-1}\end{aligned} \tag{III.19}$$

(Weymann 1965). Prior to decoupling the temperature of the radiation field and matter are governed by adiabatic expansion of the relativistic photon gas. Molecular cooling by H_2 arises from excitation of rotational and vibrational

levels by collisions with H and free electrons followed by radiative decay. Collisional excitation of H_2 by other species is negligible. Thus,

$$\Lambda_{H_2} = n_H n(H_2) L_H(T_{mat}) + n_e n(H_2) L_e(T_{mat}) \quad \text{erg cm}^{-3}\ \text{s}^{-1}, \tag{III.20}$$

where $L_H(T_{mat})$ is the cooling rate coefficient due to H - H_2 collisions and $L_e(T_{mat})$ is the cooling rate coefficient due to e - H_2 collisions. We adopt $L_H(T_{mat})$ as given by Hollenbach and McKee (1979) in the low density limit. $L_e(T_{mat})$ is computed from the cross sections of Crompton *et al.* 1969, Chang and Temkin 1969, Crompton *et al.* 1970, Gibson 1970, Henry 1970, and Linden and Schmidt 1971.

Using relation (III.8) and conservation of baryons, it is easy to show that $\frac{1}{n}\frac{dn}{dt} = \frac{3}{T_{rad}}\frac{dT_{rad}}{dt}$. Thus, the equation to be solved is

$$\frac{dT_{mat}}{dT_{rad}} = 2\frac{T_{mat}}{T_{rad}} + \frac{2}{3nk}\left(\frac{dT_{rad}}{dt}\right)^{-1}(\Gamma - \Lambda) \quad \text{erg cm}^{-3}\ \text{s}^{-1}, \tag{III.21}$$

where $\Gamma - \Lambda$ is given by equations (III.19) and (III.20). The exact value of T_{mat} must be calculated from equation (III.21) after decoupling has occurred. However, prior to decoupling $T_{rad} \approx T_{mat}$ such that $\frac{dT_{mat}}{dT_{rad}} \approx 1.0$. Now (III.21) can be rewritten to give

$$T_{mat} \approx \frac{gT_{rad}\left(0.2266 x_e T_{rad}^2 - w\right)}{1 + 0.2266 g x_e T_{rad}^2}, \tag{III.22}$$

where

$$w = 2.226 \times 10^{36} n(H_2) T_{rad}^{-3} \left[L_H(T_{mat}) + L_e(T_{mat})\right]$$
$$g = \left[\frac{3R + 4\kappa_o}{2(\kappa_o + R)^{\frac{3}{2}}}\right]. \tag{III.23}$$

It can easily be seen that without molecular cooling ($w = 0$) the exact moment of decoupling depends on x_e and on the expansion rate in terms of the change

in T_{rad} and R. Therefore, decoupling is a function of Ω only. If molecular cooling is significant, then decoupling may occur earlier.

d) *Partition Functions*

At the temperatures and densities to be explored in this calculation, excited electronic states of atomic species may be significantly populated. In order to accurately determine the ionization balance of such an environment, the atomic partition functions must be calculated. The partition function for a neutral or ionic species ξ is given by

$$Q_\xi(\mathrm{T}) = \sum_{n=1}^{\infty} g_{n\xi} \exp\left(-\frac{E_{n\xi}}{kT}\right),$$

where n is the principal quantum number, $g_{n\xi}$ is the statistical weight of the nth level, and $E_{n\xi}$ is the excitation energy. This sum formally diverges when carried out over an infinite number of energy levels. It is physically more meaningful to express the partition function as

$$Q_\xi(T, n_i) = \sum_{n=1}^{\infty} W_\xi(T, n_i) g_{n\xi} \exp\left(-\frac{E_{n\xi}}{kT}\right). \qquad \text{(III.24)}$$

The probability that the nth energy state exists is given by the function $W_\xi(T, n_i)$ which depends on the gas temperature and number density of charged particles n_i. A probability $W_\xi(T, n_i)$ of less than unity arises from the fact that atoms in an actual gas are not at infinite distances. Thus, there cannot be an infinite number of bound states as there is for an idealized atom. It can be shown that $W_\xi(T, n_i) \propto n^{-4}$ (*cf.* Fischel and Sparks 1971, and references therein).

The general partition function can be written as the sum of three terms

$$Q_{1\xi}(T) = \sum_{n=1}^{\alpha} g_{n\xi} \exp\left(-\frac{E_{n\xi}}{kT}\right), \tag{III.25}$$

$$Q_{2\xi}(T, n_i) = \sum_{n=\alpha}^{\beta} g_{n\xi} \exp\left(-\frac{E_{n\xi}}{kT}\right), \tag{III.26}$$

$$Q_{3\xi}(T, n_i) = \sum_{n=\beta}^{\infty} W_{\xi}(T, n_i) g_{n\xi} \exp\left(-\frac{E_{n\xi}}{kT}\right), \tag{III.27}$$

where $Q_{1\xi}(T)$ is an exact sum over low-lying levels. Above the αth level, the excited states are approximately hydrogenic. $Q_{2\xi}(T, n_i)$ is a sum over such hydrogenic levels for which $W_{\xi}(T, n_i)$ is unity. The final term, $Q_{3\xi}(T, n_i)$, is a sum over levels for which $W_{\xi}(T, n_i) < 1$. In order to solve for the partition functions of He, He^+, H, and D with minimal computing effort, the formulation of Fischel and Sparks (1971) has been employed. This method approximates the sums $Q_{2\xi}(T, n_i)$ and $Q_{3\xi}(T, n_i)$ in a closed form representation containing several Riemann ζ-functions. For this work, the ζ-functions have been approximated by integrals. The value of β is found using a formula given by Fischel and Sparks which is appropriate to a primarily ionized plasma. However, other forms may be better suited for systems in which the linear Stark effect is not the dominant perturbation. The contribution to the partition function from excited levels becomes negligible by the time the recombination plasma has departed significantly from equilibrium and equations (III.10) and (III.11) have become important.

e) *The Chemical Network*

Since primordial nucleosynthesis strongly favored the production of a limited number of species, the chemistry around the epoch of recombination involved only processes of H, D, He, and to a small degree Li. Since the density was low and grains were absent, the chemistry during this period took place strictly through binary gas phase reactions. The chemistry cannot have initiated until the recombination of helium had begun, thus providing neutral species for ion–neutral reactions to take place.

Molecular hydrogen formation began with the radiative association process

$$H + H^+ \rightarrow H_2^+ + h\nu, \tag{III.28}$$

which is followed by charge transfer

$$H_2^+ + H \rightarrow H_2 + H^+. \tag{III.29}$$

Photodissociation of H_2^+

$$H_2^+ + h\nu \rightarrow H + H^+ \tag{III.30}$$

and dissociative recombination

$$H_2^+ + e^- \rightarrow H + H \tag{III.31}$$

limit the total rate of H_2 formation by reactions (III.28) and (III.29). The distribution of vibrational states in the H_2^+ ion determines the rate of destruction by processes (III.30) and (III.31). H_2^+ in $v > 3$ can also be removed through formation of HeH^+

$$H_2^+(v > 3) + He \rightarrow HeH^+ + H \tag{III.32}$$

in the presence of neutral helium. A second route to the formation of H_2 is started by radiative attachment to form the hydrogen negative ion

$$H + e^- \rightarrow H^- + h\nu, \tag{III.33}$$

which may be followed by associative detachment with H

$$H^- + H \rightarrow H_2 + e^-. \tag{III.34}$$

Owing to a threshold of only 0.75 eV, hydrogen negative ions are rapidly removed from the sequence by the process of photodetachment

$$H^- + h\nu \rightarrow H + e^- \tag{III.35}$$

and by the mutual neutralization processes

$$H^- + H^+ \rightarrow H + H, \tag{III.36}$$

$$\begin{aligned} H^- + H_2^+ &\rightarrow H + H + H \\ &\rightarrow H_2 + H. \end{aligned} \tag{III.37}$$

As discussed elsewhere (Chapter 2 and Appendix A) molecular hydrogen cannot form by direct radiative association of ground state H atoms. However, as the recombination of H became rapid, there may have been a source of H_2 formed by the excited atom association process

$$H\,(n = 2) + H\,(n = 1) \rightarrow H_2 + h\nu, \tag{III.38}$$

where the $n = 2$ population was determined by the rate of recombination (Peebles 1968). The period when reaction (III.38) may have been important was short lived and is not expected to have altered the final H_2 abundance

after the recombination period ceased. The abundance of H_2 was limited at early times primarily by photodissociation, collision-induced dissociation, and electron-impact excitation leading to dissociation. All these destruction processes rapidly became ineffective due to the decreasing temperatures of the radiation field and matter (Dalgarno and Lepp 1987). Therefore, H_2 formation after recombination is limited only by the decrease in density due to the expansion of the Universe.

The first molecules formed were likely to have been He_2^+ followed by HeH^+. The formation of both these species was initiated by radiative association of neutral helium with He^+ and H^+, respectively. Their relative abundances, especially that of He_2^+, are expected to have been low, however. The isotopic form of molecular hydrogen, deuterium hydride or HD, probably contributed to cooling during the formation of the first stars (Dalgarno and Wright 1972). HD is formed by processes analogous to the formation of H_2. In addition, there may have been a small contribution by radiative association of H and D. This differs from H_2 in that the HD molecule has a small dipole moment which makes ground electronic state vibrational transitions permitted (Lepp and Shull 1984). The ionization of D is determined by the charge transfer reaction

$$D + H^+ \rightleftarrows D^+ + H. \qquad \text{(III.39)}$$

This allowed for rapid formation of HD by the process

$$D^+ + H_2 \rightarrow HD + H^+ \qquad \text{(III.40)}$$

after a significant H_2 abundance had been created.

A complete listing of the chemical processes used in this calculation may be found in Table III.1 (Appendix B). The network includes only the elements H, D, and He. Photo and kinetic rates are determined by T_{rad} and T_{mat}, respectively. The time-dependent system of differential equations has been solved using standard techniques over the range of temperature T_{rad} = 20,000 K ($z \approx 7500$) to T_{rad} = 10 K ($z \approx 2.7$). Conservation of charge and total elemental abundances has been maintained at all times. Heating and cooling of the primordial gas has been followed throughout, and the moment of decoupling determined for several different models both with and without "dark" matter.

3.3 RESULTS

The atomic and molecular processes in the expanding Universe around the epoch of recombination have been examined for several different values of the cosmological expansion parameter, both with and without the presence of dark matter. In addition, the effects of differing elemental abundances have been explored. Figures III.1 – III.3 illustrate the variation of abundances with z for several such such models. A number of parameters for each model may be found in Table III.2 along with the final relative abundances of H_2 and HD. The fractional abundances presented are with respect to the total hydrogen in all forms. The calculations were started at $T_{rad} = 20{,}000$ K, just as He^{++} is recombining rapidly to form He^{+}. Primordial elemental abundances most often used in the models are H : He : D = 1.0 : 0.08 : 1.7×10^{-5}. Other elemental abundances were determined by setting $\Omega = \Omega_{bary}$ in the model of Wagoner (1973). It should be noted that the abundance of D as found by this method is inconsistent with the current best estimate of the primordial deuterium fractional abundance of $\gtrsim 10^{-5}$ (Rogerson and York 1973; Vidal-Madjar *et al.* 1983; Laurent 1983) when $\Omega_{bary} \gtrsim 0.25$. These models (6, 8, and 9) are listed for completeness, but will not be discussed at length. Models 12 and 13 are for a $H_o = 100$ universe. The general properties of the models are as follows. The recombination of helium is rapid with the abundances

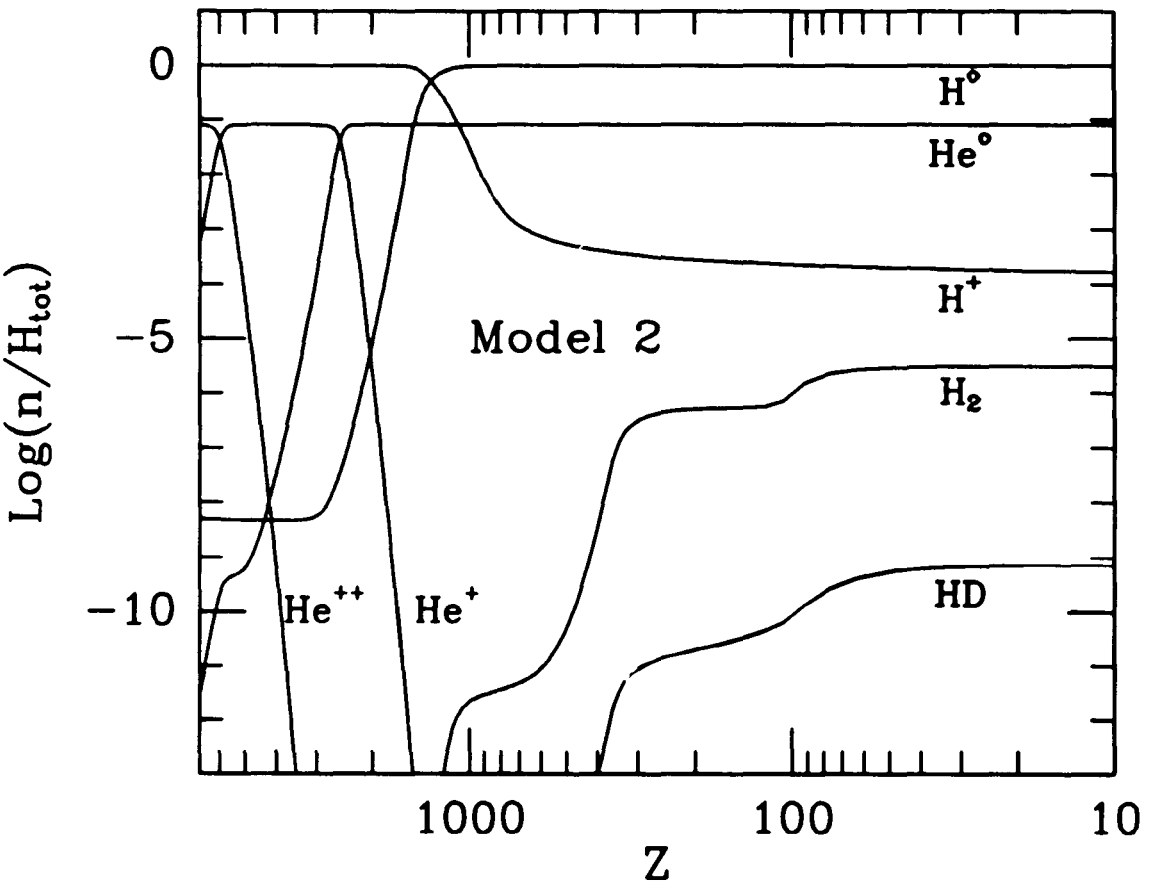

Figure III.1a: The variation in atomic and molecular fractional abundances versus z around the epoch of recombination for a number of species. These are abundances by number relative to hydrogen in all forms. Elemental abundances are H : He : D = 1.0 : 0.080 : 1.7×10^{-5}. For this model $\hat{\Omega}_{tot} = 1.0$ and $\hat{\Omega}_{bary} = 0.1$. The final H_2 fraction is 3.1×10^{-6}, and the final ionization fraction $(n_e/n_H = x_e)$ is 1.8×10^{-4} (Model 2 of Table III.2).

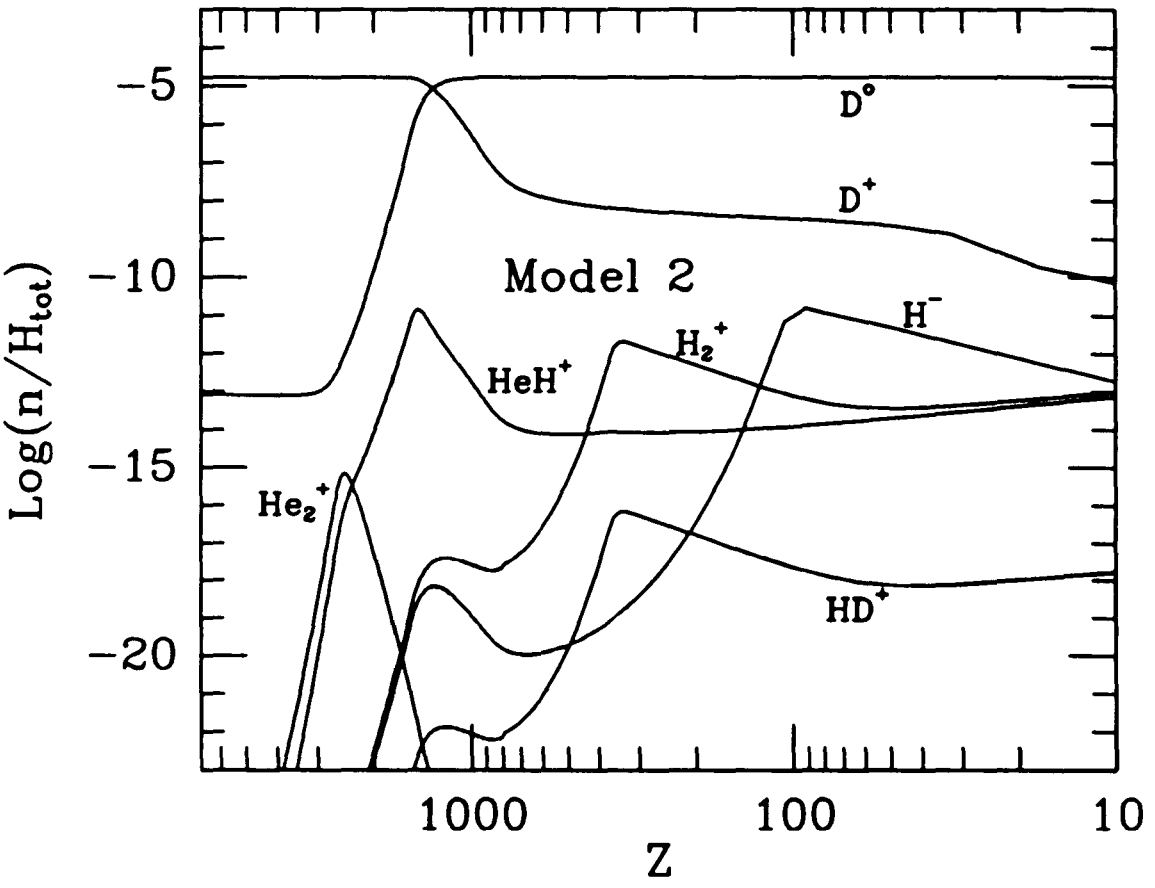

Figure III.1b: Some additional species calculated in the model described in Figure III.1a (Model 2 of Table III.2).

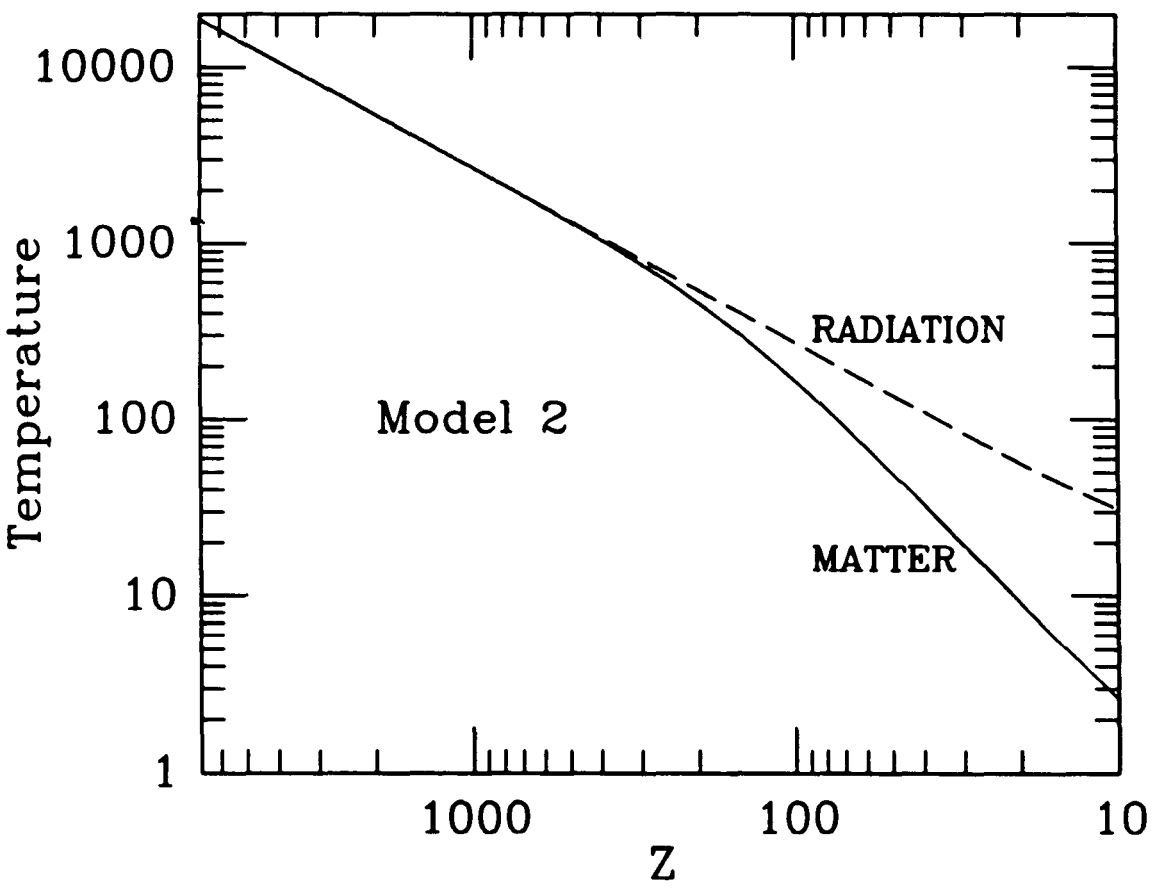

Figure III.1c: The variation of matter temperature and radiation temperature with z in Model 2 of Table III.2. Decoupling occurs at $z = 948$.

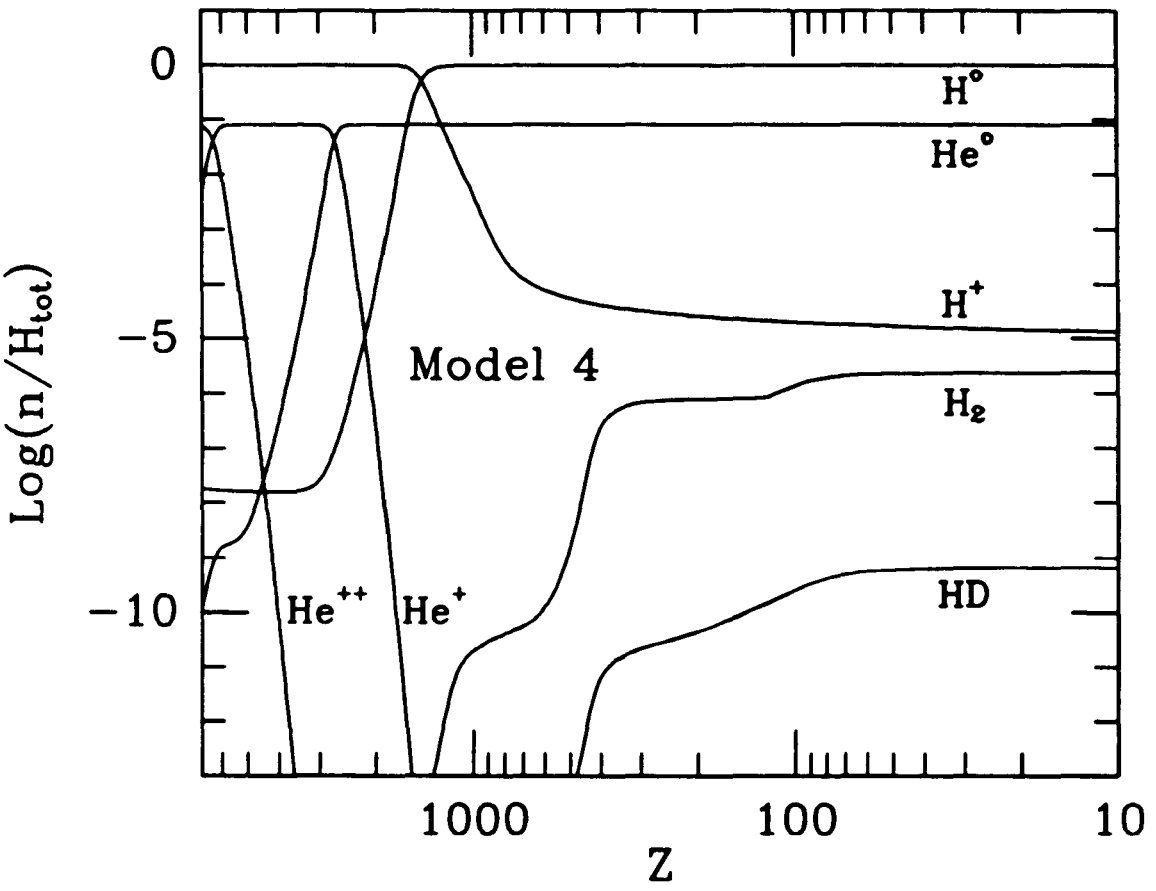

Figure III.2a: The variation in atomic and molecular fractional abundances versus z around the epoch of recombination for a number of species. These are abundances by number relative to hydrogen in all forms. Elemental abundances are H : He : D = 1.0 : 0.080 : 1.7×10^{-5}. For this model $\hat{\Omega}_{tot} = \hat{\Omega}_{bary} = 1.0$. The final H_2 fraction is 2.4×10^{-6}, and the final ionization fraction ($n_e/n_H = x_e$) is 1.4×10^{-5} (Model 4 of Table III.2).

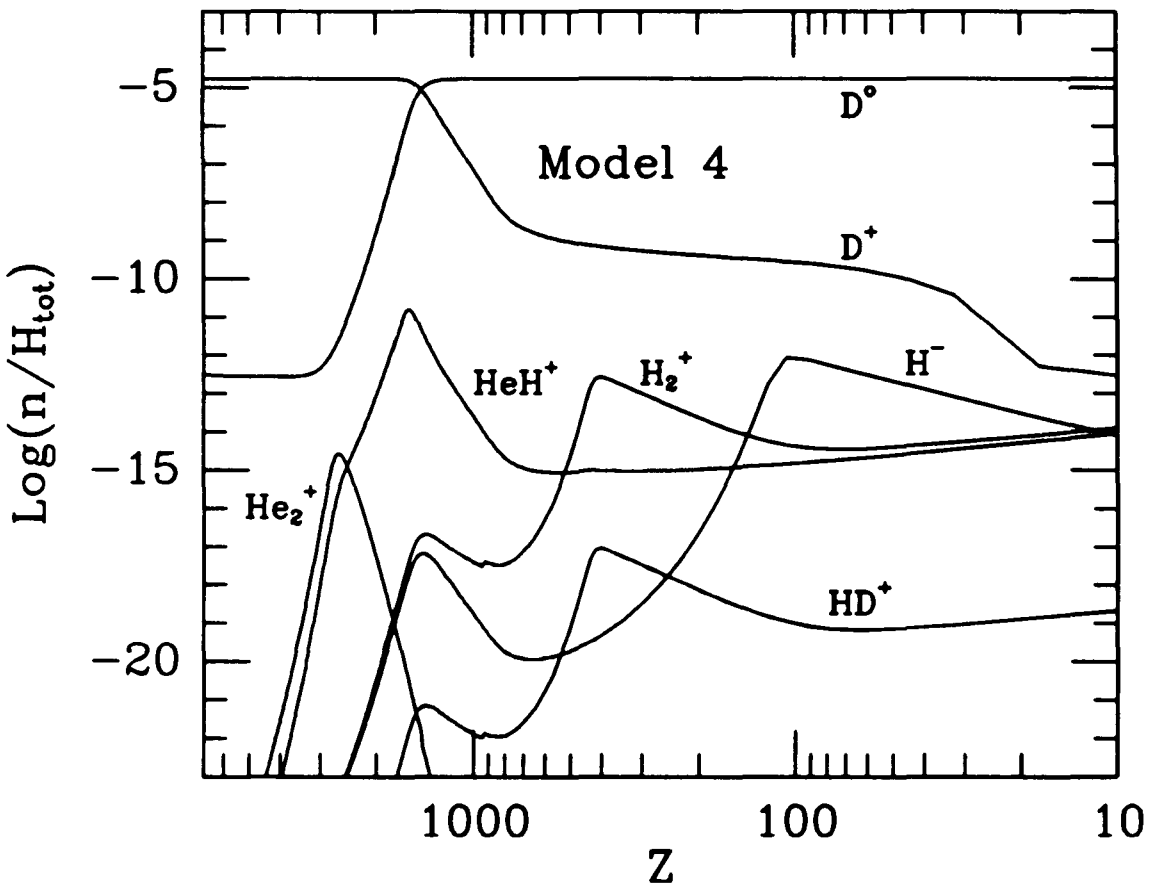

Figure III.2b: Some additional species calculated in the model described in Figure III.2a (Model 4 of Table III.2).

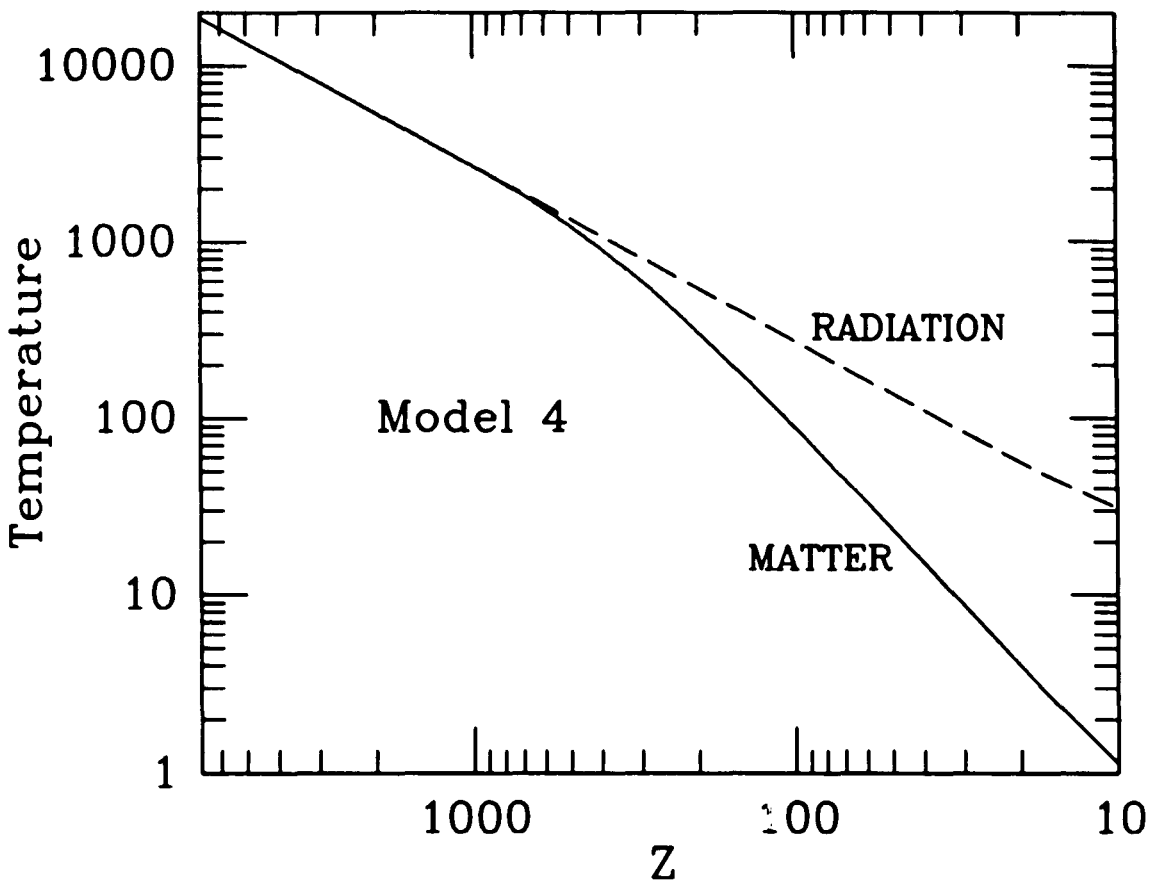

Figure III.2c: The variation of matter temperature and radiation temperature with z in Model 4 of Table III.2. Decoupling occurs at $z = 1075$.

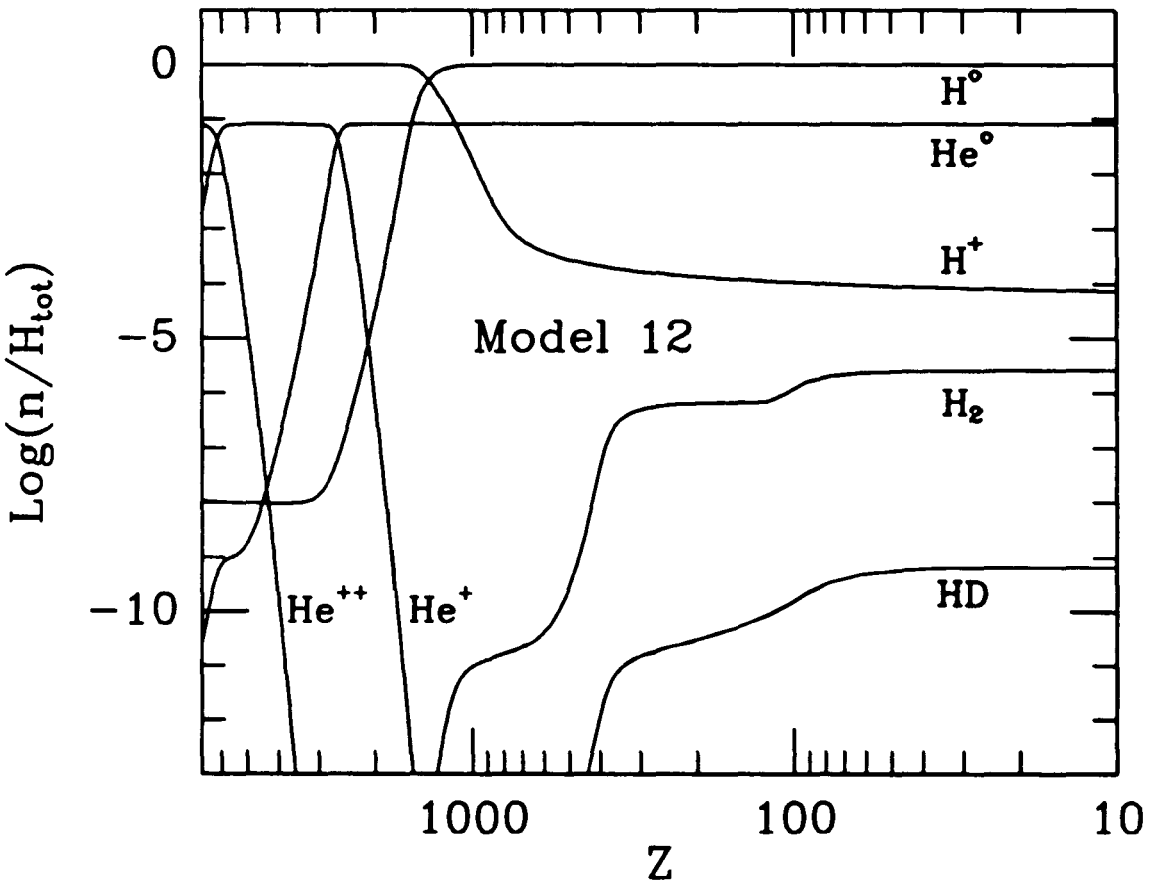

Figure III.3a: The variation in atomic and molecular fractional abundances versus z around the epoch of recombination for a number of species. These are abundances by number relative to hydrogen in all forms. Elemental abundances are H : He : D = 1.0 : 0.080 : 1.7×10^{-5}. For this model $\hat{\Omega}_{tot} = 4.0$ and $\hat{\Omega}_{bary} = 0.4$. The final H_2 fraction is 2.6×10^{-6}, and the final ionization fraction $(n_e/n_H = x_e)$ is 7.8×10^{-5} (Model 12 of Table III.2).

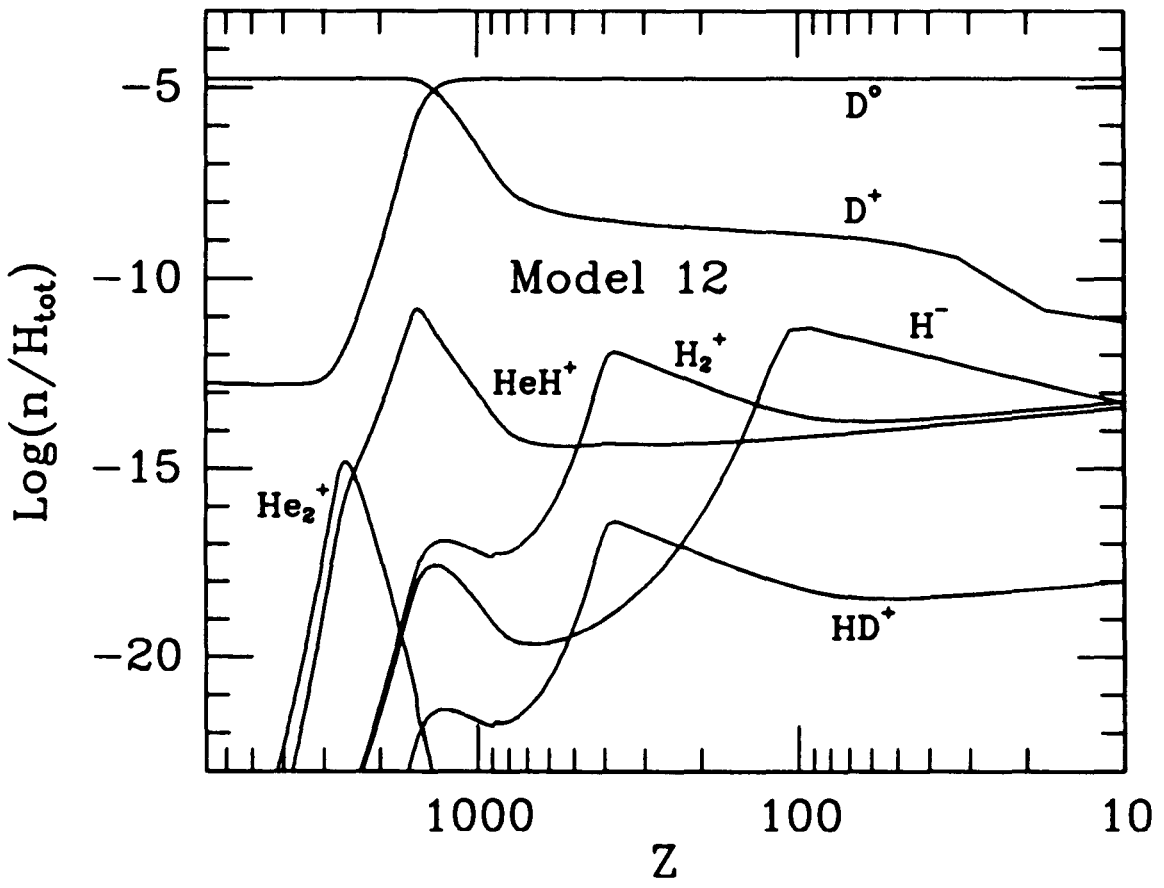

Figure III.3b: Some additional species calculated in the model described in Figure III.3a (Model 12 of Table III.2).

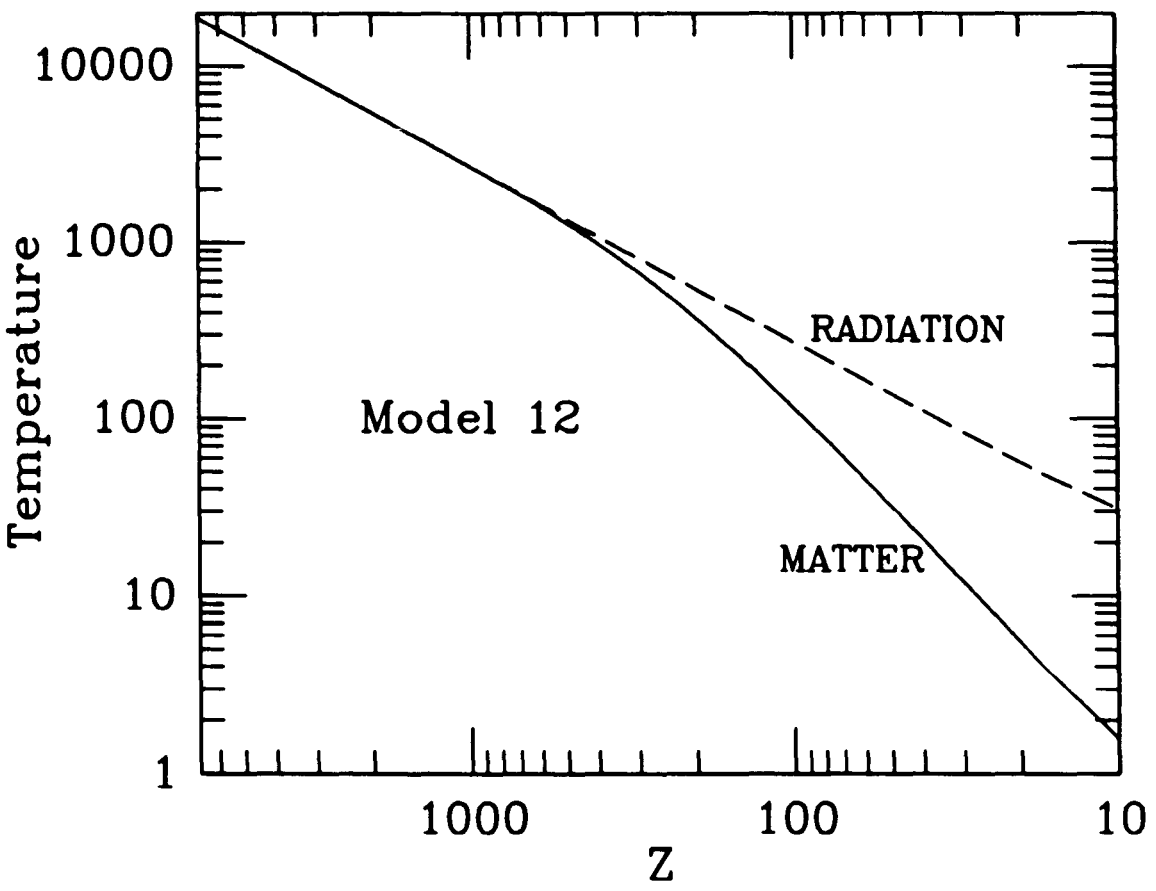

Figure III.3c: The variation of matter temperature and radiation temperature with z in Model 12 of Table III.2. Decoupling occurs at $z = 1025$.

TABLE III.2

Final Abundances[a]

Model	$\hat{\Omega}^b_{tot}$	$\hat{\Omega}^b_{bary}$	n_H (cm^{-3})	x_e	$x(H_2)$	x(HD)	$z_{x_e=0.5}$	z^c_{decple}	M_{Jeans} ($M_\odot$)	T_{mat} (K)	Notes
1	0.1	0.1	1.3(-3)	6.1(-5)	3.6(-6)	8.9(-10)	1340	936	5.1(4)	7.3	d,g
2	1.0	0.1	1.3(-3)	1.8(-4)	3.1(-6)	7.2(-10)	1312	948	4.8(4)	7.1	d,g
3	0.1	0.1	1.3(-3)	6.1(-5)	3.6(-6)	8.9(-10)	1340	936	5.1(4)	7.3	d,h
4	1.0	1.0	1.3(-2)	1.4(-5)	2.4(-6)	6.6(-10)	1442	1075	4.4(3)	3.1	d,g
5	0.5	0.5	6.7(-3)	2.2(-5)	2.6(-6)	6.9(-10)	1411	1030	9.0(3)	4.0	d,g
6	0.5	0.5	6.7(-3)	2.2(-5)	2.6(-6)	2.5(-11)	1410	1029	9.1(3)	4.0	e,g
7	1.0	0.5	6.7(-3)	3.1(-5)	2.6(-6)	6.7(-10)	1402	1032	9.0(3)	3.9	d,g
8	1.0	0.5	6.7(-3)	3.1(-5)	2.6(-6)	2.4(-11)	1401	1031	9.1(3)	4.0	e,g
9	1.0	1.0	1.3(-2)	1.5(-5)	2.4(-6)	4.8(-12)	1440	1073	4.5(3)	3.1	f,g
10	0.5	0.5	6.7(-3)	2.2(-5)	2.6(-6)	6.9(-10)	1411	1030	9.0(3)	4.0	d,h
11	1.0	1.0	1.3(-2)	1.4(-5)	2.4(-6)	6.6(-10)	1442	1075	4.4(3)	3.1	d,h
12	4.0	0.4	5.4(-3)	7.8(-5)	2.6(-6)	6.6(-10)	1363	1025	1.1(4)	4.3	d,g
13	4.0	4.0	5.4(-2)	5.9(-6)	2.2(-6)	7.4(-10)	1503	1172	1.1(3)	2.0	d,g

[a]Final values of density, temperature, and abundances refer to $T_{rad} = 50$ and $z = 17.5$. $T_{rad} = 2.7(1+z)$.

[b]$\hat{\Omega} = \Omega\left(\frac{H_0}{50}\right)^2$; [c]$z_{decple}$ is when $\frac{T_{rad}-T_{mat}}{T_{rad}} > 10^{-4}$.

[d]H : He : D = $1.0 : 0.080 : 1.7 \times 10^{-5}$

[e]H : He : D = $1.0 : 0.085 : 6.1 \times 10^{-7}$

[f]H : He : D = $1.0 : 0.088 : 1.2 \times 10^{-7}$

[g]Ionization function of Peebles (1968)

[h]Ionization function of Jones and Wyse (1985)

of He^{++} and He^{+} decreasing at a rate much faster than the cosmological expansion. The abundance of ionized hydrogen maintains a high level due to the process described by equation (III.11) and the increasing importance of the expansion. H^{+} has reached an asymptotic value by $z \approx 100$ in all models. Deuterium ionization remains much higher than its equilibrium value due to charge transfer with H^{+} (reaction III.39).

Molecule formation is efficient. It is evident that the first molecule to have formed in the early Universe was He_2^{+}. The abundance of He_2^{+} first rises with the increasing presence of He and is rapidly destroyed by photodissociation. Its formation rate drops as He^{+} vanishes. The next molecule to have formed was HeH^{+}, which had an initial peak in abundance due to the radiative association of He and H^{+}. At $z \approx 700$ the abundances of H_2^{+}, H^{-}, HD, and H_2 begin to increase rapidly. The abundance of H_2 rises in steps with the first rise due to the exchange reaction of H with HeH^{+} to form H_2^{+}. This process ceases to be important by $z \approx 600$. Indeed, the earliest formation of molecular hydrogen is dominated for a short time by the excited atom association process (III.38). This period was brief and did not alter the final asymptotic abundance of H_2 in any model (see Figure III.4). The next step is caused by H_2 formation via the H_2^{+} process (III.28) and (III.29). A final rise to an asymptotic abundance as $z \rightarrow 0$ is due to the H^{-} process, (III.33) and (III.34), which becomes effective only when the radiation has become too cold to threaten H^{-} through reaction (III.35). HD follows a similar sequence as a result of reaction (III.40), which is controlled at later times by the molec-

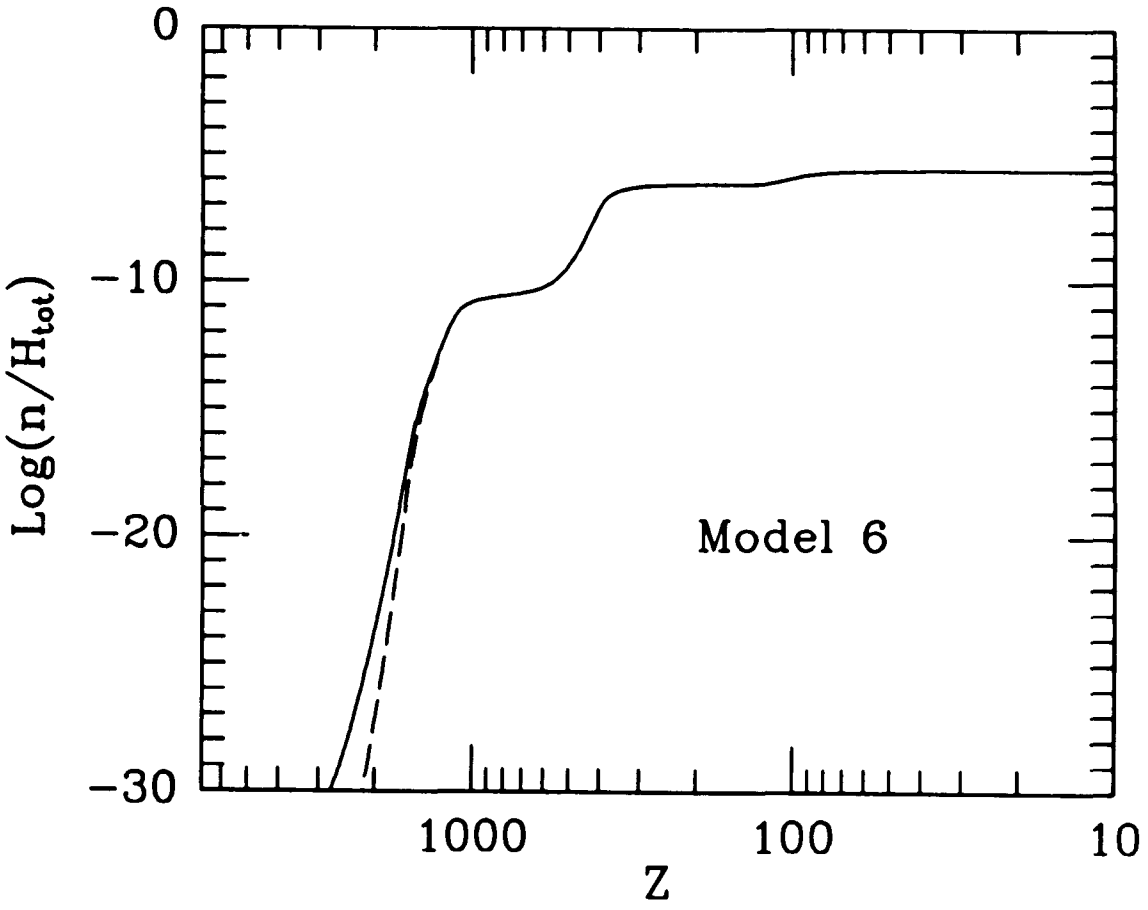

Figure III.4: The variation of molecular hydrogen abundance versus z for Model 6 of Table III.2. This plot demonstrates the relative importance of the excited atom radiative association process to form H_2 (reaction III.38) around the epoch of recombination. The dashed curve has been calculated with the excited atom radiative association process excluded. The solid curve is the result of a calculation which included the excited atom formation process.

ular hydrogen abundance. For completeness and because of its importance to interstellar chemistry, the molecular ion H_3^+ was also followed. As expected for a polyatomic molecule in a very dilute gas, the final abundance of this species is negligible. The power of the cosmological expansion to control the chemistry is evident by the rapid approach to asymptotic abundances of the most important species, H^+, H_2, and HD.

An interesting result appears if the final deuterium hydride to molecular hydrogen ratio is examined. For a particular model (Model 2 of Table III.2), the primordial D/H ratio is 1.7×10^{-5}. Since the formation and destruction processes of H_2^+ and HD^+ are similar and occur at similar rates, it is not surprising to find that $HD^+/H_2^+ = D/H = 1.7 \times 10^{-5}$. However, for the model considered, the HD/H_2 ratio is 2.3×10^{-4}. Thus, HD/H_2 was fractionated in the early Universe by a factor of 13.6 in favor of HD. This is opposite to that found at the present epoch within galactic diffuse clouds. The interstellar HD/H_2 ratio has been observed and modeled to be a factor of $\sim 1 - 30$ less than the cosmic D/H ratio of 1.5×10^{-5} (van Dishoeck and Black 1986). This difference is easily understood. Diffuse clouds are exposed to harsh UV starlight. While the self-shielding of H_2 reduces photodissociation by the interstellar radiation field, self-shielding of HD is inefficient owing to its much lower abundance. The survivability of H_2 in such an environment makes up for the faster formation of HD by processes (III.39) and (III.40). In the early Universe there is no self-shielding from the ambient radiation field, and the dominant destruction prosesses of H_2 are the same as for HD. Thus, the faster formation of HD

raises the HD/H_2 ratio above the primordial D/H ratio. The possiblity of fractionated HD in the early Universe was discussed by Dalgarno and Lepp (1987).

Looking in more detail at Table III.2 quickly reveals that there is no significant difference in the final ionization fraction x_e when the Jones and Wyse (1985) ionization formula is used. This result was not unexpected (see their Table 1). A more important finding is that the final relative H_2 abundance does not vary by more than 39% over the entire list of models. Indeed, all models have an abundance $> 10^{-6}$. The lowest baryon density models (1 and 2) have the largest asymptotic H_2 abundance. This results from a larger ionization fraction leading to a more rapid H^- process in these models. A similar trend is seen in the relative HD abundance, except in Model 13. Here the large HD abundance is a result of the low ionization fraction slowing destruction by electron impact and the reverse of reaction (III.40). The canonical models in which only 10% of the matter is baryonic and the Universe is just closed ($\rho = \rho_{crit}$) are Models 2 and 12. It is interesting to note that these models have the largest final ionization fractions. Recombination and decoupling occur earlier in the higher density model (Model 12). Fractionation of HD is larger in Model 12 than in Model 2 by 8.5%. In general, a larger baryon density results in earlier recombination and decoupling (compare Models 2, 4, and 12). The effect of a slower expansion retarding the recombination can be seen by comparing $z_{x_e=0.5}$ in Models 1 and 2.

The general results found here are similar to those of Lepp and Shull (1984). The final molecular hydrogen abundances determined by this calculation are a factor of $\sim$ 1.8 greater than that of the earlier work. A key difference is that the HD fractionation did not appear in their model.

3.4 DISCUSSION

a) *H_2 and HD as Coolants and Primordial Star Formation*

As we have seen, the net result of atomic and molecular processes around the epoch of recombination is a non-zero asymptotic molecular fraction as $z \rightarrow 0$. Depending on the density parameter Ω, it has been shown that $x(H_2) \sim 2 \times 10^{-6}, x(HD) \sim 7 \times 10^{-10}$, and $x(HeH^+) \sim x(H_2^+) \sim x(H^-) \sim 10^{-13}$. As discussed in an earlier section, the cooling of the material in the early Universe by molecules was calculated explicitly. It was found that for the conditions which may have existed during and just after the recombination, cooling by collisional excitation of rotational and vibrational levels of H_2 never competed with the adiabatic cooling of expansion. At the most favorable time ($z \approx 330$) molecular cooling is 4 orders of magnitude slower than the rate of cooling by expansion. In addition, since decoupling in all of the models occurs well before a significant molecular fraction has formed, the presence of molecular coolants did not alter the moment at which decoupling occurred. However, the persistence of a large ionized fraction after decoupling means that Thomson heating continues to be significant. Indeed, the matter temperature is higher by a factor of ~ 7 for Model 2 and ~ 4 for Model 12 than if only adiabatic cooling had been considered over the range $892 \geq z \geq 17.5$. Thus, the usual picture that adiabatic cooling dominated the matter temperature after decoupling is unchanged by this work. Although heating by electron scattering

after decoupling is small, it may be important if an accurate estimate of the matter temperature is required.

In spite of their lack of importance to the thermal history of the Universe, molecular coolants are vital to the formation of the first stars. Collisional excitation of vibrational and rotational transitions of the molecules created in the early Universe is effective at cooling gas with temperatures from 10^2 to 10^4 K. This is a temperature range where the lowest excited states of H and He are energetically inaccessible. For temperatures below ~ 300 K the lowest H_2 quadrupole transition is ineffective at cooling since it lies 510 K above the ground state (Dalgarno and Wright 1972). At these lower temperatures, the less abundant hydrides HD and LiH are important coolants due to their dipole-allowed transitions. The variation with temperature of cooling due to H, H_2, and HD is displayed in Figure III.5. The abundances and density used are from Model 2. The cooling functions were calculated from the expressions of Dalgarno and McCray (1972) and Hollenbach and McKee (1979). Collision strengths for H excitation by electron impact are from Giovanardi, Natta, and Palla (1987).

The importance of results found in this work become clear if the rate at which a cloud in free–fall collapse must cool to maintain collapse is considered. As discussed by Lepp and Shull (1984) the rate of cooling by molecular hydrogen must exceed the rate of heating by gravitational collapse

$$n(\mathrm{H_2})L(\mathrm{H_2}) \geq \left(\frac{3}{2}\right)\left(\frac{32G\rho}{3\pi}\right)^{\frac{1}{2}} n_H kT, \qquad \text{(III.40)}$$

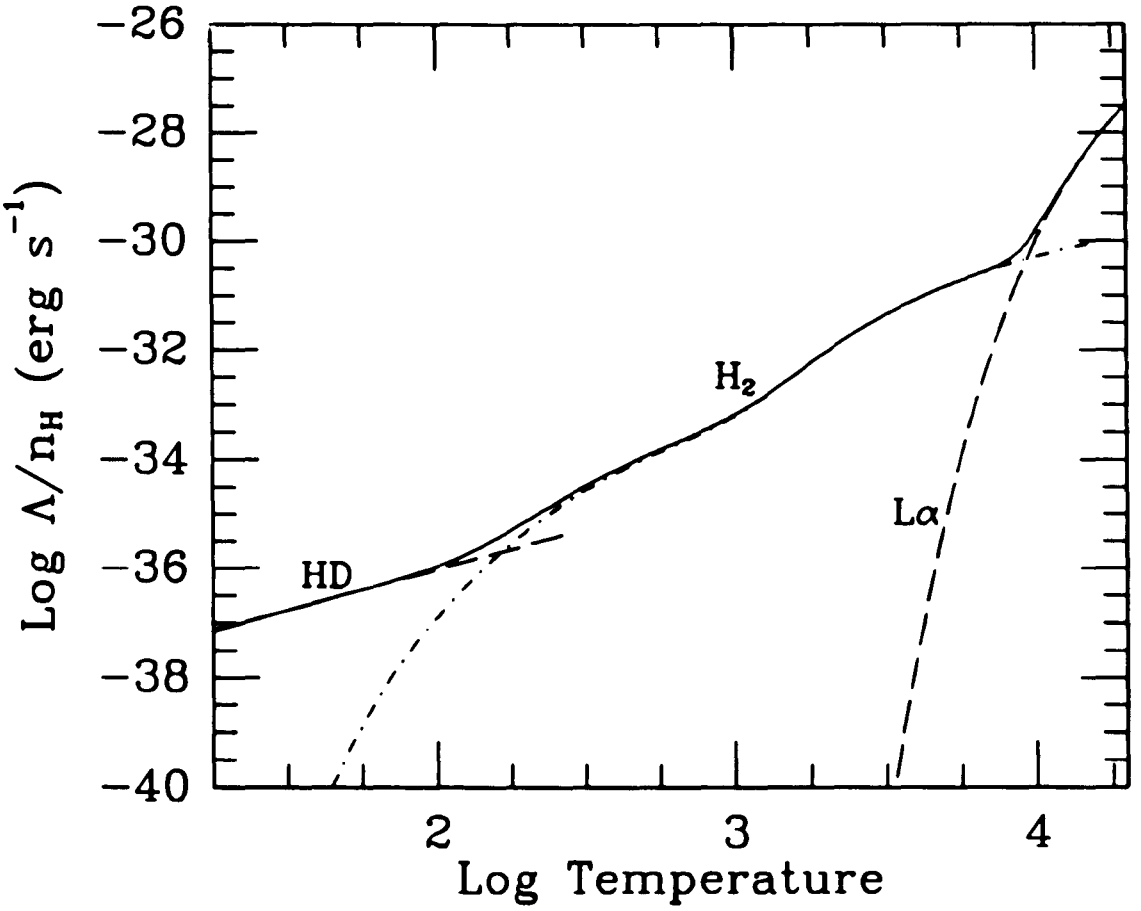

Figure III.5: The variation with temperature of cooling rates due to H, H_2, and HD (see text). The abundances and density are appropriate to Model 2 of Table III.2 at $z = 17.5$.

or

$$x(\mathrm{H_2}) \geq \left(\frac{3}{2}\right)\left(\frac{32G\rho}{3\pi}\right)^{\frac{1}{2}} \frac{kT}{L(\mathrm{H_2})}, \qquad \text{(III.41)}$$

where $L(\mathrm{H_2})$ is the cooling rate per $\mathrm{H_2}$ molecule ($\approx \Lambda_{\mathrm{H_2}}/n(\mathrm{H_2})$ in equation (III.20)). For conditions typical of the early Universe, Lepp and Shull use equation (III.41) to show that a cloud in adiabatic collapse requires $x(\mathrm{H_2}) \geq 10^{-6}$ in order to radiate away the gravitational potential energy released during collapse. It is important to note that every model computed in this work safely exceeds that limiting abundance for $z < 200$.

Molecular cooling at low temperatures can affect the value of the Jeans mass (the mass at which gas pressure can no longer prevent gravitational collapse),

$$M_{Jeans} = 94.0 T_{mat}^{\frac{3}{2}} n_H^{-\frac{1}{2}} \quad M_\odot, \qquad \text{(III.42)}$$

by lowering the temperature in a parcel of gas. The calculated Jeans mass at $z = 17.5$ is displayed in Table III.2 for each model. The value at earlier epochs can be determined by using $T_{mat} \propto (1+z)^2$ after decoupling, $T_{mat} = T_{rad} \propto (1+z)$ before decoupling, and $n_H \propto (1+z)^3$. Thus, fragmentation of a Jeans unstable clump can occur if low temperature cooling is efficient. It is unclear whether fragmentation can continue to stellar mass scales in this simple scenario. However, the initial raw material containing a molecular fraction of species which can radiate effectively to low temperatures is provided just after the Universe recombined. As a collapsing condensation forms, its density will

rise and molecule formation will begin again. Indeed, three-body processes

$$H + H + H \rightarrow H + H_2$$
$$H + H + H_2 \rightarrow H_2 + H_2 \qquad \text{(III.43)}$$

become increasingly important for densities $> 10^9$ cm^{-3}. It has been shown that conversion of H into molecular form by these processes can be complete (Palla, Salpeter, and Stahler 1983) as can the conversion of D into HD (Palla and Zinnecker 1987). The atomic and molecular processes which take place in collapsing clouds of primordial abundance have been discussed by others (Palla, Salpeter, and Stahler 1983; Lepp and Shull 1984; Palla and Zinnecker 1987; Dalgarno and Lepp 1987). An important result of this work is that the conclusion of Lepp and Shull has been confirmed. There would have been sufficient molecule formation during the epoch of recombination to allow for the initial collapse of primordial clouds.

b) *Damping of Fluctuations Prior to Decoupling*

An intriguing feature of the recombination models calculated as part of this work is that there is a small, but non-negligible neutral fraction of atomic hydrogen before the "recombination" begins (see Figures III.1 - III.3). As shown by the partition function, the number of possible states in which a hydrogen atom can exist increases with temperature within the relatively low density environment of the Universe just before recombination. The fact that the ionization fraction appears to be constant is a consquence of the partition function varying at a rate similar to that of the expansion. Prior to recombination, the ionization is described by the Saha formula (III.9). For the

neutral fraction to be constant with z, $n_e n_{H^+}/n_H \propto T_{mat}^3$. By comparing the dominant terms in equations (III.25 – III.27) as given by Fischel and Sparks (1971) it is found that such a relation does indeed approximately hold, at least as long as the assumptions that went into determining the partition function remain valid. Breakdown would clearly occur in the extremely high density and temperature of the very early Universe.

Since a neutral hydrogen atom in an excited state has a large cross section for continuum (bound – free) absorption, it seems reasonable to assess the impact such absorption may have had on the damping of adiabatic fluctuations just before recombination. It is noted at the outset that this previously unexplored damping source is shown by a simple calculation to be negligible. However, because of its importance to the formation of structure, the primary cause of damping (Silk damping) will be described. How neutral hydrogen may have played a role can then be seen.

It is not known at what time inhomogeneities which led to galaxy and star formation in the primordial Universe arose. For large scale structures of the type observed today to have been generated by gravitational attraction, the degree of inhomogeneity need not have been large. It seems likely that any non-uniformities developed early in the history of the Universe (an alternative will be discussed in the following section). Such fluctuations could not have been static. The competition between gravity and pressure would have resulted in an inhomogeneity which oscillated and propagated through the plasma much like a sound wave. For $z > z_{decouple}$ such acoustic oscillations can be damped

by photon diffusion through baryons (Börner 1988 and references therein). Photons with a mean free path for interaction with the matter greater than the size of the fluctuation can escape, reducing the effectiveness of the radiation field to maintain an oscillation.

During the epoch prior to decoupling the strongest interaction between radiation and matter was through Thomson scattering. The photon mean free path is

$$\lambda_T = (n_e \sigma_T)^{-1} = c\tau_o, \tag{III.44}$$

where σ_T is the Thomson cross section ($= 6.652453 \times 10^{-25}$ cm^2) and τ_o is the mean free time to Thomson scattering. The diffusion time of an adiabatic oscillation of wavelength λ is then

$$\tau_D = \left(\frac{\lambda}{\lambda_T}\right)^2 \tau_o = \frac{\lambda^2}{c\lambda_T}. \tag{III.45}$$

If λ is such that τ_D is less than the age of the Universe at decoupling then the oscillation will have been strongly damped. This gives a characteristic minimum wavelength for inhomogeneities which may have survived through decoupling of

$$\lambda \gtrsim \left(c\lambda_T t_{decouple}\right)^{\frac{1}{2}}. \tag{III.46}$$

In Model 2 of Table III.2 this turns out to be $\sim .2$ Mpc. Therefore, the only fluctuations to survive the dissipative forces in the Universe prior to decoupling would have been of galaxy cluster size or larger.

If bound - free absorption by neutral hydrogen had been important, then damping would have been reduced by an effective decrease in the mean

free path for interaction. Therefore, surviving fluctuations would have been smaller than in the case where electron scattering dominates. During the earliest history of the Universe, coupling between matter and radiation was so strong that damping by photon diffusion was slow. It is therefore only important to examine damping during the period just before decoupling. Thus, the details of the atomic physics which has gone into determining the ionization fraction will remain valid. If the impact of neutral hydrogen on photon diffusion is important then the damping length for pure electron scattering in a time t will be altered such that $\lambda = \lambda_o(\tau/\tau_o)^{1/2}$, where τ_o is the mean free time for Thomson scattering only and

$$\frac{\tau_o}{\tau} = \frac{(n_e\sigma_T)^{-1}\int_0^\infty d\nu B_\nu(T_{rad})}{\int_0^\infty d\nu B_\nu(T_{rad})\left(n_e\sigma_T + \sum_{states} n_{Hi}\sigma_{\nu i}\right)^{-1}}. \qquad \text{(III.47)}$$

$B_\nu(T_{rad})$ is the Planck function for a blackbody radiation field. The cross section for bound – free absorption of a photon with frequency ν by an atom in principal quantum level n is

$$\sigma_{\nu n} = \frac{512\pi^7 me^{10}}{3\sqrt{3}ch^6n^5}\frac{g(\nu,n)}{(2\pi\nu)^3}, \qquad \text{(III.48)}$$

where $g(\nu,n)$ is the bound – free gaunt factor. It is of interest to determine how the ratio τ_o/τ evolves with time up to the point of recombination.

Equation (III.47) was solved in a straight forward manner by numerically integrating the denominator. Thermodynamic equalibrium was assumed in determining populations in excited states and ionization. Gaunt factors are from Karzas and Latter (1961). Truncation of the sum over states was deter-

mined by the method of Dickinson (1971). Several values of Ω_{tot} and Ω_{bary} were tested.

The result is not surprising. The ratio τ_o/τ does not differ from unity by more than a few parts in 10^5 for much of the period prior to recombination. The situation is not altered significantly if the neutral fraction is arbitrarily increased by 3 orders of magnitude. While there may have been large numbers of neutral atoms, there were few in the important excited levels as the plasma approached recombination. Thus, a strong interaction between neutral hydrogen and radiation could not have taken place. The damping length for any adiabatic fluctuations which may have existed prior to decoupling was clearly dominated by electron scattering. Helium was completely neutral by this time. But, the threshold for bound – free absorption by helium made such transitions energetically inaccessible.

c) *A Possible Instability at Recombination*

In the previous section the origin of fluctuations in a structure–free primordial universe was ignored. The extreme uniformity of the Universe in the standard big bang model makes difficult the identification of an instability which could have generated even star sized structures. An inflationary scenario helps on large scales, since small fluctuations would have been diffused away. Invoking exotic physics is unsatisfying. Clearly, the matter will not be settled here. In a recent work, Hogan (1989) suggested that a radiation driven instability may have arisen as the recombination of hydrogen commenced. He also

demonstrated that this instability would have been damped for finite wavelength perturbations. Since this work has dealt with the epoch of recombination in some detail, it seems reasonable to review the work of Hogan. This discussion should make clear why a detailed examination into the microphysics of the helium recombination may be important.

The instability is straightforward to describe. As the recombination begins, Lα photons are produced in great numbers. A region adiabatically expanding faster than the surrounding plasma will recombine at a higher rate, generating even more Lα photons. These photons contribute on the order of 5 times more pressure than the electrons and protons which produced the photons. It can now be seen how the pressure of a lower density region can exceed that of the surrounding medium. The result may have been a rapidly growing instability. In order for this instability to work the effective compressibility $dp/d\rho$ must go negative. Using the equations of Peebles (1968), Hogan has shown that such a condition did indeed exist at the onset of hydrogen recombination. The compressibility due to Lα photons is

$$\frac{dp_\alpha}{dp} = \frac{8\pi E_\alpha \sigma}{3m_p \lambda_\alpha^3} \frac{dN_\alpha}{dn}, \tag{III.49}$$

where σ is the Lα line width, E_α is the energy of a Lα photon, and N_α is the number of photons per mode in the Lα resonance line as given by Peebles. As the recombination begins, the dominant term in the derivative can be shown to be

$$\frac{dN_\alpha}{dn} \approx -e^{\frac{E_2}{kT_{rad}}} \frac{h^3}{(2\pi m_e kT_{rad})^{\frac{3}{2}}} \frac{n_e^2}{n_H n_{1s}} \frac{E_2}{kT_{rad}} \frac{d\ln T_{rad}}{d\ln n_H}. \tag{III.50}$$

Thus, for parameters appropriate at $z \approx 1600$, the compressibility turns out to be of the order -1.7×10^{14} cm^2 s^{-2}.

The instability remains when subjected to a linear analysis which includes the important radiation damping terms. The growth of the instability will not be damped by radiation drag for scales smaller than

$$\lambda_d \lesssim \frac{3\pi m_e |c_s|}{2\rho_\gamma c \sigma_T}, \tag{III.51}$$

where c_s is the sound speed (which is now imaginary). This length is about 2×10^{18} cm which encloses a mass of $\approx 50\ M_\odot$.

The instability is shown to fail because, in this context, the net recombination rate is governed by Balmer continuum photons, not the trapped Lyman continuum. The main opacity source in the Balmer continuum is Thomson scattering, which is optically thin for a path length of 10^{18} cm. Thus, the radiation temperature at Balmer frequencies is isothermal for the undamped scales of less than 10^{18} cm. The critical condition for the instability to work is that the radiation which controls the recombination must adjust its temperature adiabatically with the matter.

The physical processes in the early Universe seem to have once again conspired to stop an instability which may have led to the formation of the first stars. As discussed earlier, the helium recombination occurred rapidly and may have been influenced by metastable states in a manner similar to hydrogen. It is easy to imagine that the instability described here may have an analogy during helium recombination. In this earlier epoch of higher temperatures, photon

opacities may have been large enough to allow an instability to grow without being terminally damped. It appears that there is now strong motivation for a detailed examination into the microphysics of the helium recombination epoch.

3.5 SUMMARY

In this chapter the atomic and molecular processes around the epoch of recombination in the early Universe have been examined. The results from detailed integrations of these processes through the recombination period have been presented. In addition, some of the implications of these results were discussed. To summarize, it was shown that:

1) Molecule formation at the epoch of recombination in the early Universe was efficient. The first molecule to have formed was He_2^+ followed by HeH^+.

2) HD/H_2 was fractionated by a factor of $\sim$ 13.6 over the primordial D/H ratio.

3) In order to assess the contribution to cooling in the early Universe by molecules, the cooling rate was explicitly calculated. The most important heating and cooling processes were included. It was found that cooling by collisional excitation of molecular hydrogen never competed with the adiabatic cooling of expansion. In addition, the moment of decoupling was not altered by the presence of molecular coolants.

4) The persistence of a large ionized fraction after decoupling meant that Thomson heating continued to be significant. It was shown that the matter temperature remains higher by a small factor than if only adiabatic cooling is considered.

5) An important result is that, in every recombination model calculated, the asymptotic molecular hydrogen abundance relative to the total hydrogen is $> 10^{-6}$. This minimum abundance of H_2 was required to provide sufficient cooling of gravitationally unstable regions for the initial collapse to continue. Without an initial abundance of molecular coolants, a collapsing region would be halted before renewed molecule formation could begin.

6) It was shown that a small neutral atomic hydrogen fraction before recombination did not influence the damping of adiabatic fluctuations prior to decoupling.

7) The possibility of a radiation driven instability during the helium recombination epoch was considered.

Acknowlegments: I cannot end this chapter without thanking John Black and Craig Hogan. John provided the initial idea for the work presented here. If there is anything worthwhile contained in this chapter, it is because of him. Craig's enthusiasm for new and different ideas is contagious. Much of this chapter is a direct result of his search for something new. Unfortunately none of it worked!

CHAPTER 4

CHEMICAL EVOLUTION IN THE EXPANDING ENVELOPE OF SN 1987A

4.1 INTRODUCTION

When the explosion of Supernova 1987A was detected on 1987 February 23, it quickly became the most exciting and studied object in the sky. For the first time, atomic and molecular processes which take place within the expanding ejecta of a supernova have been observable in detail. The first detection of a molecule in a supernova came with the identification of CO emission in the infrared spectrum of SN 1987A (Catchpole and Glass 1987; Oliva, Moorwood, and Danziger 1987; Danziger *et al.* 1988; Elias *et al.* 1988; Spyromilio *et al.* 1988). In addition, observations of CO^+, SiO, and CS have recently been claimed (see Meikle *et al.* 1989).

The fundamental ($\Delta v = 1$, $\lambda 4.6$ μm) and first overtone ($\Delta v = 2$, $\lambda 2.3$ μm) bands of carbon monoxide have been prominent features in the infrared spectrum of SN 1987A. Although highly broadened by expansion, these

features are sufficiently strong that detailed analyses can be made, resulting in a knowledge of the physical characteristics in the emitting region (*e.g.* McCray 1989). Due to the paucity of relatively nearby supernovae, such studies of molecular emission have not previously been possible. Indeed, it was not entirely expected that such emission would be observed arising from the harsh environment of a supernova.

In addition to the use of molecules as probes of temperature, density, and velocity within the supernova, SN 1987A provides a unique environment in which to study rapidly evolving chemical processes. The elemental abundances are highly stratified and hydrogen poor in the inner regions. The expansion velocity is large and cooling is fast. As will be discussed in more detail later in this chapter, the chemistry of such an environment will likely be much different from that found in the more general interstellar medium. Aside from abundance variations, molecular processes within supernovae resemble the chemistry of strong shocks. There are significant differences, however. For example, in the core of a supernova, little or no hydrogen is expected. The usual routes for CO formation require the presence of hydrogen bearing molecules. For this reason, it is difficult to understand how CO can be present in the abundance implied by observation.

Due to the importance of SN 1987A, study of its characteristics has been intense and the literature into its every aspect has been voluminous. Reviews of some of this material have been presented by McCray (1989) and McCray and Li (1989). Summaries of infrared observations, in which molecular

emission is present, have been compiled by Meikle *et al.* (1989) and Bouchet *et al.* (1989).

Since it may be possible to use molecular emission as a diagnostic probe of the evolution of SN 1987A, it seems prudent to attempt to model the time-dependent chemistry of the expanding envelope. The exploration of molecules in supernovae is just beginning. McCray (1989) and Petuchowski *et al.* (1989) have examined molecular processes in the hydrogen-poor inner regions of the ejecta. In this chapter, we consider the formation and destruction processes of molecules in the rapidly expanding outer envelope of SN 1987A. Using a simple model, we find that large abundances of molecules, in particular CO, form rapidly after the recombination front passes. Indeed, with reasonable abundances for the outer envelope, CO should be the dominant molecular species while hydrogen remains mostly in atomic form.

4.2 THE MODELING METHOD

a) *The Physical Model*

We have used the simplest, physically realistic model available to represent the supernova. As described by McCray and Li (1989), the supernova may be approximated by a homologously expanding sphere. The radius of the outer surface is given by $R(t) = 3.5 \times 10^{13} t_{day}(E_{51}/M_{10})$ cm and is assumed to expand at the velocity $V_{outer} = 4100(E_{51}/M_{10})$ km s^{-1}, where E_{51} is the energy deposited in the envelope in units of 10^{51} ergs and M_{10} is the envelope mass in units of 10 solar masses. The total number density is given approximately by $n(t) = 6.47 \times 10^{16} t_{day}^{-3} E_{51}^{-3/2} M_{10}^{5/2}$ cm^{-3}. We assume $E_{51} = M_{10} = 1$. The velocity of a gas element interior to the surface is given by $v(r) = [r/R(t)]V_{outer}$ km s^{-1}. For this work we have considered only the outer mantle and envelope. This is a region with $v \gtrsim 2000$ km s^{-1} and $M \approx 8\ M_{\odot}$ (McCray 1989). We assume free expansion and ignore interactions with circumstellar material. At later times, such assumptions will not be justified. In addition, we have not included dust formation in the model. There is little evidence for such a process having taken place in the first two years since the explosion (see, however, Smith, James, and Aitken 1988 and Dwek 1989).

The aims of a simple model are to establish the general properties of the chemistry and to identify the diagnostics that may be used for continued study of the supernova evolution. Several key parameters remain uncertain. These

include the kinetic temperature of the gas, the radiation field in the envelope, ionization by energetic particles, and the possible stratification of elemental abundances. We have used the model to assess the sensitivity of molecule formation to each of these parameters over a broad range. We note that if there exist sources of dissociating radiation within the envelope itself, then the molecular destruction rates considered here will have been underestimated. This must be considered a key uncertainty of the simple model.

Initially, the entire envelope is ionized after the shock front passes through. As the gas cools, by radiation losses and expansion, a recombination front begins to form in the outer regions and propagates inward through the expanding material (Falk and Arnett 1977; McCray 1989). The calculation is begun at this time, when the density is high enough that the initial ionization balance approaches LTE conditions. From this initial state, the molecular formation and destruction processes in a parcel of gas are followed as the density drops and the temperature and radiation field vary.

b) *The Chemical Network and Method of Calculation*

While it is possible to maintain a simple model for the physical structure of SN 1987A, it is also necessary that the routes for chemical reactions be complete for a wide range of temperature and density. Throughout the time of expansion explored, the density remains high enough ($10^8 - 10^{11}$ cm^{-3}) that binary gas phase reactions are rapid compared with expansion. Three-body

processes, while included for completeness at the highest densities, are not significant. During the earliest stages of molecule formation, high temperature neutral – neutral reactions and ion – molecule reactions dominate the chemistry.

As pointed out by Lepp, Dalgarno, and McCray (1988), an important route to CO formation in the supernova may be the radiative association process

$$C^+ + O \rightarrow CO^+ + h\nu \qquad \text{(IV.1)}$$

followed by the charge transfer reaction

$$CO^+ + O \rightarrow CO + O^+. \qquad \text{(IV.2)}$$

While this mechanism is likely to be important in regions of low hydrogen abundance, such as the core, it will compete with

$$C^+ + OH \rightarrow CO^+ + H \qquad \text{(IV.3)}$$

and

$$CH^+ + O \rightarrow CO^+ + H \qquad \text{(IV.4)}$$

followed by

$$CO^+ + H \rightarrow CO + H^+ \qquad \text{(IV.5)}$$

in regions where hydrogen is abundant.

Since the thermal rate coefficient of reaction (IV.1) has not been determined by a quantal calculation, we carried out a semi-classical calculation using the method of Bates (1951a; see Chapter 2) in order to estimate its value. We found in Chapter 2 that $k_{IV.1} \approx 5 \times 10^{-19}[\ln(T_{kinetic}) - 1.91]$ cm^3 s^{-1}

($50 \leq T_{kinetic} \leq 5000$ K; see Table II.2). The rate coefficients for (IV.3) and (IV.4) are $k_{IV.3} = 8.0 \times 10^{-10}$ cm^3 s^{-1} and $k_{IV.4} = 3.4 \times 10^{-10}$ cm^3 s^{-1}, respectively. Therefore, reactions (IV.3) and (IV.4) will dominate in regions of even modest OH and CH^+ abundance.

If grain surface processes are absent and electrons and protons are present, molecular hydrogen can be formed via the H_2^+ process

$$H + H^+ \rightarrow H_2^+ + h\nu \qquad \text{(IV.6)}$$

$$H_2^+ + H \rightarrow H_2 + H^+. \qquad \text{(IV.7)}$$

If neutral hydrogen and electrons coexist, then the H^- process will form H_2:

$$H + e^- \rightarrow H^- + h\nu \qquad \text{(IV.8)}$$

$$H^- + H \rightarrow H_2 + e^-. \qquad \text{(IV.9)}$$

Silicon monoxide is formed via

$$Si + OH \rightarrow SiO + H \qquad \text{(IV.10)}$$

and is destroyed by the charge transfer reaction

$$SiO + H^+ \rightarrow SiO^+ + H. \qquad \text{(IV.11)}$$

After the ejecta have become primarily neutral through recombination, self-shielding, and reduction of the radiation field, CO synthesis proceeds primarily by

$$C + OH \rightarrow CO + H \qquad \text{(IV.12)}$$

and

$$O + CH \rightarrow CO + H, \qquad \text{(IV.13)}$$

if the region is not depleted in hydrogen. Photodissociation of CO occurs through absorption of discrete ultraviolet photons to predissociating states (van Dishoeck and Black 1988; Mamon, Glassgold, and Huggins 1988; Viala *et al.* 1988) at wavelengths $\lambda > 912$ Å. This process is rapidly self-shielding for even small column densities of CO. Other CO destruction routes are slow or cause no net loss by cycling back to CO with high probability.

Throughout the calculation, we keep track of 31 chemical species, 13 neutral and 18 ionic. The species considered contain H, He, C, O, and Si. A total of 171 reactions is incorporated (see Table IV.1 in Appendix B). Self-shielding of C and Si is explicitly calculated. This time-dependent calculation requires the simultaneous solution of a system of stiff differential equations, for which we have chosen the Gear method (Gear 1971) and a well tested algorithm. Conservation of charge and total elemental abundances are maintained at all times.

4.3 RESULTS

We have examined molecule formation in the envelope for different cooling rates and elemental abundances. Figure IV.1 illustrates the temporal variation of abundances (relative to the total hydrogen) for one such model. In this case, the elemental abundances are appropriate for the Large Magellenic Cloud with the observed oxygen enhancement from Fransson *et al.* (1989). The envelope cools adiabatically with expansion. The figure shows that the abundances of CO, H_2, and OH increase rapidly, with CO and H_2 reaching asymptotic abundances by $\sim$ 200 days. Following an initial rise and decline, the abundances of CH and HCO^+ continue to increase throughout the calculation. The abundance of OH is limited by charge transfer with H^+ and reaches a final relative abundance of 3.4×10^{-11}. We have explored both Case B and Case C recombination of hydrogen by using the appropriate rate coefficients for radiative recombination (Osterbrock 1974; McCray 1989). The difference was found to be negligible within the uncertainties of this calculation.

In the model of Figure IV.1 the final CO abundance is approximately a factor of two larger than that of molecular hydrogen. Most of the atomic carbon and a large fraction of the atomic oxygen are converted into CO. Most of the hydrogen remains in atomic form, however. The formation of H_2 is inhibited by slow reactions (IV.6–IV.9) while CO is formed rapidly and not

readily destroyed. Throughout the expansion H^+ is the dominant ion. A final ionization fraction of 3.0×10^{-6} is achieved by 400 days after the blast.

Self-shielding of carbon from the photospheric radiation field is effective. As a result, photoionization of carbon is not an important source of C^+. On the other hand, silicon is found to be only marginally self-shielding owing to its lower abundance. Thus, the onset of self-shielding is strongly dependent on abundance. For the models decribed here, silicon was constrained to be self-shielding at the outset (*i.e.* photoionization of silicon was ignored). However, it is likely that inhomogeneities in the real supernova ejecta will cause regions to exist with little, or no self-shielding. At early times this may have resulted in variations in Si^+ abundances in the envelope of several orders of magnitude. Since SiO is formed primarily via (IV.10), this may have led to regions of negligible SiO abundance. For the model shown, SiO reaches a maximum relative abundance of $\sim 4.7 \times 10^{-10}$ at $\sim$ 220 days and then declines to an asymptotic value of 7.5×10^{-12}.

The same qualitative properties of molecule formation are found if the hydrogen abundance is reduced. Figure IV.2 shows the results of a calculation in which hydrogen was depleted by a factor of 1000 from that of the model shown in Figure IV.1. Again, carbon monoxide is the dominant molecular species with H_2 nearly two orders of magnitude less abundant. In this case, however, CO reaches an asymptotic limit in abundance well before it incorporates all of the carbon available. When H is depleted, He competes more effectively for H^+ through radiative association. As a result, HeH^+ appears

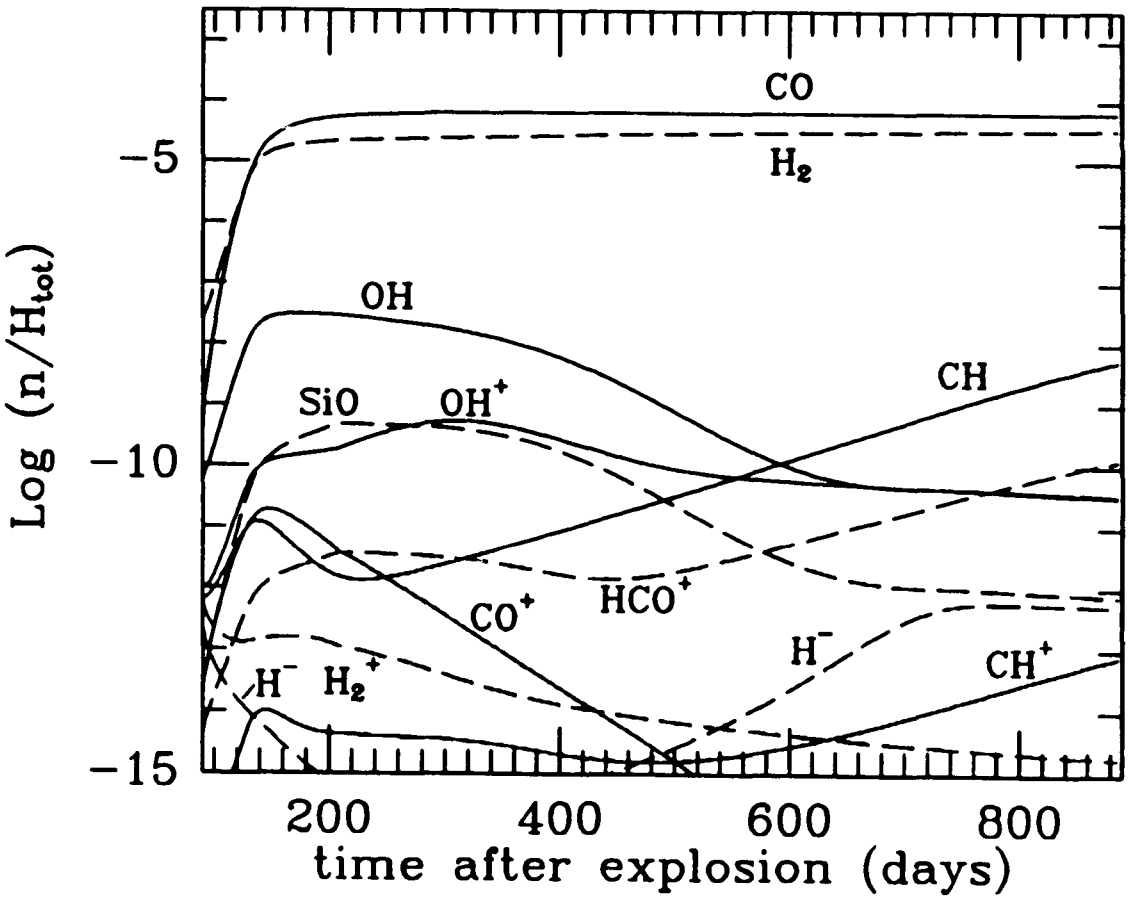

Figure IV.1: Molecular abundances versus time (in days) after detonation of SN 1987A. These are abundances by number relative to hydrogen in all forms. Elemental adundances are 0.25 times solar with O enhanced. This model has no hydrogen depletion. Cooling is adiabatic with initial temperature and total number density of T_o = 5000 K and n_o = 10^{11} cm^{-3}, respectively. Initial density of hydrogen nuclei in all forms is $n_H(initial)$ = 9.0×10^{10} cm^{-3}. Final values of temperature and total hydrogen density are $T(final)$ = 225 K and $n_H(final)$ = 8.3×10^7 cm^{-3} at 887 days (Model 1 of Table IV.2).

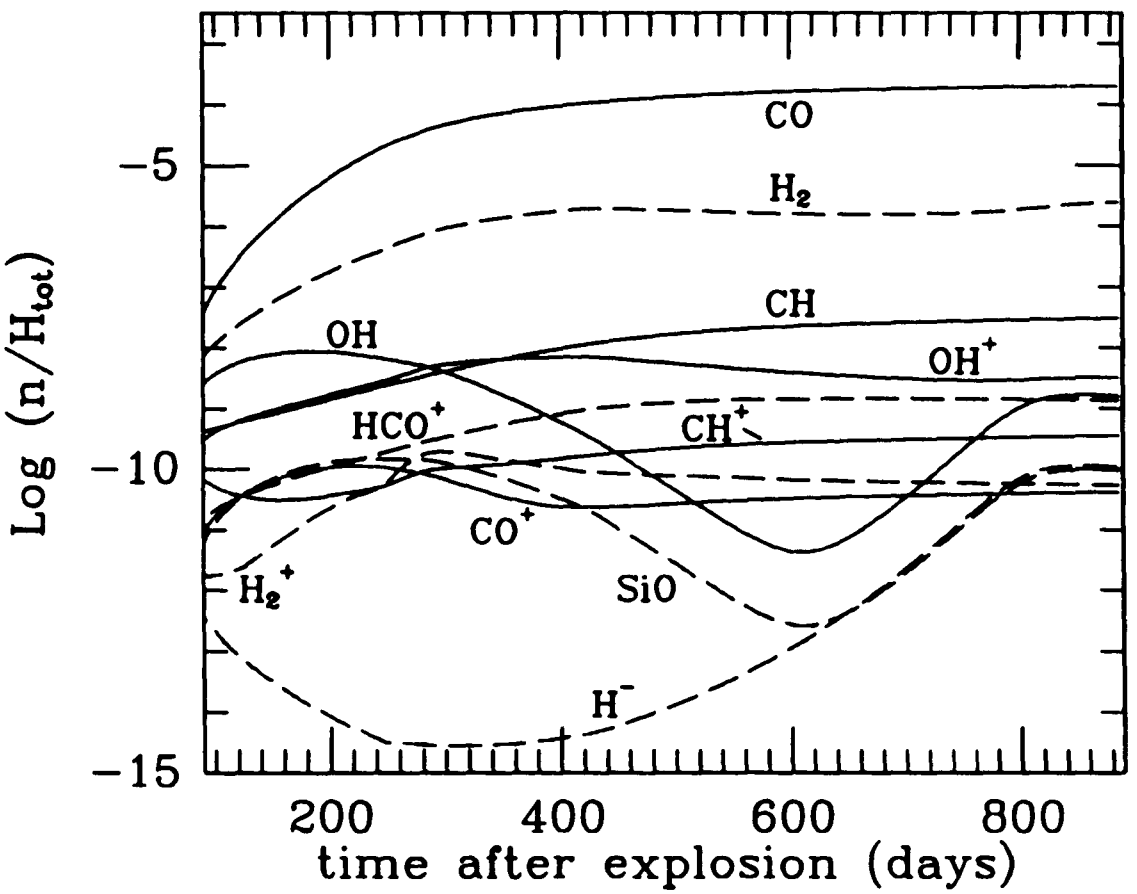

Figure IV.2: As in Figure IV.1, but with hydrogen depleted by a factor of 1000. For this case: $n_H(initial) = 9.7 \times 10^8$ cm^{-3} and $n_H(final) = 9.0 \times 10^5$ cm^{-3} at 887 days (Model 5 of Table IV.2).

with an abundance rivaling those of other molecular ions such as CH^+ and OH^+ (for the model shown in Figure IV.2, $x(HeH^+) \sim 10^{-10}$ at ~ 800 days). In addition, reduction of the hydrogen abundance causes the ejecta to remain mostly atomic. The total ionization fraction is increased and H^+ maintains a final relative abundance of 10^{-3}. This is almost three orders of magnitude larger than if hydrogen is not depleted.

As expected, if the envelope continues to be heated by energetic processes in the core such that the gas temperature remains constant, molecular abundances are found to be significantly reduced. The general trend in such an environment is for the molecular abundances to reach asymptotic limits rapidly. This occurs in models both with and without depletion of hydrogen. Beginning at approximately day 700 there is a short period of renewed molecule formation. This results primarily from rapid H^- formation as the radiation field decreases.

In Table IV.2 we display the final fractional abundances of selected species in different envelope models. In column 4, $\mathcal{N}(H)$ is the total number of hydrogen nuclei in all forms contained within the final envelope volume $\mathcal{V}$. Column 5 is the emission measure of the envelope. Models 1 and 5 are displayed in Figures IV.1 and IV.2, respectively. The general properties depend most sensitively on the temperature variation in the expanding envelope. In the outer regions being considered here, we expect the gas temperature to be determined by adiabatic cooling. This will be especially true at later times when the density has dropped and the envelope becomes increasingly transpar-

TABLE IV.2

Final Abundances[a]

Model	$T(final)$ (K)	$n_H(final)$ (cm^{-3})	$N(H)$	$n(H^+)n(e)\mathcal{V}$ (cm^{-3})	$x(CO)$	$x(H_2)$	$x(SiO)$	$x(CO^+)$	$x(H^+)$	Notes
1	225	8.3(7)	1.0(58)	7.4(54)	6.5(-5)	3.5(-5)	7.5(-13)	2.0(-17)	2.9(-6)	b,c
2	5000	8.3(7)	1.0(58)	3.2(56)	1.5(-7)	2.6(-7)	9.6(-12)	1.9(-13)	2.0(-5)	d
3	225	8.3(6)	1.0(57)	5.8(55)	1.6(-4)	3.4(-5)	1.8(-11)	1.1(-12)	7.6(-5)	c,e
4	5000	8.3(6)	1.0(57)	3.0(57)	1.4(-4)	1.0(-6)	1.1(- 8)	4.8(-9)	5.9(-4)	d,e
5	225	9.0(5)	1.1(56)	1.1(56)	2.0(-4)	2.5(-6)	9.4(-11)	4.1(-11)	9.9(-4)	c,f
6	5000	9.0(5)	1.1(56)	2.3(57)	6.2(-5)	1.5(-7)	1.3(-8)	8.2(-9)	4.4(-3)	d,f

[a] All model envelopes have initial values of temperature and density, $T_o = 5000$ K and $n_o = 10^{11}$ cm^{-3}, respectively. Final values of densities, temperatures and abundances refer to $t = 887$ days, when the envelope radius is $R(t) = 3.1 \times 10^{16}$ cm.

[b] Element abundances are 0.25 times solar, but O enhanced.

[c] Adiabatic cooling governs the variation of T with time.

[d] Constant temperature with time.

[e] H depleted by a factor of 100.

[f] H depleted by a factor of 1000.

ent to radiation and energetic particles. The most abundant molecular species (CO and H_2) reach asymptotic abundances rapidly. This takes place at a time when the radiation field is well approximated by a 5000 K blackbody. Therefore, the final abundances are not strongly dependent on how the radiation field is modeled at later times. Photometric observations (Bouchet *et al.* 1989; Dopita *et al.* 1988) indicate that the use of a blackbody to model the radiation field will overestimate the UV flux, however.

4.4 DISCUSSION

In this chapter, we have shown that molecule formation in the rapidly expanding outer envelope of SN 1987A is not only possible, but very efficient. Molecules such as CO and H_2 are likely to form in considerable abundance. Other important molecular species are found to be abundant as well. In addition, molecule formation is not strongly inhibited if hydrogen is depleted. Molecular abundances are reduced if heating of the envelope persists, however. It should be noted that this calculation has ignored the outermost reaches of the envelope, where pre-existing circumstellar and interstellar matter is swept up by the remnant. This is a region of relatively low mass where the density gradient is large. The contribution to the total molecular content of the supernova by this material will be small.

Unfortunately, observation of molecular emission from SN 1987A will likely continue to be difficult. It would be desirable to observe rotational transitions of CO ($J = 1 \rightarrow 0$ or $2 \rightarrow 1$) at millimeter wavelengths. To estimate the intensity of such emission, we refer to the detectability of the galactic carbon star IRC+10°216 if it were at the distance of the LMC (50 kpc; Walker 1987). This object has a CO envelope more than an order of magnitude larger than that of SN 1987A at 887 days (McCabe, Connon Smith, and Clegg 1979; Lafont, Lucas, and Omont 1982), and has a total number of CO molecules comparable to that of the supernova envelope (Allen and Knapp

1978; McCabe *et al.* 1979). We have assumed a distance to IRC+10°216 of 200 pc (Lafont *et al.* 1982). Using the expressions from Ulich and Haas (1976) and Maloney (1987), we predict an antenna temperature for IRC+10°216 of $T_A \sim 6 \times 10^{-3}$ K in the CO J = 1 → 0 line at 50 kpc for an error-free 12 m antenna. Such antenna temperatures are not unusual in CO observations of galaxies. The problem of detectability is, however, compounded by the large expansion velocity and higher gas temperature of the supernova. Rotational line intensities will be further reduced if adiabatic cooling does not dominate, and the gas temperature remains high. Confusion with ambient CO emission may be important. The factor of 4 decrease in beam size at 230 GHz and the increasing angular extent of the supernova shell may make detection of the J = 2 → 1 transition possible some time in the near future with a large telescope. Interferometeric observations may be promising.

Model spectra of the $v = 2 \rightarrow 0$ band of CO at $\lambda 2.3$ μm used by Spyromilio *et al.* (1988) indicate that there is $\sim 4.7 \times 10^{-5}$ $M_\odot$ of CO in the core at 255 days. We have found that the envelope may contain as much as 1.3×10^{-2} $M_\odot$ of carbon monoxide. In order to assess the contribution of the envelope to the observed emission, we have used simplifying assumptions to model the $\lambda 2.3$ μm emission. A description of the modeling technique to simulate CO spectra in LTE may be found in Thompson and Jannuzi (1989). A velocity dispersion of 2000 km s^{-1} was used to represent the effect of expansion on line formation. This procedure may underestimate the flux at a given wavelength. The parameters appropriate to Model 1 at 255 days yielded

a spectrum qualitatively similar to that of Spyromilio *et al.* for the same epoch. The model spectra indicate that at 1200 K the envelope will be optically thin to radiation from the core and may contribute $\sim$ 2 % to the observed flux at λ2.3 μm. The larger velocity of the envelope reduces the emission at each wavelength, thus, the integrated intensity of the large predicted CO mass of the envelope is spread out over a broader band profile. While the model spectra discussed here neglect the radiative transfer effects in an expanding sphere, they reveal that emission from the envelope may be important to a full description of the CO band profile.

Infrared transitions of H_2 are unlikely to be observable in SN 1987A. At best, the abundance of H_2 is comparable to that of CO in the models summarized in Table IV.2. The vibration – rotation lines of H_2 are inherently weak, electric quadrupole transitions while those of CO are strong, electric dipole transitions. In the most favorable case of LTE line emission in Model 2 at day 887, the predicted flux in the H_2 (1,0) S(1) line at λ2.121 μm is $f \approx 4 \times 10^{-17}(\frac{50\mathrm{kpc}}{D})^2$ ergs s^{-1} cm^{-2} at Earth, which is roughly a million times too weak to be discernible in spectra like those of Spyromilio *et al.* (1988).

Although large abundances of OH and H_2O are predicted, it is unclear whether conditions for maser emission from these species can be satisfied in the envelope. Because the velocity dispersion is large, it is unlikely that significant optical depth and maser gain can be achieved. Large inhomogeneities of small internal velocity dispersion might support maser emission, however.

Non-uniformities of this type have been postulated to explain the observed spectrum (McCray, personal communication).

As the envelope evolves, it will continue to cool. The ejecta will approach conditions similar to that of a small molecular cloud (*cf.* McCray and Li 1989). The outer regions will be strongly influenced by the interstellar radiation field and cosmic rays. Chemical processes in this region will resemble those of "normal" interstellar clouds aside from the possible absence of dust grains. The inner regions will continue to be exposed to energetic particles. If a pulsar has formed (see Middleditch *et al.* 1989), the effects of synchrotron emission will become increasingly important. Eventually, this small molecular cloud will vanish through continued expansion. The molecules will become increasingly vulnerable in this environment. Finally, an almost fully atomic diffuse remnant will form and molecular processes will cease to be important.

This calculation has shown that molecule formation can take place in an extreme environment. Molecule formation in other expanding systems of similar temperature and density have already been explored: the epoch of recombination in the early Universe (Lepp and Shull 1984; Dalgarno and Lepp 1987; Chapter 3, this work) and high velocity protostellar winds (Glassgold, Mamon, and Huggins 1989). Indeed, the chemistry of the supernova envelope resembles that of the protostellar wind modeled by Glassgold *et al.* A qualitatively similar result is that hydrogen remains primarily atomic while a large fraction of the heavy elements are converted into molecules. The expansion velocity of the supernova is more than an order of magnitude faster, however.

It can now be argued that significant molecular abundances are likely to form in a variety of other extreme environments. The key requirement is that the rate of molecular synthesis be faster than the rate of expansion. In both the supernova envelope and protostellar winds, *in situ* formation of molecules may be important to our understanding of emission from these regions. Molecular emission need not arise from pre-existing material swept up in the expansion.

For a number of years Supernova 1987A will continue to be an excellent laboratory for many types of astrophysical processes. Molecule formation is only one of these. The use of molecular emission as a probe may lead to a deeper understanding of supernova physics in general. Further analysis of the molecular emission in the infrared spectrum (particularly CO) should continue to yield new insights even though the emission has already weakened. Although the envelope is calculated to form large quantities of molecules like CO, the large expansion velocity limits its contribution to the observed molecular line emission; the core probably dominates as discussed by Lepp, Dalgarno, and McCray (*cf.* McCray 1989). A detection of rotational transitions from carbon monoxide in the envelope may eventually be possible.

NOTE: After the completion of this work, it was brought to the author's attention that dust formation has taken place in the ejecta of SN 1987A. The composition of the dust is unknown, and it is believed to have a clumpy distribution (R. Kirshner, private communication; Lucy *et al.* 1990). While the appearance of dust may have an effect on the future chemical evolution of the

supernova, it occurred at a sufficiently late date that the main conclusions of this work are not altered. It may be of interest to examine the effects of dust formation on the continued chemical evolution within the supernova envelope. However, in the case of SN 1987A, results of such a study will remain difficult to confirm observationally.

Acknowledgements: I would very much like to thank Philip Maloney and Adam Burrows for useful comments and discussions. An early conversation with R. McCray provided the inspiration for this chapter, and I thank him for a critical reading of the manuscript. B. Jannuzi's patience and modeling of the CO spectrum are much appreciated. It is a pleasure to thank A. Dalgarno for reading the manuscript and providing several valuable comments. Of course, I thank John Black for a great deal of invaluable assistance.

CHAPTER 5

NEAR-INFRARED OBSERVATIONS OF THE PROTO-PLANETARY NEBULA CRL 618

5.1 INTRODUCTION

As a star begins to evolve off the asymptotic giant branch (AGB) on the HR diagram to become a planetary nebula, it may (or will) take on the spectacular hourglass form of a bipolar nebula. Such objects are characterized by symmetric lobes of gas and dust flowing outward from an obscured central star. This apparently brief period ($\sim$ 1000 yrs, or less than one millionth of its life expectancy) in a star's life is also one of the least understood. Models have been presented which describe the origin of these objects as a result of stellar mass-loss in a close asynchronous binary system (Morris 1981). Although quite successful in reproducing the observed characteristics of bipolar nebulae (in particular CRL 2688, "the Egg Nebula," and HD 44179, "the Red Rectangle"), there is little evidence for binary central stars in any of the known proto-planetary nebulae (Cohen 1987). However, it has been shown that a number of fully fledged PNs may have close binary central stars (Bond 1989).

Observations have indicated that asymmetric mass-loss on the AGB may be very common (Cohen and Schmidt 1982; Latter and Maloney 1989). While there is good reason to believe that duplicity shapes bipolar nebulae, it may not be the only mechanism. Another hypothesis is that of rapid stellar rotation causing a preferred direction for mass ejection (*i.e.* Kwok and Bignell 1984; Calvet and Peimbert 1983; Morris 1981). This suggestion is, however, difficult to test. With the successful flight of the *Infrared Astronomical Satellite (IRAS)* and improved millimeter and sub-millimeter instrumentation, proto-planetary nebulae (PPN) have become the source of much recent discussion (*e.g.* Knapp *et al.* 1989; Volk and Kwok 1989).

Of particular interest is the highly-evolved object CRL 618. First identified as a classical bipolar nebula by Westbrook *et al.* (1975), it has been examined in detail from visible to radio wavelengths. The bright, compact ($\sim 0''.4$) infrared source studied by Westbrook *et al.* lies midway between two visible nebulosities and has a color temperature of $T \approx 275$ K. The bipolar structures are separated by $\sim 7''$ in the east – west direction (Calvert and Cohen 1978). Centimeter wavelength radio observations reveal an elongated compact source ($0''.4 \times 0''.1$) that has the same axis of symmetry as the bipolar lobes (Kwok and Bignell 1984). Optical spectropolarimetry shows the two lobes to be reflection nebulae (Schmidt and Cohen 1981). Analysis of the reflected spectrum indicates that the central star is of type B0, which gives an implied distance of 1.8 kpc (Westbrook *et al.* 1975; Schmidt and Cohen 1981). The total luminosity has been found to be $\sim 2.6 \times 10^4\ L_\odot$, with the infrared spec-

trum dominated by dust continuum emission which arises primarily from the compact source (Kleinmann *et al.* 1978; Russell, Soifer, and Willner 1978). CO observations as reported by Lo and Bechis (1976), Thronson and Mozurkewich (1983), Knapp and Morris (1985), and Bachiller *et al.* (1988) indicate a rapid expansion velocity of about 20 km s^{-1} and a mass-loss rate on the order of 10^{-4} $M_{\odot}$ yr^{-1}.

Most recently, observations of the CO (2 $\rightarrow$ 1) and (3 $\rightarrow$ 2) rotational lines (Gammie *et al.* 1989; Cernicharo *et al.* 1989) indicate the presence of outflow velocities $>$ 190 km s^{-1}. In addition, there exists an expanding central HII region (Kwok and Feldman 1981; Kwok and Bignell 1984) and high velocity H_2 (1,0) S(1) emission (Burton and Geballe 1986). The ionization and forbidden line emission from the lobes may be explained by low velocity shocks (see, however, Schmidt and Cohen 1981). The expansion velocity of the lobes derived from visible spectroscopy is $\sim$ 80 km s^{-1} (Carsenty and Solf 1982). All this evidence indicates that CRL 618 is a rapidly evolving object which may be on the verge of producing a full-blown planetary nebula. The low-velocity component appears to be the remnant AGB circumstellar envelope, while the high-velocity component suggests that ejection of the star's outer layers has begun. Indeed, CRL 618 has visibly brightened on a human timescale, increasing $\sim$ 2 magnitudes since 1940 (Gottlieb and Liller 1976).

In this chapter, we present newly acquired H and K band images and discuss near-infrared spectoscopy of CRL 618 in the range $\lambda\lambda 0.950 - 1.330$ μm. Such spectra may open up a new window on the evolutionary state of PPN.

At least some of the emission observed is expected to be a result of fluorescent excitation of H_2. This hypothesis will be tested by detailed modeling of the spectrum in Section 5.3. Earlier observations of molecular hydrogen emission (*i.e.* Thronson 1981; Beckwith, Beck, and Gatley 1984; Burton and Gaballe 1986) have provided insight into the physical conditions in the nebula. We will discuss how the new observations strengthen or alter the earlier work. In the next section, we describe the observations and present the data.

5.2 OBSERVATIONS

a) Spectroscopy

Observations of CRL 618 were obtained by D. Kelly and G. H. Rieke on 25 and 26 February 1989 using the Steward Observatory 2.3 m telescope and the new germanium diode spectrometer. The spectrometer is currently under development at Steward Observatory. High resolution mode produces a resolving power of $\Delta\lambda/\lambda = 6.3 \times 10^{-4}$ at 1.164 μm. This instrument acquires simultaneous sky and object spectra, greatly speeding up the observing sequence. A 6″ circular aperture was used, thus taking in the majority of the eastern lobe of CRL 618. Data reduction followed conventional techniques. The standard star HD 106965 (spectral type A2) was used to flux calibrate the data. Removal of telluric absorption was facilitated by observations of the nearby star HD 29645 (spectral type G0). Error in absolute flux calibration is estimated to be $\sim$ 15%. The data are presented in Figure V.1.

b) Imaging

In collaboration with P. Maloney, the Steward Observatory 64 × 64 pixel Rockwell HgCdTe array (Rieke, Rieke, and Montgomery 1987) and 2.3 m telescope were used to obtain infrared images of CRL 618 in the H and K bandpasses. Observations were made on 27 September 1988. The array was operated at 77 K. Cold reimaging optics gave a plate scale of about 0.″25

per pixel. The standard star HD 44612 (spectral type A0) was observed for flux calibration. Sky flats were obtained after each exposure by wobbling the telescope $\sim 1'$ to a region clear of infrared sources. Data reduction was carried out using standard IRAF routines.

Figure V.1: Near-infrared spectrum of CRL 618 acquired with the new Ge spectrometer. Prominent atomic lines are labeled. Many of the weaker lines can be identified with molecular hydrogen vibration – rotation transitions.

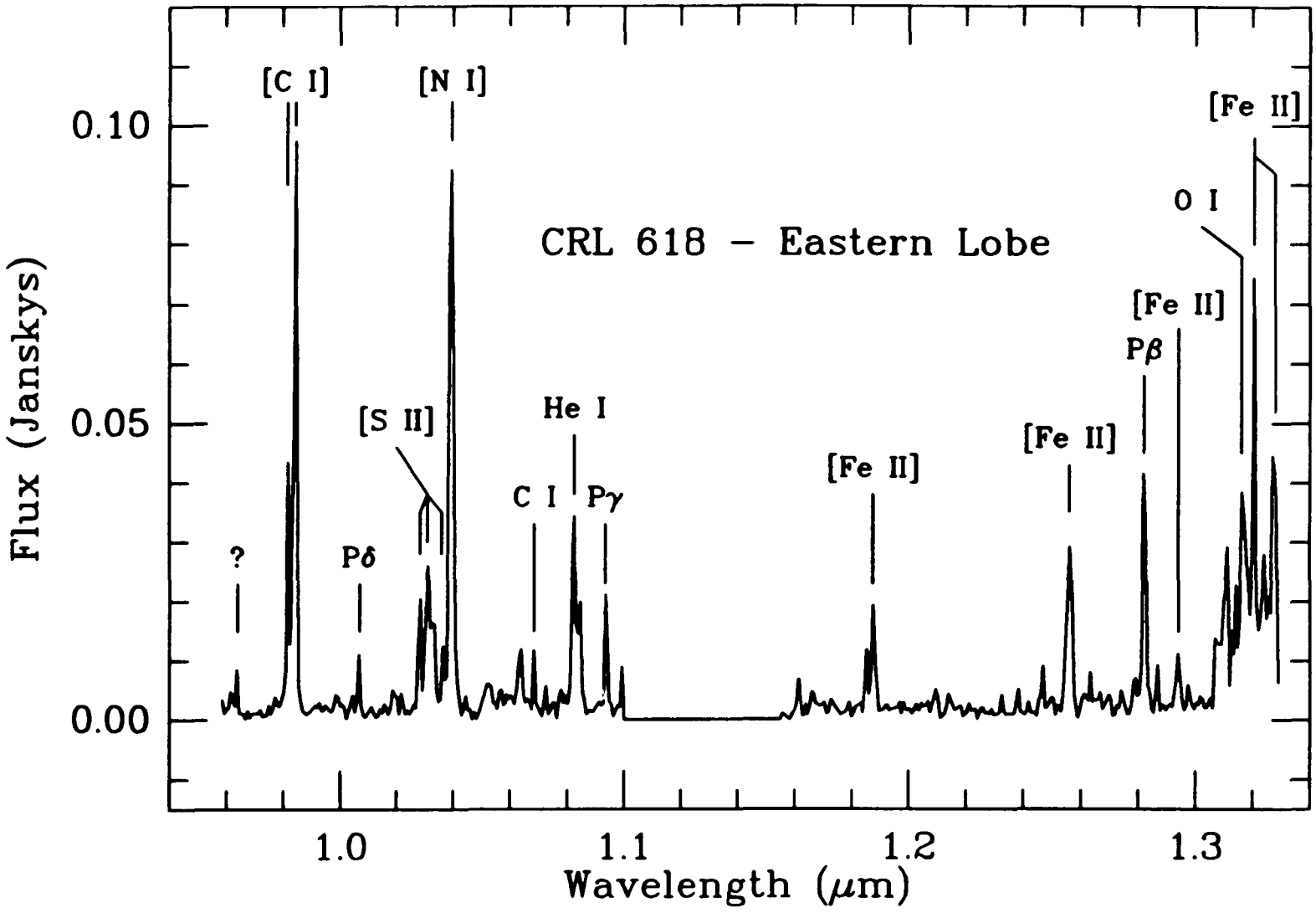
CRL 618 – Eastern Lobe
Flux (Janskys)
0.10
0.05
0.00
1.0
1.1
1.2
1.3
Wavelength (μm)
[C I]
[N I]
[Fe II]
O I
[Fe II]
Pβ
[Fe II]
[Fe II]
He I
[S II]
C I
Pγ
?
Pδ

5.3 THE INFRARED IMAGES

The new infrared images are displayed in the form of contour plots in Figures V.2 and V.3. The integrated magnitudes are $H = 11.59 \pm 0.1$ and $K = 8.60 \pm 0.1$. The K magnitude determined here is somewhat brighter than that found by Westbrook *et al.* (1975) at 2.2 μm ($m_{2.2} = 9.3$). However, it appears that Westbrook *et al.* may have underestimated the total brightness at this and longer wavelengths (see Kleinmann *et al.* 1978). Seeing at the time of the observations was $\sim 0''.7$.

The bipolar morphology is evident in both images, although the western lobe appears much less extended. It is clear that the emission at both H and K is dominated by a small, unresolved source just inside the eastern lobe. While apparently not directly between the lobes, the position of this source is consistent with the placement of the peak 2.1 μm continuum as found by Beckwith, Beck, and Gatley (1984). The total extent of the nebula as represented by the lowest contours is smaller in H than in K as expected when the faint emission is attributable to cool dust.

It is likely that the unresolved compact source, just inside the eastern lobe, is the $0''.4$ source observed by Westbrook *et al.* (1974) and Wynn-Williams (1977). We find it to be $\sim 1''$ east of the center of bipolar symmetry. We do not have an absolute position for the source, therefore we cannot compare with the placement of Wynn-Williams (1977) at 15 GHz. The morphology

displayed in these images is consistent with a bipolar axis highly inclined to the line-of-sight, such that the eastern lobe lies nearest the Earth. Carsenty and Solf (1982) determined just such an orientation with an analysis of the radial velocity structure. They found the polar axis to be inclined to the plane of the sky at an angle of $\sim 45°$. This type of viewing geometry can also account for the apparent smaller size of the western lobe as seen in these and optical images.

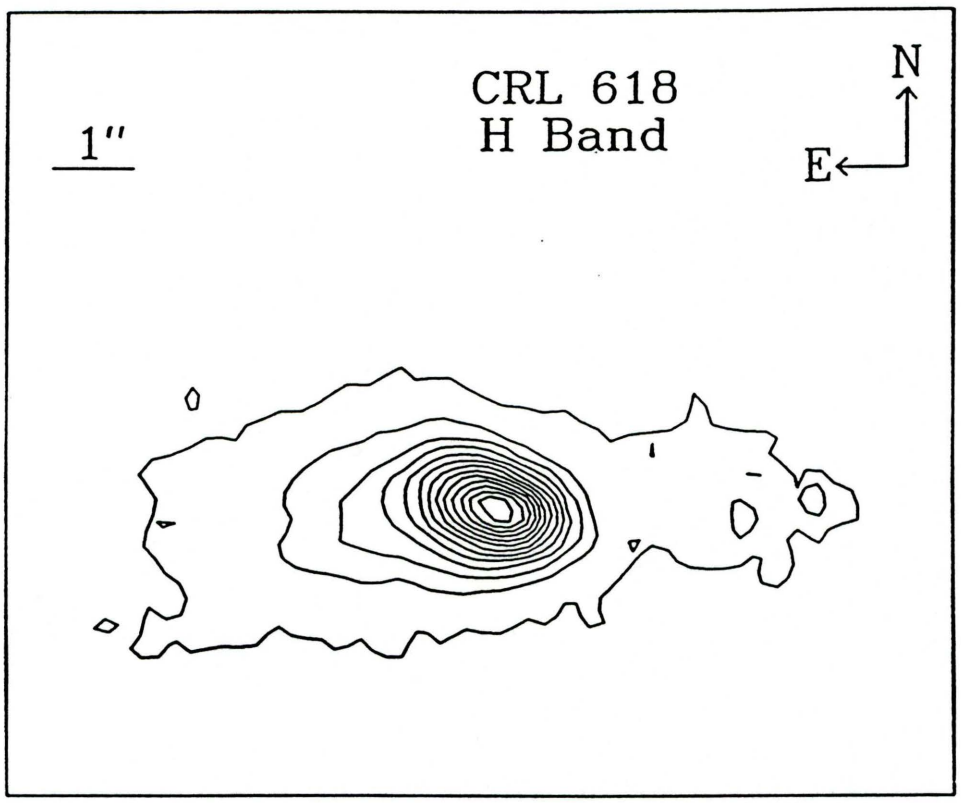

Figure V.2a: H-band image of CRL 618 taken with the Steward Observatory 2 μm camera. The plate scale is 0.″25 per pixel (1″ per 1.1 cm on this plot). Contours are at linear spacings with lowest at 1.9×10^{-5} Jy and highest at 4.8×10^{-4} Jy. Contour spacings are 3.8×10^{-5} Jy.

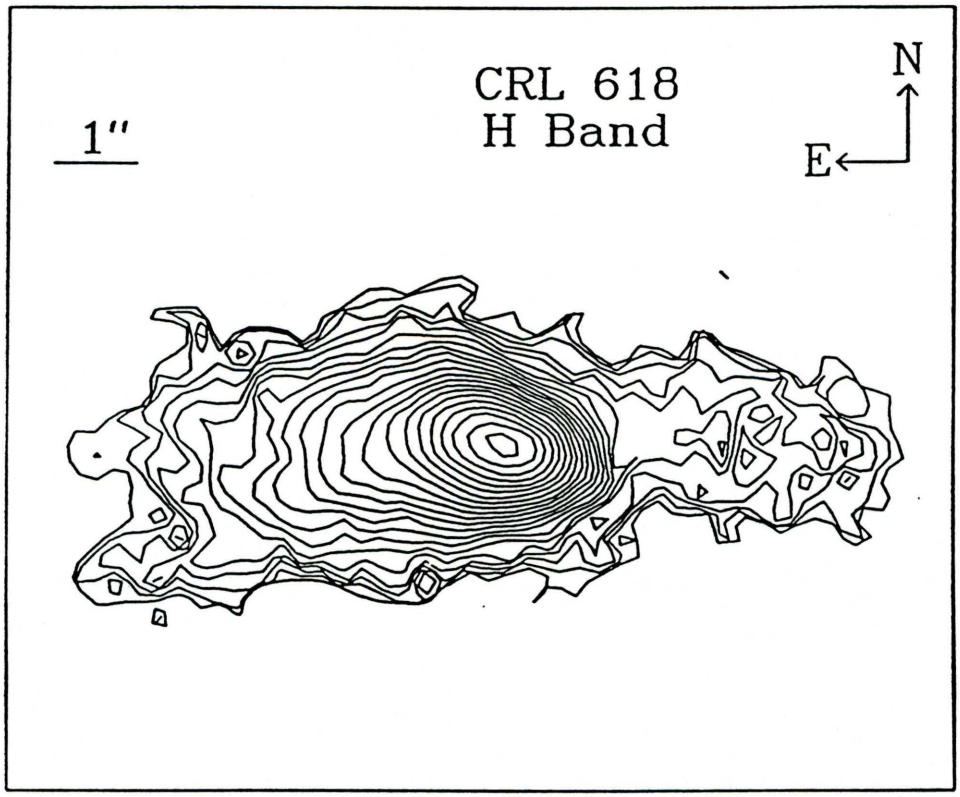

Figure V.2b: Same as Figure V.2a plotted with logarithmic contour spacing in order to display the lowest flux levels with greater clarity.

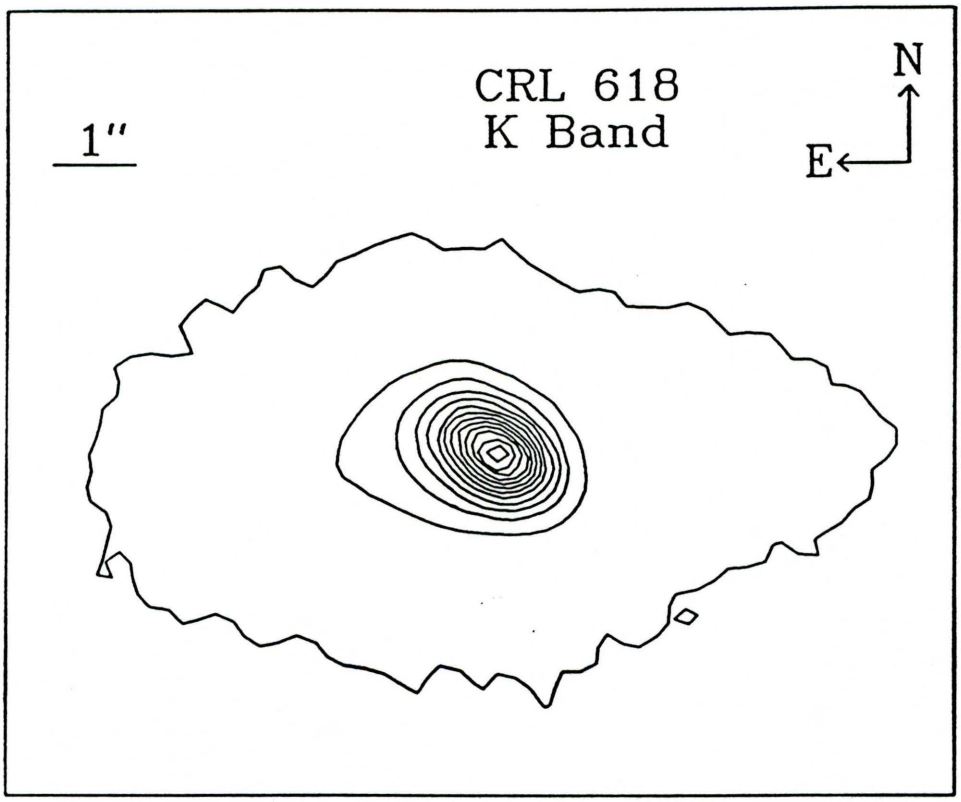

Figure V.3a: K-band image of CRL 618 taken with the Steward Observatory 2 μm camera. The plate scale is 0.″25 per pixel (1″ per 1.1 cm on this plot). Contours are at linear spacings with lowest at 3.0×10^{-5} Jy and highest at 7.8×10^{-3} Jy. Contour spacings are 6.0×10^{-4} Jy.

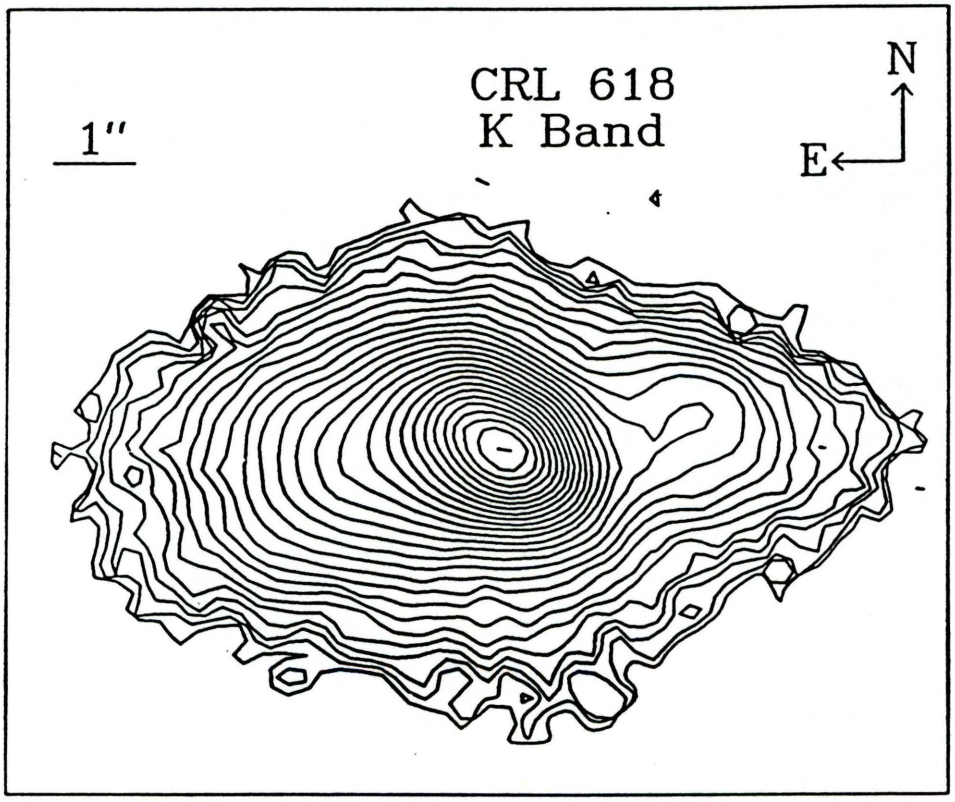

Figure V.3b: Same as Figure V.3a plotted with logarithmic contour spacing in order to display the lowest flux levels with greater clarity.

5.4 THE ATOMIC LINE SPECTRUM

Atomic lines prominent in the near-infrared spectrum of CRL 618 are noted in Figure V.1. Other features are attributable to emission from vibration – rotation quadrupole transitions in the ground electronic state of molecular hydrogen. A number of atomic features identified here have already been reported by Westbrook *et al.* (1975) in their long wavelength visible spectrum. These include [C I] at 9823 and 9849 Å, [S II] at 10287, 10320, 10338, and 10373 Å, and hydrogen Pγ at 10049 Å. Schmidt and Cohen (1981) have analysed the visible spectrum in the range $\lambda\lambda 3750 - 7050$ Å in detail. The atomic spectrum presented here will be discussed in greater length elsewhere (Kelly *et al.* 1990). However, it is worthwhile to make a brief examination.

As already seen in the visible spectrum of Schmidt and Cohen (1981), the IR spectrum is also dominated by forbidden line emission. In the earlier work, it was shown that most of the visible permitted line radiation observed from the lobes originates within the central region. It is then scattered into the line-of-sight by dust. The forbidden line radiation arises from the lobes themselves. Without polarization measurements, we cannot judge whether the infrared line radiation behaves similarly. However, for all but the O I line at 1.316 μm ($3p\ ^3P - 4s\ ^3S^o$), this would be a reasonable assumption. It is unlikely that the O I line results from recombination in the central H II region, since no other O I lines are seen. Nor can it be collisionally excited in the forbidden

line region due to a large transition probability ($A = 3.04 \times 10^7$ s^{-1}). If the identification is correct, then it is possible that this line is excited by continuum fluorescence in the $2p^4\ ^3P - 4s\ ^3S^o$ λ1040 Å resonance transition. If so, similar pumping would occur in the $2p^4\ ^3P - 3d\ ^3D^o$ λ1026 Å transition resulting in emission at 11287 Å, which is a wavelength unfortunately not observed in this spectrum. Comparison of Einstein A-values yields fluorescence probabilities of 0.283 (λ1026 pumping) and 0.112 (λ1040 pumping) for λ11287 and λ13160 lines, respectively. If it is assumed that the UV flux is equal at 1040 and 1026 Å, then $I_{\lambda 11287}/I_{\lambda 13165} \approx 6.5$. The apparent flux ratio would be reduced to $\approx$ 1.4 by the 5.3 mag of visual extinction implied by the H_2 line intensity ratios (see §5.5.a). Another line of O I at 8446 Å, which is expected to have an intensity 10.2 (or 0.85 if $A_v = 5.3$) times that of the 13165 Å line, was not seen by Westbrook *et al.* (1975). The radiative excitation of O I lines has been discussed previously by Grandi (1975). Grandi's line ratios differ from those presented here because he did not assume equal fluxes of pumping radiation at 1040 and 1026 Å. All three lines are observed from the early-type star η Carinae (Thackeray 1962; Allen, Jones, and Hyland 1985; McGregor, Hyland, Hillier 1988) in which the excitation mechanism may be similar. UV fluorescence of molecular hydrogen may be weakly present in CRL 618 (see below). Thus, if the O I line at λ13165 is shown to be due to UV pumping, then constraints may be placed on the abundance ratio of O and H_2 in the region exposed to the stellar radiation.

5.5 THE MOLECULAR HYDROGEN EMISSION

a) Extinction to the H_2 Emitting Region

Observations of CO (*e.g.* Thronson and Mozurkewich 1983) demonstrate that a great deal of molecular material surrounds CRL 618. This material is likely to be the remnant of mass-loss from CRL 618 prior to its evolution to a bipolar nebula. As a result, a large amount of attenuation due to dust in the extended circumnebular material is expected. Using a standard interstellar extinction law, Thronson (1981) used four pairs of H_2 lines in the range $\lambda\lambda 1.9-2.5$ μm to determine a visual extinction of $A_v = 8 \pm 6$ magnitudes toward the H_2 emitting lobes. It is easy to argue that a standard interstellar extinction law is inappropriate for an object like a PPN. Unfortunately, it is currently impossible to know how much the true extinction law may differ from that found for the general interstellar medium.

With the new observations presented here, we now have a longer spectral baseline over which to determine the amount of extinction, possibly improving upon the estimate of Thronson (1981). In the spectral region covered by the Ge spectrometer, there are 5 lines which share the same upper state with lines present in the spectrum of Thronson (1981). Comparison of observed and predicted intensity ratios from such lines provide a measure of the attenuation. These lines are: $v = 2 \rightarrow 0$ S(0) ($\lambda 1.189$ μm), S(1) ($\lambda 1.162$ μm), Q(2) ($\lambda 1.242$ μm), Q(3) ($\lambda 1.247$ μm), and Q(5) ($\lambda 1.263$ μm) share the same upper

state with $v = 2 \rightarrow 1$ S(0) (λ2.355 μm), S(1) (λ2.247 μm), S(0), S(1), S(3) (λ2.073 μm), respectively. For lines originating from the same upper state, a predicted line ratio is just the ratio of the products $\Delta E_i A^i_{ul}$, where ΔE_i is the energy of transition i and A^i_{ul} is the Einstein transition probability for the same transition. Our best estimate using a standard interstellar extinction law is $A_v = 5.3 \pm 2.5$ magnitudes. The relatively large uncertainty is a result of scatter in the extinction as determined from single line pairs and the uncertainty in individual line fluxes. This value is well within the errors on A_v as found by Thronson. It is important to note that there is an uncertainty in A_v, which cannot be estimated, associated with the form of the extinction law. The differential extinction between 1.2 and 2.2 μm is, however, directly determined from the observations.

On the basis of the Balmer decrement and visible line ratios, an extinction of $A_v \sim 3.5$ mag (Westbrook *et al.* 1975; Calvet and Cohen 1978; Schmidt and Cohen 1981) has been found. While the difference between this value and that determined above is not significant if the errors are considered, it is easy to imagine how such a difference could be real in an object like CRL 618. If the bulk of attenuation arises from the same region, then a non-universal extinction law could result in such a difference. In addition, the complex structure of CRL 618 may come into play. For example, Thronson (1981) found $A_v \gtrsim 28$ mag to the Brackett γ emitting region. Thus, if the difference in visual extinction as determined from the visible and infrared is real, then there must be differing amounts of obscuring material between

the sources of emission. It has already been suggested by Schmidt and Cohen (1981) that the lobes are clumpy. Also, it may be incorrect to assume a case B recombination spectrum for the intrinsic Balmer decrement in a compact, very dense nebula (*c.f.* Thompson 1987 and references therein). As discussed by Thronson (1981), the Bγ emitting region is the compact H II region which lies behind a thick, dusty torus surrounding the central star, obscuring it from view at visible wavelengths.

b) Origin of the H_2 Spectrum

As demonstrated by Black and van Dishoeck (1987), reflection nebulae are likely to be ideal sources of fluorescent H_2 emission. Thus, CRL 618 should be an excellent object in which to search for such emission. Ultraviolet photons with $\lambda > 912$ Å are able to escape the ionized nebula and illuminate the lobes where they can be absorbed in the Lyman ($B^1\Sigma_u^+ - X^1\Sigma_g^+$) and Werner ($C^1\Pi_u - X^1\Sigma_g^+$) bands of molecular hydrogen. Approximately 10% of the resulting downward transitions will be to the vibrational continuum of the ground electronic state, thus leading to dissociation of the molecule (This process was first described by Solomon in 1965 and discussed by Field, Somerville, and Dressler 1966). The remaining transitions to bound vibration - rotation levels of the ground state result in UV line fluorescence and produce a distinctive infrared spectrum of slow electric quadrupole transitions. This process is described in detail by Black and Dalgarno (1976), van Dishoeck and Black (1986), and Black and van Dishoeck (1987). Emission from low lying

vibration – rotation levels can be collisionally excited in regions of relatively high excitation temperature $T_{ex} \gtrsim 1000$ K as may result from the passage of a shock.

We have attempted to reproduce the observed H_2 emission from CRL 618 using the modeling techniques described by van Dishoeck and Black (1986) and Black and van Dishoeck (1987). Both fluorescent emission spectral models and models assuming thermal equilibrium have been calculated. In the fluorescent models, formation of H_2 is primarily by grain surface reactions and destruction is photodissociation by absorption of UV radiation followed by decay to an unbound vibrational state. The abundance of H_2 is assumed to be in steady state. The calculation solves the equation of transfer for 22,445 absorption lines simultaneously in a plane-parallel cloud illuminated on one side by an external ultraviolet radiation source. Statistical equilibrium equations are solved for the populations of 211 vibration – rotation levels in the $X^1\Sigma_g^+$ state, 629 levels in the $B^1\Sigma_u^+$ state, and 476 levels in the $C^1\Pi_u$ state. Multiple steps are taken through the cloud at each of which the cascade of 2937 vibration – rotation transitions in the $X^1\Sigma_g^+$ state is calculated.

The intensity of the radiation field at the boundary is parameterized by the factor I_{UV}, such that $\phi(\lambda = 1000\ \text{Å}) = 4.5 \times 10^{-8} I_{UV}$ photons cm^{-2} s^{-1} Hz^{-1}. Enhanced H_2 excitation may occur in regions where the Lα flux is large due to accidental resonances with the $B^1\Sigma_u^+ - X^1\Sigma_g^+$ (1,2) P(5) and R(6) lines, provided that $v = 2$ levels are already significantly populated. To explore this possibility in CRL 618, we have examined the effect of a large Lα

flux on the IR fluorescence spectrum. As described by Black and van Dishoeck (1987), the Lα radiation is characterized by a Gaussian profile

$$\phi_\nu^\alpha = \phi_\circ^\alpha \exp\left\{-1.686 \times 10^5 \left[(\lambda - \lambda_\alpha)/\Delta V\right]\right\} \quad \text{cm}^{-2}\ \text{s}^{-1}\ \text{Hz}^{-1}, \qquad \text{(V.1)}$$

and is parameterized by the quantity $\alpha = 310.5\phi_\circ^\alpha \Delta V / I_{UV}$. Here ΔV is the full width half-maximum (FWHM) of the Lα profile in kilometers per second.

Thronson (1981) has determined an H_2 vibration - rotation excitation temperature based on line fluxes in the 2 μm region which were not corrected for extinction. In order to minimize error in the thermal model of H_2 emission, we have corrected the fluxes presented by Thronson for $A_v = 5.3$ mag. We then determined a new excitation temperature based on the corrected fluxes, even though the change was expected to be small. Assuming a Boltzmann distribution and including all 15 available lines in a least-squares fit to a plot of $N(v,J)/g_J$ versus $T_u = E(v,J)/k$ (see, *e.g.*, Thronson 1981), it was found that $T_{ex} = 2262$ K. However, as was also shown by Thronson, the four $v = 2 \rightarrow 1$ lines all appear to be systematically stronger than would be expected for TE, based on the $v = 1 \rightarrow 0$ lines. Since these are also the weakest lines in the spectrum, this may be a result of measurement error. In addition, scatter in the $N(v,J)/g_J$ vs. T_u diagram is much larger in the $v = 2 \rightarrow 1$ lines. It therefore seems prudent to leave these lines out of the fit (as was also done by Thronson) and determine a T_{ex} based only on the $v = 1 \rightarrow 0$ lines. For such a least-squares fit, it was found that $T_{ex} = 1926$ K. This can be compared to the value found by Thronson of $T_{ex} = 1950 \pm 200$ K. Uncertainty in the new value is the same as that given by Thronson.

Results of the modeling exercise are presented in Figure V.4. A fluorescence model appears on the bottom. The thermal model is displayed below the data. The thermal model was adjusted to give the same intensity in the $1-0$ S(1) line as that observed by Thronson (1981). This resulted in an H_2 column density of $N_{H_2} = 7.2 \times 10^{18}$ cm^{-2} for $T_{ex} = 1926$ K. The fluorescence model has been calculated for $I_{UV} = 2 \times 10^4$, $\alpha = 0.20$, $n_H = 10^5$, and $T = 2000$ K. These values of I_{UV} and α give a UV radiation field appropriate for a B0 star embedded in an H II region seen at a distance of 8×10^{16} cm, which is comparable to the linear scale of the lobes in CRL 618. Both models have been corrected for 5 magnitudes of visual extinction. The fluorescence model predicts more and stronger lines than are observed. A satisfactory fit is obtained by the thermal emission model. However, a number of features appear stronger in the data than predicted. These lines include $2-0$ S(7) (λ1.064 μm), $3-1$ S(3) (λ1.185 μm), $2-0$ Q(7) (λ1.287 μm), $4-2$ S(1) (λ1.311 μm), $3-1$ Q(1) (λ1.314 μm), and $3-1$ Q(3) (λ1.324 μm). The last three are in a region crowded by other lines. Models were calculated with the values of I_{UV} and α varied over many orders of magnitude. A better fit was not obtained. It is possible that these lines are confused with unidentified atomic or molecular features. In addition, the plane-parallel geometry used in the models may fail to adequately represent the actual geometry of CRL 618. Thus, fluorescent excitation of these lines remains likely. The [Fe II] line at λ1.2750 μm appears broadened due to a blend with the relatively weak $v = 2 \rightarrow 0$ Q(6) line of H_2 at λ1.2740 μm.

Figure V.4a: The spectrum plotted in Figure V.1 compared to models of thermal and fluorescent emission from H_2. The wavelength range has been reduced for clarity. The data appears on top, thermal model in the middle, and the fluorescence model on the bottom. Parameters for the models are: $T_{ex} = 1926$ K and $N_{H_2} = 7.2 \times 10^{18}$ cm^{-2} (thermal), $I_{UV} = 2 \times 10^4$, $\alpha = 0.20$, $n_H = 10^5$, and $T = 2000$ K (fluorescence; see text). The predicted fluxes have been corrected for $A_v = 5$ magnitudes. Note that the atomic lines have been labeled in Figure V.1. The flux scale is referenced to the data.

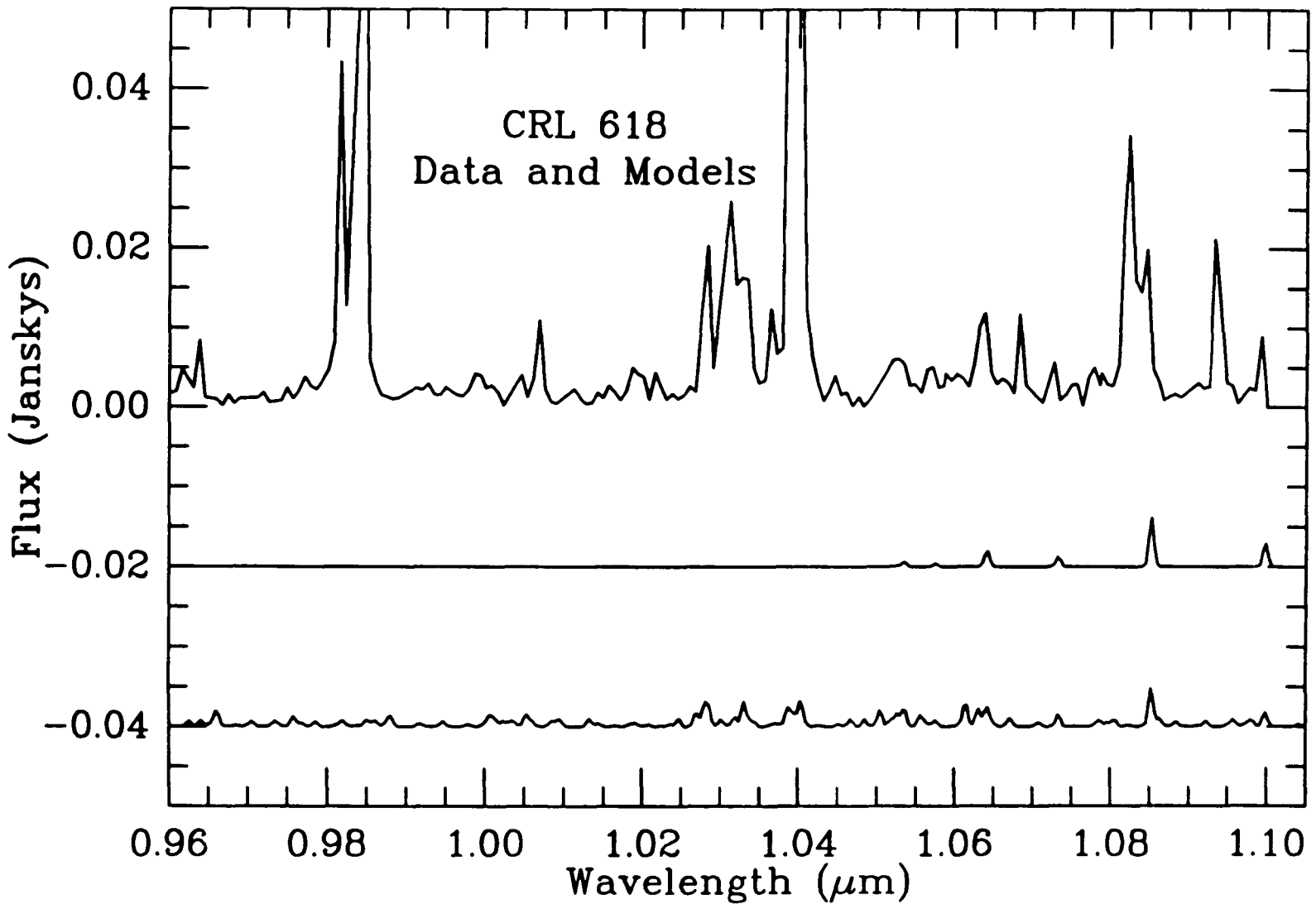
CRL 618
Data and Models
Flux (Janskys)
0.04
0.02
0.00
−0.02
−0.04
0.96
0.98
1.00
1.02
1.04
1.06
1.08
1.10
Wavelength (μm)

Figure V.4b: Same as in Figure V.4a. The longer wavelength part of the spectrum is displayed.

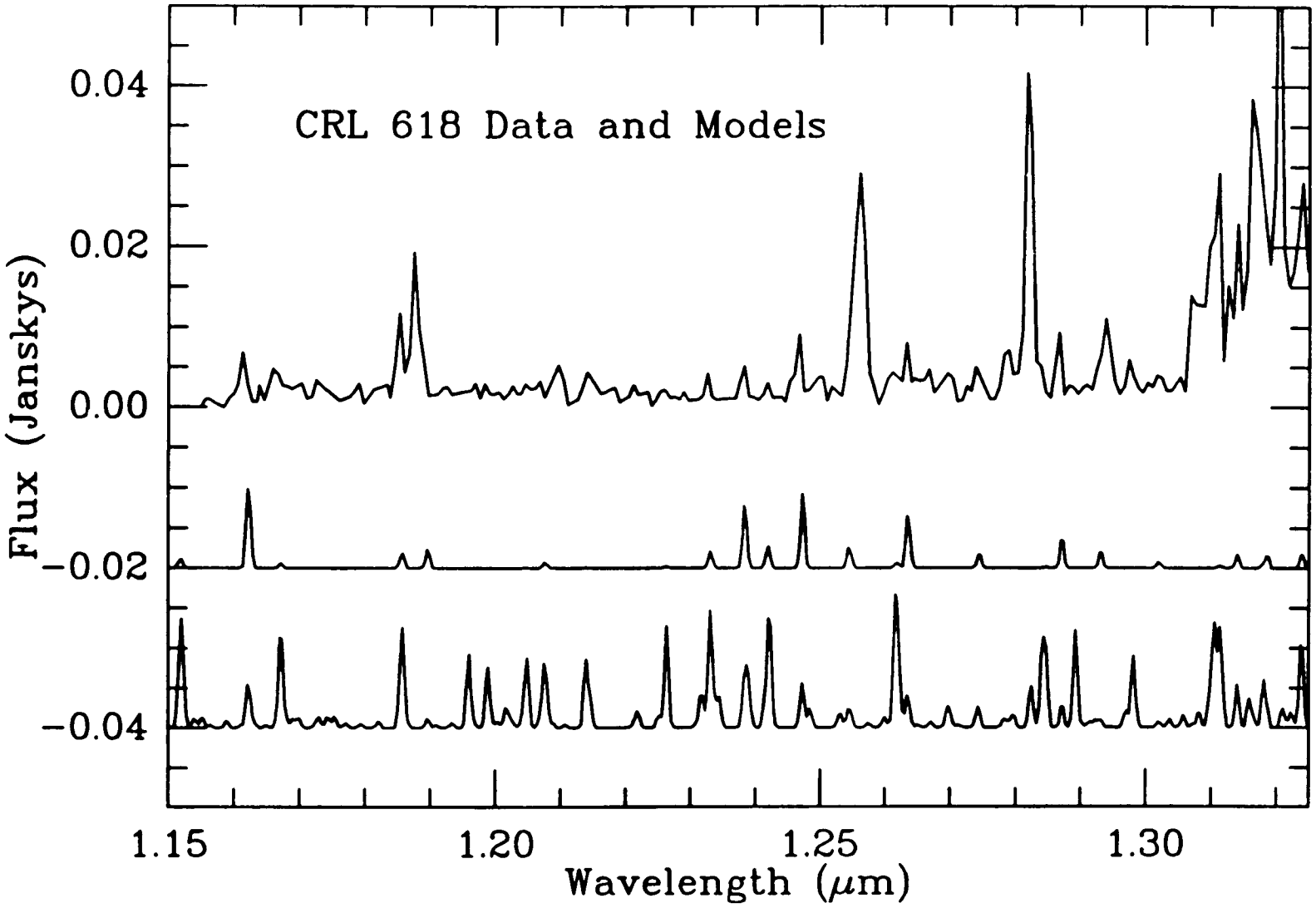
CRL 618 Data and Models
0.04
0.02
0.00
−0.02
−0.04
Flux (Janskys)
1.15
1.20
1.25
1.30
Wavelength (μm)

5.6 DISCUSSION

The H_2 (1,0) lines in the 2 μm region are rather intense and exhibit a rotational excitation temperature in $v = 1$ levels of $T \approx 2000$ K (Thronson 1981). This leads to an immediate presumption that there is an important component of high-temperature thermal emission, perhaps even in lines of the (2,0) band in the spectral region accessible to the Ge spectrometer ($\lambda \lesssim 1.6$ μm). If the excitation temperature were $T_{ex} \leq 2000$ K for all levels, however, little emission would be expected in transitions arising in $v' \geq 3$. Detection of such highly excited lines would reveal a component of fluorescent emission. We have calculated spectral models of H_2 fluorescence emission which show that such emission was not obviously seen in the near-infrared spectrum presented in §5.2. While fluorescent emission is expected from bright reflection nebulae like CRL 618, its possible absence provides new information into the detailed morphology of this object.

If fluorescent emission is absent, or only weakly present in the spectrum of CRL 618, the UV flux incident on the lobes must be highly extingushed in the region surrounding the central star. Another alternative is that the lobes have a shape which prevents the observed surface from having a direct view of the stellar photosphere. Also, fluorescent emission could be present. However, the large amount of circumnebular material may have extingushed it beyond detectable limits of the spectrum presented here. Total obscuration of

the central star from the lobes is unlikely due to the presence of reflected stellar continuum in spectra acquired at visual wavelengths (Schmidt and Cohen 1981). Therefore, a combination of the above scenarios seems the most probable. The detection of O I, λ13165 Å emission, if shown to arise from UV fluorescence, may be particularly useful in determining how the UV flux is distributed. In addition, higher signal-to-noise spectra acquired through a small aperture at various points on the bright eastern lobe could be revealing.

Models of H_2 thermal emission were also compared to the data. These reproduced the observed spectrum adequately for an excitation temperature of $T_{ex} \sim 2000$ K. A component of fluorescent emission may be present, however. Thronson (1981) has discussed the origin of the thermal emission in detail. He argued that the molecular hydrogen is excited by shocks with velocities of ~ 10 km s^{-1}. The total mass of shocked H_2 is given to be $M_{H_2} \sim 10^{-4}$ $M_\odot$, assuming TE, an absolute $v = 1 \rightarrow 0$ S(1) line intensity, and a distance of 1 kpc. For a column density derived from the models of $N_{H_2} = 7.2 \times 10^{18}$ cm^{-2}, an assumed distance of 1.8 kpc, and a spherical lobe with $r = 4 \times 10^{16}$ cm, we find $M_{H_2} \sim 4 \times 10^{-4}$ $M_\odot$. This assumes that the emitting H_2 is uniformly distributed throughout the eastern lobe, which is surely not the case. Therefore, our results are not discrepant with those of Thronson. If shocks are responsible, then the emission would be expected to arise from a relatively small region. It is not clear that this must be the case, however. As mentioned above, better spatial resolution is required to determine the distribution of H_2 emission in the lobes. While shock excitation is sufficient

to explain the observed emission, it may not be necessary. There are regions within CRL 618 which are at high enough density and temperature (see, *e.g.*, Schmidt and Cohen 1981) that H_2 may be present in LTE at $T \sim 2000$ K.

We have compared H_2 line fluxes observed by the Ge spectrometer with those of Thronson. A differential extinction between 1.2 and 2.2 μm implies an attenuation at visual wavelengths to the H_2 emitting lobes of $A_v = 5.3 \pm 2.5$ magnitudes. While we cannot be certain that the extinction law for objects like CRL 618 is the same as the interstellar law, this amount of attenuation implies a significant amount of material outside the emitting lobes. This material has been observed to be molecular with an expansion velocity consistent with it being the remnant mass-loss shell (*i.e.* Knapp and Morris 1985).

Near-infrared images of CRL 618 have been presented which display a bright, compact source believed to be at the position of the central star. This object is probably a warm dust torus surrounding the central star and H II region. Weak, extended emission arising from cool dust in the bipolar lobes is also observed. The apparent morphology seen in these images is consistent with a bipolar nebula having a bipolar axis highly inclined to the plane of the sky. The dust torus, which may be directing outflow into the lobes, obscures the central regions from view at visual wavelengths.

The observations presented in this chapter reinforce the general description for the structure of CRL 618. The complex distribution of gas and dust is vividly displayed in both spectrum and images. Follow-up observations have been suggested. Since this clearly is a rapidly evolving object at one of the

most mysterious points in stellar evolution, continued monitoring of key features is justified. As material flows away from the central star, its density will drop. Obscuration of UV starlight will decrease. Perhaps fluorescent emission from molecular hydrogen will increase in the foreseeable future. Fluorescent emission has been observed from at least one compact young planetary nebula, Hubble 12 (Dinerstein *et al.* 1988). The wavelength range accessible to the Ge spectrometer is particularly discriminating to the presence of fluorescent emission. A survey for this type of emission from the nearest PPN and young PN may help to reveal additional insights into the evolution of these objects.

Acknowledgements: This chapter would not have been possible without the spectrum kindly supplied by G. Rieke and D. Kelly. I would like to thank G. Schmidt and H.-W. Rix for a number of useful discussions. J. H. Black has been enormously helpful by aiding in the production of the spectral models. I also thank P. Maloney for comments on an early version of this chapter.

CHAPTER 6

LARGE MOLECULE PRODUCTION BY MASS-LOSING STARS

6.1 INTRODUCTION

In recent years much progress has been made toward identifying the carrier of the so-called diffuse interstellar bands and unidentified infrared emission features. The diffuse interstellar bands (DIBs), which have been known for many years to arise in the interstellar medium (Merrill 1934), consist of $\sim$ 50 absorption features in the wavelength range extending from 4430 Å into the near infrared (van der Zwet 1987). Since the advent of infrared astronomy, the unidentified infrared emission features (UIRs) have been observed to arise from a number of sources including planetary nebulae, reflection nebulae, H II regions, and galaxies. The UIRs appear as band-like features at $\lambda\lambda$3.28, 6.2, 7.7, 8.6, and 11 – 13 μm and probably result from UV-pumping of molecular vibrational transitions (Allamandola, Tielens, and Barker 1987a; Witteborn *et al.* 1989). It has been suggested that the carriers of these features are large molecules, in particular polycyclic aromatic hydrocarbons (PAHs), which are

distributed throughout the ISM (Duley and Williams 1981; Léger and Puget 1984; Allamandola, Tielens, and Barker 1985; Léger and d'Hendecourt 1985; van der Zwet and Allamandola 1985; Crawford, Tielens, and Allamandola 1985). Indeed, such large molecules were hypothesized to exist as early as 1956 (Platt 1956) and the suggestion that they may be PAHs was put forward in 1968 (Donn 1968). If such particles are responsible for the UIR features, then the strengths of these features suggest that the particles contain several percent of the available carbon and have an abundance relative to hydrogen of $10^{-8} - 10^{-7}$ (see, *e.g.*, Léger and Puget 1984; Léger and d'Hendecourt 1987). Thus, they may be one of the most abundant interstellar molecules. The importance of large molecules in the ISM extends beyond the identification of the DIBs and UIRs. The chemistries of both dense and diffuse clouds have been shown to be significantly altered by the inclusion of PAHs (Lepp and Dalgarno 1988; Lepp *et al.* 1988; Bohme, Wlodek, and Wincel 1989). Recent reviews of the subject include Allamandola, Tielens, and Barker (1987a, 1987b), Omont (1986), Léger, d'Hendecourt, and Boccara (1987), and Allamandola, Tielens, and Barker (1989). A thorough discussion of the emission mechanisms of interstellar PAHs has been made by Léger, d'Hendecourt, and Défourneau (1989).

In this chapter, we will briefly review the structure and chemistry of polycyclic aromatic hydrocarbons. It is frequently asserted that PAHs originate in the mass-loss winds of carbon-rich asymptotic giant branch stars (see, *e.g.*, Jura 1987b; Allamandola *et al.* 1989). Using recent models of PAH formation, we will explore this possibility. In addition, we will use simple arguments to

determine if the ISM can be well mixed in large molecules assuming their only source is AGB carbon stars. A number of suggestions for further study will be discussed.

6.2 Structure and Chemistry of PAHs

Due to the inherent complexity of polycyclic aromatic hydrocarbons, a complete review of their structure and chemistry is well beyond the scope of this chapter. The purpose of this section is to introduce the general properties of PAHs and the most important chemical processes which may involve large molecules in the interstellar and circumstellar medium. More detailed discussions can be found in the above mentioned reviews and in Lepp and Dalgarno (1988), Lepp *et al.* (1988), and Frenklach and Feigelson (1989).

a) *Structure*

PAHs are large planar, fused ring molecules. Terrestrial examples include napthalene ($C_{10}H_8$), chrysene ($C_{18}H_{12}$), pyrene ($C_{16}H_{10}$), and coronene ($C_{24}H_{12}$). The basic ring structure consists of six carbon atoms in a hexagonal cycle with hydrogen atoms bonded on the outside at each carbon. The well known benzene ring (C_6H_6) is the simplest PAH. Three general complex structures may be modeled (Omont 1986; see, also, Schmidt 1987; Léger *et al.* 1989). These include molecules in which the aromatic hexagonal cycles are bound linearly with a single C–C bond (*e.g.* biphenyl), linear structures in which two adjacent cycles share a common side ($C_{4n+2}H_{2n+4}$ where n is the number of rings), and quasi-circular structures in which there are i "layers" of rings around a central hexagonal cycle (*e.g.* coronene). The latter type has the

chemical formula $C_{6i^2}H_{6i}$, where $i-1$ is the number of layers or crowns, and are made up of $3i^2+3i+1$ rings. More complex variations of these basic structures are known to exist, *i.e.* ovalene ($C_{32}H_{14}$) and dicoronene ($C_{48}H_{20}$). Due to their extreme stability in harsh conditions, it is the quasi-circular structures and their variants which are most often assumed to exist in the interstellar medium. The most likely composition of PAHs in the ISM, however, is some mixture of these structures, dominated by the quasi-circular type, as is generally found in soot. Indeed, Allamandola *et al.* (1985) find a remarkable similarity between the Raman spectrum of auto exhaust and the 7.7 μm emission from the Orion bar region.

It has been shown that PAHs with ~ 20, or fewer, carbon atoms will be rapidly destroyed in the interstellar radiation field by the process of photothermodissociation. Larger molecules with an enormous number of vibrational modes are thought to be so efficient at internal conversion of absorbed energy that they may be almost indestructible by UV photodissociation. The mean size of interstellar PAHs is usually taken to be about 50 – 90 carbon atoms (Léger and Puget 1984; Allamandola *et al.* 1985; Léger and d'Hendecourt 1987; Omont 1986; Léger *et al.* 1989). A very broad range in sizes is likely to exist, however. It is interesting to note that the radius of a quasi-circular PAH is approximately $r = 0.9\sqrt{N_c}$ Å, where N_c is the total number of carbon atoms and a typical C–C distance is 1.4 Å (Omont 1986). Thus, for a 50 atom molecule, $r \approx 6.4$ Å. The surface area is $\sigma \approx 125$ Å^2.

b) *Chemistry*

The hydrogen bonds around the periphery of a PAH are especially susceptible to photolysis in the ambient UV radiation field. Thus, the hydrogens are likely to be removed from the molecule rapidly by photodissociation. Open bonds (radical sites) may be replaced by other atomic species and molecular ions and radicals. Ejection of hydrogen atoms may assist the survivability of PAHs in the ISM by cooling the molecule without disrupting the carbon bonds. There is much discussion as to how much an interstellar PAH will be dehydrogenated. It has been shown that interstellar PAHs with more than $\sim$ 25 carbon atoms will cool by infrared fluorescence at a rate faster than C–H bond breakage (Tielens *et al.* 1987; Allamandola *et al.* 1989). However, direct photolysis following absorption of a UV photon may be significant. If the number of radical sites on an interstellar PAH is large, the molecule will be highly reactive (Omont 1986). While most interactions will result in simple replacement of the hydrogen, other important reactions are possible. These reactions could result in growth by accretion of C atoms, or partial destruction of the molecule by reactions with O (Duley and Williams 1986; Duley 1987). Such processes are currently only poorly understood, however.

As pointed out by Omont (1986), if present in the numbers suggested, PAHs may play a prominent role in the chemistry of interstellar clouds. Due to a low first ionization potential ($\sim 6-7$ eV; Duley 1986; Omont 1986), PAHs exposed to UV radiation will be easily ionized. The large electron affinity of $\sim$ 3 eV (Léger and d'Hendecourt 1985) and cross section of a PAH make it an

important sink for free electrons in comparison with positive atomic ions, which recombine slowly, and small molecular ions, which are rare. Thus, there may be a large abundance of negatively charged PAHs within interstellar clouds. It is this ability to acquire charge which makes PAHs important to the chemistry in interstellar environments.

The dominant processes which determine the abundance of charged and neutral PAHs are photoionization and photodetachment

$$\mathrm{PAH} + h\nu \rightarrow \mathrm{PAH}^+ + e^-, \tag{VI.1}$$

$$\mathrm{PAH}^- + h\nu \rightarrow \mathrm{PAH} + e^-, \tag{VI.2}$$

and the inverse processes of radiative recombination and attachment

$$\mathrm{PAH}^+ + e^- \rightarrow \mathrm{PAH} + h\nu, \tag{VI.3}$$

$$\mathrm{PAH} + e^- \rightarrow \mathrm{PAH}^- + h\nu. \tag{VI.4}$$

Among the most important reactions which can involve PAHs and ions are charge transfer

$$\mathrm{X}^+ + \mathrm{PAH} \rightarrow \mathrm{X} + \mathrm{PAH}^+, \tag{VI.5}$$

and mutual neutralization

$$\mathrm{X}^+ + \mathrm{PAH}^- \rightarrow \mathrm{X} + \mathrm{PAH}. \tag{VI.6}$$

If the ionization potential of X is less than that of the PAH, then extraction of a hydrogen atom can occur in the reaction

$$\mathrm{X}^+ + \mathrm{PAH} \rightarrow \mathrm{XH}^+ + \mathrm{PAH}. \tag{VI.7}$$

This will likely be followed by dissociative recombination of the molecular ion.

The chemistry of neutral PAHs is up for debate. If reactions occur primarily at radical sites as proposed by Omont (1986), then Lepp *et al.* (1988) suggest that the formation of CO and CN may occur through

$$O + PAH \rightarrow CO + PAH, \tag{VI.8}$$

$$N + PAH \rightarrow CN + PAH. \tag{VI.9}$$

PAH^- will react with C, N, and O to form CH_4, NH_4, and H_2O by associative detachment. A neutral PAH may also form CH_4 in reactions with C and H at a radical site, assuming the C is not part of the lattice skeleton. We note, however, that Duley and Williams (1986) conclude that reactions of PAHs with H and O atoms will result in rapid destruction of the PAH molecule in less than 10^5 yrs.

In laboratory experiments, Bohme *et al.* (1989) have found that the reactions

$$\begin{aligned} Si^+ + C_{10}H_8 &\rightarrow SiC_{10}H_8^+ \\ &\rightarrow C_{10}H_8^+ + Si \end{aligned} \tag{VI.10}$$

occur in the ratio of 7 to 1. Thus, silicon can readily be incorporated into complex organic compounds. It was also found that $SiC_{10}H_8^+$ reacts rapidly with acetylene and diacetylene to form SiC_2H_2 and SiC_4H_2. A slow reaction with O_2 was seen which results in the formation of SiO_2. No reactions were observed for D, N, and C_6H_6 with $SiC_{10}H_8^+$. Bohme *et al.* suggest that these results imply that more general reactions of the type

$$SiPAH^+ + M \rightarrow PAH^+ + SiM \tag{VI.11}$$

and

$$XPAH^+ + M \rightarrow PAH^+ + XM \qquad \text{(VI.12)}$$

are likely if charge transfer does not dominate in processes like reaction (VI.10), which initates the sequence.

Recently, PAH chemistry has been included into the "standard" interstellar chemistries of both dense and diffuse molecular clouds by Lepp and Dalgarno (1988) and Lepp *et al.* (1988). In both cases, the presence of PAHs dramatically alters the ionization structure of the cloud. A PAH abundance relative to hydrogen of $\gtrsim 10^{-8}$ within a dense cloud results in most of the free electrons being taken up into PAH^-. In addition, the steady state abundances of carbon-bearing molecules in dense clouds are expected to be significantly enhanced. Since reactions with PAH^- replace dissociative recombination in the removal of H_2D^+, Lepp and Dalgarno propose that the measured DCO^+/HCO^+ abundance ratio can be used to obtain an upper limit to the abundance of PAHs in dense clouds. By examining observations of a number of clouds, they find that the abundance of PAHs in dense clouds cannot exceed $\sim 6 \times 10^{-6}$, which is in line with the abundances required to produce the UIRs.

Lepp *et al.* (1988) present detailed models of diffuse clouds which include PAH chemistry. Comparisons with observed abundances in the ζ Persei and ζ Ophiuchi clouds are made. In light of the effects of PAHs on the number of free electrons, the possibly important set of reactions

$$\begin{aligned} H_3^+ + PAH &\rightarrow PAH^+ + H + H_2 \\ &\rightarrow PAH^+ + H + H + H, \end{aligned} \qquad \text{(VI.13)}$$

$$\begin{aligned} H_3^+ + PAH^- &\rightarrow PAH + H + H_2 \\ &\rightarrow PAH + H + H + H, \end{aligned} \qquad \text{(VI.14)}$$

were included. They find that discrepancies between cloud densities inferred directly from level populations and from ionization balance are resolved if PAHs are present in abundances of $\sim 10^{-7}$ for ζ Persei and $\sim 6 \times 10^{-7}$ for ζ Ophiuchi.

As stated earlier, it is unlikely that PAHs in the interstellar medium are in a pure form. Indeed, in much of the chemistry just described, the polycyclic aromatic hydrocarbon could be replaced by a number of different species of very large molecules. The interstellar cloud models of Lepp and co-workers indicate that these large molecules must be present in large numbers. It is by inference to the large abundance of an unknown mixture of PAHs which is required to explain the UIRs, that we can assume that these unobserved large molecules are also PAHs.

6.3 CARBON STARS AND LARGE MOLECULES

There has been considerable discussion of how and where interstellar polycyclic aromatic hydrocarbons form. While it is possible that PAHs form in the gas phase within diffuse clouds (see, *e.g.*, Duley 1987), a more plausible alternative is that they arise from the fracturing of grains in shocks waves (Duley and Williams 1986; Omont 1986; Duley 1987). While interstellar and circumstellar carbon grains appear to be made up of PAH-like structures, the proposal that interstellar PAHs may be released by the cleaving of such grains remains unconfirmed. There continues to be much laboratory and observational work to be done. An alternative scenario is that they form by cyclization of long-chain hydrocarbon molecules (Ghosh 1987). However, a predicted abundance of $\sim 10^{-12}$ is in disagreement with that assumed for interstellar PAHs.

Another obvious source of PAH molecules may be the high temperature, carbon-rich environment of circumstellar envelopes surrounding mass-losing AGB carbon stars. PAH formation by oxygen-rich stars will be negligible because nearly all the available carbon is bound up in CO molecules. Keller (1987) and Gail and Sedlmayr (1987) have used thermodynamic calculations and considerations of non-TE effects to show that PAH production can be efficient in carbon star envelopes. In a more recent study, Frenklach and Feigelson (1989; hereafter F&F) employed a detailed chemical reaction network for gas phase PAH formation in model circumstellar envelopes. Based on reac-

tions that form soot in hydrocarbon flames, this study showed that PAHs can be formed in large abundance in carbon star winds. The results of Keller and Gail and Sedlmayr differ from those of F&F in the temperature range of peak PAH production (700 - 900 K and 900 - 1100 K, respectively) and maximum carbon atom content of a PAH (millions as opposed to 10^3 for F&F).

A number of recent studies have demonstrated that mass-loss from highly evolved carbon stars is a major contribution to the total amount of processed material returned to the ISM (Knapp and Morris 1985; Claussen *et al.* 1987; Thronson *et al.* 1987; Jura and Kleinmann 1989). These stars lose mass at rates of $10^{-8} - 10^{-4}\ M_\odot\ \mathrm{yr}^{-1}$ and may contribute as much as half the total quantity of material returned to the ISM by all AGB stars (see, *e.g.*, Knapp and Morris 1985; Knapp, Rauch, and Wilcots 1990). It is clearly evident from the above studies that the total mass loss rate by all carbon stars is dominated by a few of the most prolific objects. Since F&F find that the rate of PAH production is also greatest in stars with the highest mass-loss rates, it is of interest to assess how PAH production by these stars may affect the general ISM.

Defining the PAH yield Y as the fraction of carbon atoms originally in acetylene (C_2H_2) which are converted into PAHs of at least two rings, F&F have shown that

$$Y \approx 1\% \left(\frac{f_{C_2H_2}}{10^{-4}} \right)^3 \left(\frac{\dot{M}}{10^{-4}\ M_\odot\ \mathrm{yr}^{-1}} \right)^{2.5} . \qquad \text{(VI.15)}$$

For the carbon star IRC+10°216, the observed C_2H_2 abundance is $[C_2H_2]/[H_2] = f_{C_2H_2} \approx 2 - 3 \times 10^{-4}$ (McCabe, Connon Smith, and Clegg 1979; Lafont,

Lucas, and Omont 1982; Betz 1987). As discussed by F&F, it is difficult to assess how this abundance relates to the abundance at the inner PAH formation region. Indeed, if PAH formation is efficient, then it may be much higher than observed values. In the discussion which follows, we will accept an acetylene abundance of $[C_2H_2]/[H_2] = 3 \times 10^{-4}$.

If we assume that the stars losing mass at the highest rates were originally $\sim 2.5\ M_\odot$ objects (see Aaronson and Mould 1986; Thronson *et al.* 1987; Jura and Kleinmann 1989), then their lifetimes on the AGB as mass-losing stars are approximately 2×10^4 yrs. One star produces a total number of PAH molecules

$$N_{PAH} \approx 1.1 \times 10^{53} \left(\frac{Y}{0.3}\right) \left(\frac{f_{C_2H_2}}{3 \times 10^{-4}}\right) \times \left(\frac{\dot{M}}{10^{-4}\ M_\odot\ \mathrm{yr}^{-1}}\right) \left(\frac{t_*}{2 \times 10^4\ \mathrm{yr}}\right) \tag{VI.16}$$

during its mass-losing lifetime t_*, assuming each PAH survives much longer than t_*. If the molecules fill a spherical volume of radius r, then the mean density of PAHs at the the end of the mass-loss phase is

$$n_{PAH} \approx 1 \times 10^{-2} \left(\frac{Y}{0.3}\right) \left(\frac{f_{C_2H_2}}{3 \times 10^{-4}}\right) \left(\frac{\dot{M}}{10^{-4}\ M_\odot\ \mathrm{yr}^{-1}}\right) \times \left(\frac{t_*}{2 \times 10^4\ \mathrm{yr}}\right)^{-2} \left(\frac{V_\infty}{20\ \mathrm{km\ s}^{-1}}\right)^{-3}\ \mathrm{cm}^{-3}. \tag{VI.17}$$

V_∞ is the rate of expansion of the envelope. Thus, if high mass-loss rate carbon stars produce PAH yields like those of F&F, then the density of PAHs in the neighborhood of these stars will be large.

In order to assess the total number of PAHs in the Galaxy which may have come from carbon stars, we must know the lifetime τ_{PAH} of an

interstellar PAH and the birthrate ϕ_* of high mass-loss rate stars. Both of these parameters are highly uncertain. We will define a PAH "envelope" as a region which contains the total number of PAHs produced by a carbon star as given by equation (VI.16). This is simply a bookkeeping device to keep track of PAH production by a number of stars. The mean number of PAH envelopes in the Galaxy is then $\langle N_e \rangle \approx \phi_* \tau_{PAH}$, assuming steady state. If the mean number of PAHs per envelope is $\langle \mathcal{N}_{PAH} \rangle$, then their total number is $N_{PAH} = \langle N_e \rangle \langle \mathcal{N}_{PAH} \rangle$.

The birthrate of mass-losing carbon stars has been been determined by a number of techniques (Claussen *et al.* 1987; Thronson *et al.* 1987; Jura and Kleinmann 1989). However, it is not clear what the birthrate should be for the most extreme mass-losing stars. This birthrate depends upon whether all AGB carbon stars go through a brief phase of extreme mass-loss, repeated phases, or only certain objects attain rapid mass-loss. To avoid this uncertainty, we will make the assumption that the product of ϕ_* and τ_* is the mean number of high mass-loss rate carbon stars, which can be estimated from current data.

Due to their short lifetime, extreme mass-losing stars are rare. From the data of Knapp and Morris (1985; their Figure 22) it can be estimated that $n_* \sim 1.1 \times 10^{-9}$ pc^{-3} for carbon stars with $\dot{M} \approx 10^{-4}$ $M_\odot$ yr^{-1}. This is $\sim 3\%$ of the surface density of high mass-loss rate carbon stars in the solar neighborhood (for scale height $h_* = 200$ pc) as found by Jura and Kleinmann (1989), and is fully consistent with their having found no stars with $\dot{M} \geq 5 \times 10^{-5}$ $M_\odot$ yr^{-1} within 1 kpc of the Sun. However, we note that one extreme object which

appears in both studies (AFGL 2688) is found to have $\dot{M} \approx 1.6 \times 10^{-4}\ M_{\odot}\ \mathrm{yr}^{-1}$ by Knapp and Morris, while Jura and Kleinmann find it to have a factor of 4 slower $\dot{M}$ by a different method (see discussion in §III of Jura and Kleinmann). Since $\dot{M}$ appears in equations (VI.15) and (VI.16) to high powers, the accuracy in determining of mass-loss rates is an important uncertainty. In any case, we estimate the number of carbon stars with $\dot{M} \approx 10^{-4}\ M_{\odot}\ \mathrm{yr}^{-1}$ to be

$$N_{*} \approx 310 \left(\frac{R_{Gal}}{15\ \mathrm{kpc}} \right)^{2} \left(\frac{h_{*}}{200\ \mathrm{pc}} \right). \qquad \text{(VI.18)}$$

The dependence on galactic radius appears since the number density of carbon stars in the Galaxy appears to be constant with galactic radius (Thronson *et al.* 1987; Jura, Joyce, and Kleinmann 1989). The scale height $h_{*} \approx 200$ pc for dusty carbon stars is taken from Claussen *et al.* (1987) and Jura and Kleinmann (1989).

The lifetime of a free PAH in the interstellar medium is by no means well constrained. As mentioned earlier, Duley and Williams (1986) and Duley (1987) argue for rapid destruction of free PAHs. They suggest a lifetime of $\lesssim 10^{5}$ yrs. Such a short lifetime would require that PAHs be formed *in situ* where they are observed in the interstellar medium. On the other hand, Omont(1986) states that large PAHs are stable against chemical disruption and can survive weak shocks. If PAHs have characteristics similar to small grains in terms of their behavior in shocks and the hot coronal gas, then their mean lifetime will be governed by exposure to supernova remnants. Thus, interstellar PAHs may survive as long as a few $\times\ 10^{8}$ yrs (see, also, Allamandola *et al.* 1989).

If $\tau_{PAH} \approx 10^8$ yrs, it is easy to see that $\langle N_{PAH} \rangle = N_{PAH}$ as given by equation (VI.16), since $\tau_{PAH} \gg \tau_*$. The number of PAH envelopes is $\langle N_e \rangle \approx N_* \tau_{PAH}/\tau_* = 1.6 \times 10^6$. Thus, the total number of PAH molecules produced by mass-losing carbon stars contained within the Galaxy is

$$N_{PAH} \approx 1.7 \times 10^{59} \left(\frac{Y}{0.3}\right) \left(\frac{f_{C_2H_2}}{3 \times 10^{-4}}\right) \left(\frac{\dot{M}}{10^{-4}\ M_\odot\ \mathrm{yr}^{-1}}\right) \times \left(\frac{N_*}{310}\right) \left(\frac{\tau_{PAH}}{10^8\ \mathrm{yr}}\right). \tag{VI.19}$$

In order to determine the mean density of PAHs in the Galaxy, we assume that interstellar PAHs will quickly redistribute into the general interstellar gas. The scale height for this gas is ≈ 120 pc (Spitzer 1978; Mihalas and Binney 1981). Thus, assuming a uniform disk, the mean number density of PAHs is

$$\langle n_{PAH} \rangle \approx 3.4 \times 10^{-8} \left(\frac{Y}{0.3}\right) \left(\frac{f_{C_2H_2}}{3 \times 10^{-4}}\right) \left(\frac{\dot{M}}{10^{-4}\ M_\odot\ \mathrm{yr}^{-1}}\right) \times \left(\frac{N_*}{310}\right) \left(\frac{\tau_{PAH}}{10^8\ \mathrm{yr}}\right) \left(\frac{15\ \mathrm{kpc}}{R_{Gal}}\right)^2 \times \left(\frac{120\ \mathrm{pc}}{h_{gas}}\right)\ \mathrm{cm}^{-3}. \tag{VI.20}$$

Since this is an average density in the Galaxy, it can also be taken to be the mean abundance relative to hydrogen, which has an average density of $\langle n_H \rangle \approx 1\ \mathrm{cm}^{-3}$ (Spitzer 1978). While fully appreciating the uncertainties which have gone into this simple estimate, we note that the final result is within small factors of values found from chemical models and observations of specific regions.

For a free flying lifetime of $\tau_{PAH} \sim 10^8$ yrs, the ISM will be well mixed in PAHs produced only in carbon star winds. A typical expansion

velocity of a mass-losing carbon star envelope is $V_\infty \approx 20$ km s^{-1} (Knapp and Morris 1985). At this velocity a PAH will travel an average linear distance of 6×10^{21} cm before being destroyed. This is approximately twice the mean distance between the carbon stars which act as sources of the PAHs. The actual motion, if magnetic fields are ignored, will approach a random walk through the Galaxy. Thus, PAHs will be uniformly distributed throughout the Galaxy, with the galactic gravitational potential helping them to settle into the plane. The situation is complicated by how PAHs respond to radiation pressure. The scale height and distribution of the stars responsible will depend on what light (*i.e.* UV or visible) is most effective in producing the radiation pressure. UV sources such as OB stars have a very small scale height and are located in fairly isolated regions. Stars which are sources of visible light are more evenly distributed and may have a scale height greater than the PAH producing AGB stars. The galactic magnetic field may organize the distribution, possibly causing the PAHs to collect into clouds. Perhaps more importantly, 10^8 yrs is approximately equivalent to the galactic rotation period and an order of magnitude longer than the lifetime of a typical giant molecular cloud (Blitz and Shu 1980). A detailed assessment of the mixing would involve an understanding of how a charged, planar particle like a PAH moves through the ISM, and how it is influenced by magnetic fields. It is, in any case, easy to see that PAHs are ejected from carbon star winds with sufficient velocity, and assuming $\tau_{PAH} \sim 10^8$ yrs, that they will be fully distributed throughout the ISM.

6.4 DISCUSSION

We have used reasonable estimates of parameters and the most detailed model available for the production of polycyclic aromatic hydrocarbons in carbon star winds to derive a mean abundance of PAHs in the interstellar medium, assuming no other sources. While the result presented in equation (VI.20) remains highly uncertain, it is clear that a large fraction of observed and inferred PAHs can arise from stellar mass-loss. Indeed, this type of mean abundance is very likely an underestimate for isolated regions. Whatever the mechanisms are which cause the ISM to associate into clouds, it is conceivable that large planar molecules like PAHs are more strongly influenced than small atomic species. This could arise from the large cross section in one orientation to radiation pressure and particle collisions. If the yield of F&F underestimates PAH production in stars with somewhat lower mass-loss rates than $\dot{M} \sim 10^{-4}$ $M_{\odot}$ yr^{-1}, then the interstellar abundance of PAHs could easily be increased by the much greater number of stars available.

Perhaps the most uncertain and difficult to evaluate parameter is τ_{PAH}. If the estimate $\tau_{PAH} \lesssim 10^5$ yrs of Duley and Williams (1986) and Duley (1987) is correct, then PAH production by carbon stars is negligible, even for a yield of 100%. However, it has been asserted that the majority of dust produced by carbon stars is composed of amorphous carbon (Rowan-Robinson and Harris 1983; Jura 1986; Thronson *et al.* 1987). As mentioned in §6.3, amorphous

carbon grains appear to be made up of PAH-like structures. Hydrogenation of these particles may occur in the ISM. Disruption of these grains can provide an additional source of free interstellar PAHs, independent of gas phase reactions in mass-loss winds. Again, Duley and Williams state that amorphous carbon grains will not survive long in the ambient ISM. However, they argue that the lifetime will be much longer in dense diffuse clouds or dark clouds. It remains unclear as to whether PAHs may originate from grains formed during the stellar mass-loss process.

Even with the current uncertainties, we assert that the majority of PAHs which may exist in the interstellar medium were formed in the mass-loss winds of AGB carbon stars. Other sources such as R CrB and Wolf-Rayet stars and planetary nebulae may provide an additional contribution. The chemical formation network in such objects is likely to be much different than the hydrocarbon pyrolysis reactions used by F&F due to the paucity of hydrogen (see Allamandola *et al.* 1989). Much work remains to be done. The lifetime of a free PAH in the interstellar medium must be determined with greater confidence. The chemical models of F&F need to be expanded and the contribution from moderate to high mass-loss rate objects assessed in detail. While there is disagreement with other work, the models of F&F strongly indicate that PAH production takes place within the temperature range 900 - 1100 K. The current wind models should be reassessed for accuracy in this crucial regime. If the sensitivity of PAH yield to mass-loss rate remains, an accurate assessment of the numbers of extremely high mass-loss rate stars in the Galaxy

must be made. Recent work has been heading in this direction, and such a census will soon be possible. However, determination of the mass-loss rate of individual stars needs to be more accurate. The current techniques for determining $\dot{M}$ have been reviewed by Knapp *et al.* (1990). Most of these methods presume spherically symmetric mass-loss. Perhaps the greatest difficulty in this area is asymmetry in the mass-loss wind from many stars. It has been argued (Jura 1983) that this will be a small effect unless the asymmetry is extremely large. Detailed models for individual objects may be required. In addition, an empirical determination of how C_2H_2 is distributed throughout a stellar dust envelope would be highly desirable. There is already a strong indication that the acetylene abundance increases toward the inner, hotter regions of the envelope surrounding IRC+10°216 (Betz 1987 and references therein; Keady and Hinkle 1988).

It would be of interest to consider how PAHs interact with the ISM and the galactic magnetic field. Clearly, PAHs cannot fly indefinitely through the ISM at the wind speed. Consideration of how they move may be important in light of their extreme, planar structures and large cross sections both for radiation pressure and for sweeping of gas in one orientation, but nearly negligible cross sections in other orientations. Do they tumble? It has been shown that a large fraction of PAHs will be charged. How might they align with magnetic fields? Does the galactic magnetic field constrain their travel through the ISM? If PAHs are shown to exist in the numbers currently put forth, then such questions may be vital to the determination of their impor-

tance in a number of interstellar processes including star formation, and how they might be used as molecular diagnostics.

CHAPTER 7

SUMMARY

Your point is well taken. What is it?

– J. J. Charfman

In the early days of astronomy, the Universe was thought to be a stable, placid place with little more than bright lights hanging from the celestial sphere. Our modern understanding of the Universe is much different. We now know that we are surrounded by violent, rapidly evolving systems. Indeed, the Universe itself may have formed out of a blast of incomprehensible proportions. This dissertation has examined the molecular processes which take place in a number of such systems. The diversity of this work reflects the variety of environments, both quiet and violent, in which molecules are found. To summarize:

- In Chapter 1, we briefly reviewed the contents of the interstellar and circumstellar medium. It was shown that the ISM is a complex, continuously evolving system in which molecular processes play a vital role. The most important chemical processes common in astrophysics were described.

• Molecular formation by radiative association was described in Chapter 2. A semi-classical calculation of thermal rate coefficients for the processes $H(n=2) + H(n=1) \rightarrow H_2 + h\nu$ and $C^+ + O \rightarrow CO^+ + h\nu$ was presented. The results are listed in Tables II.1 and II.2, respectively. The relative importance of the excited atom association process to form H_2 was discussed. It was shown that the excited atom process will not be important except possibly in environments where $L\alpha$ trapping is large. Examples may be the material surrounding quasars, active galactic nuclei, and bright H II regions. Other possibilities may be within rapidly evolving systems where a large transient n = 2 population of neutral hydrogen could result in a burst of molecular hydrogen formation. A rate coefficient for CO^+ radiative association was calculated specifically to test its importance in the formation of CO in SN 1987A. It was later shown in Chapter 4 that, if hydrogen is present, this process cannot compete with the more conventional routes which lead to the formation of CO. It may, however, be important in the core of the supernova.

• Chapter 3 presented a detailed review of the epoch of recombination in the early Universe. Atomic and molecular processes around this period were examined. The equations of ionization balance and molecular formation and destruction were integrated through the recombination epoch and results presented. This was followed by a detailed examination of various processes, including heating and cooling of the primordial plasma, damping of fluctuations prior to decoupling, and the possibility of a radiation driven instability at the onset of recombination. A full summary of results is given in §3.5 and will not

be reiterated here. A key result is that the asymptotic H_2 fractional abundance calculated in every model exceeds 10^{-6}. This is the minimum required to provide sufficient cooling of gravitationally unstable regions for the initial collapse to continue. A similar result was found in the earlier work of Lepp and Shull (1984). While the processes described in Chapter 3 are not directly observable today, the consequences of these processes can be seen in the form of galaxies, galaxy clusters, and stars. An understanding of how atoms, ions, and molecules evolve in the early Universe will help to unravel the mystery of how large structures may have formed.

• We explored another evolving system on a somewhat smaller scale in Chapter 4. Molecular formation and destruction processes were analyzed in the rapidly expanding outer envelope of Supernova 1987A. A calculation was presented of the time-dependent chemical evolution in a model which uses a homologously expanding sphere to represent the envelope. The aim of this chapter was to establish the general properties of the chemistry and to identify diagnostics which may be used to study the supernova evolution. Various cooling rates and hydrogen abundances in the envelope were examined. It was found that large abundances of molecules, in particular CO, form rapidly, while hydrogen remains mostly in its atomic forms. Molecule formation is not inhibited if the total hydrogen abundance is reduced by a significant amount. Possible future observations for probing the evolution of the supernova ejecta were discussed.

• Newly acquired near-infrared observations of the proto-planetary nebula CRL 618 were presented in Chapter 5. This object is a classical bipolar reflection nebula. Images in the H and K bandpasses were shown to have an appearance consistent with a bipolar axis highly inclined to the plane of the sky. An unresolved, compact source is seen in these images. This region is assumed to be the 0".4 source observed previously in the far-infrared and at radio wavelengths. The infrared spectrum of the compact source is dominated by thermal dust emission. This emission likely arises from a dust torus surrounding the central star, obscuring it from view at optical wavelengths. Faint emission from the lobes is attributable to cool dust. Spectroscopy in the range $\lambda\lambda 0.950 - 1.330$ μm was presented and discussed. Emission from molecular hydrogen is present in the spectrum. A visual extinction of $A_v = 5.3 \pm 2.5$ magnitudes to the H_2 emitting lobes was found. Models of thermal and fluorescent H_2 emission were presented and comparison with the data was made. It was found that the near-infrared H_2 spectrum is dominated by emission from thermally excited molecules at $T_{ex} \sim 2000$ K. A component of fluorescent emission from H_2 may be present, however.

• The structure and chemistry of large molecules, in particular polycyclic aromatic hydrocarbons, were briefly reviewed in Chapter 6. Such molecules have been invoked as carriers of the diffuse interstellar bands and the unidentified infrared emission features. In addition, large molecules may strongly influence molecular cloud chemistry. Through the use of recent models for PAH formation and a simple argument, it was asserted that the primary source of

interstellar PAHs is mass-losing AGB carbon stars. It is apparent that the known numbers of the most extreme mass-losing carbon stars are able to produce PAHs in sufficient quantities as to maintain an interstellar medium well mixed in such molecules at the inferred abundance.

Throughout this dissertation an attempt has been made to understand the existence of molecules and their abundances in differing environments. The primary focus has been on rapidly evolving systems. It has been shown that molecule formation in an expanding environment can be efficient. The prerequisite condition is that the rate of expansion not exceed the rate of molecular synthesis. This has now been shown to be the case for a number of environments, including novae, supernovae, protostellar winds, and the early Universe.

To reiterate a statement made in Chapter 1, it is important that we understand not only the conditions under which atomic and molecular emission occur, but also the circumstances which will lead to molecule formation. Only through this type of insight can we ever hope to decipher the complex chemical environment which makes up the Universe. It is hoped that this work has provided some additional clues.

What! You have solved it already?
Well, that would be too much to say.
I have discovered a suggestive fact,
that is all....

– Dr. Watson and Sherlock Holmes,
The Sign of Four

APPENDIX A

GRAIN SURFACE CHEMISTRY vs. THE GAS PHASE

While much of the discussion contained in this dissertation focuses on environments devoid of dust grains, it is important to understand why grain surface reactions may be extremely important within regions containing cool ($T_g \lesssim 40$ K) dust particles. The following example concentrates on the formation of the most abundant interstellar molecule, molecular hydrogen (H_2). Other important processes involving grains include depletion of heavy elements into grains and onto grain surfaces and extinction of ultraviolet radiation, both of which can strongly influence atomic and molecular abundances.

In steady state, formation and destruction processes are balanced such that

$$k_{H_2} n_H^2 = \Gamma_{H_2} n_{H_2} \qquad (A.1)$$

where k_{H_2} is the total formation rate coefficient in cm^3 s^{-1}, Γ_{H_2} is the total destruction rate, n_H is the atomic hydrogen gas number density, and n_{H_2} is the molecular hydrogen number density (Note: The time scale to equilibrium for a diffuse cloud is of the order 10^5 years for clouds with lifetimes of $\gtrsim 10^7$ years (*e.g.* Blitz and Shu 1980) and is, therefore, a good assumption). For a typical diffuse cloud: $\Gamma_{H_2} = 5 \times 10^{-11}$ s^{-1} at the boundary, $n_H = 100$, and

$n_{H_2}/n_H = 2\times10^{-6}$ (van Dishoeck and Black 1986). Thus, k_{H_2} must be $\approx 10^{-18}$ cm^3 s^{-1}. The rate coefficient for the radiative association reaction

$$H + H \rightleftarrows H_2^* \rightarrow H_2 + h\nu \qquad (A.2)$$

can be simply estimated in the following way (see Chapter 2). The probability of a stabilizing transition occurring within the particle interaction time is

$$P = A_{ul}\delta t \qquad (A.3)$$

where A_{ul} is the Einstein transition probability and δt is the collision time. To estimate δt we take $\delta t = d/\langle v\rangle$. The mean thermal velocity is $\langle v\rangle \approx 10^5$ cm s^{-1} at 100 K and $d = 1$ Å (= 2 bohr). Thus $\delta t \approx 10^{-13}$ s. In the most general case, at 100 K the atoms will be in the ground electronic state. Homonuclear molecules with a $^1\Sigma$ ground state like H_2 have no permanent electric dipole moments. As a result, they can have no allowed pure rotational transitions. Only exceedingly weak electric quadrupole transitions are possible. Therefore, the only stablizing transition in the $X^1\Sigma_g^+$ molecular ground state involves a vibrational transition for which $A_{ul} \lesssim 10^{-6}$ s^{-1}. This gives $P \lesssim 10^{-19}$. The collision rate is $\sigma\langle v\rangle$ cm^3 s^{-1} with $\sigma = 10^{-16}$ cm^2 and $\langle v\rangle = 10^5$ cm s^{-1}. We now have that

$$k_{A.2} \approx \sigma\langle v\rangle P = 10^{-11}\times10^{-19} = 10^{-30} \text{ cm}^3 \text{ s}^{-1}. \qquad (A.4)$$

Thus, reaction (A.2) is extremely slow and completely negligible.

There are other processes which are more promising and are known to be important in dust-free environments. The radiative association reaction

$$H + H^+ \rightarrow H_2^+ + h\nu, \qquad (A.5)$$

has a rate coefficient $k_{A.5} \lesssim 10^{-18}$. The resulting H_2 formation takes place by the charge transfer reaction

$$H_2^+ + H \rightarrow H_2 + H^+, \tag{A.6}$$

for which $k_{A.6} \approx 10^{-9}$ (see Table III.1 in Appendix B). But $n_H \gg n_{H^+}$ in the general interstellar medium. If we take the most optimistic case where every H_2^+ ion survives to form H_2, then the rate of H_2 formation is $\lesssim 10^{-18} n_H n_{H^+}$. With $n_{H^+} \lesssim 10^{-4} n_H$ cm^{-3}, the effective rate coefficient is $k_{H_2} \lesssim 10^{-22}$ cm^3 s^{-1}. A similar argument can be made for the H^- process

$$\begin{aligned} H + e^- &\rightarrow H^- + h\nu \\ H + H^- &\rightarrow H_2 + e^-. \end{aligned} \tag{A.7}$$

The importance of the reactions

$$\begin{aligned} C^+ + H &\rightarrow CH^+ + h\nu \\ CH^+ + H &\rightarrow C^+ + H_2 \end{aligned} \tag{A.8}$$

is more difficult to assess. The rates for reactions (A.8) are presented in Table IV.1 in Appendix B. For a temperature of $T \approx 100$ K, we can use the same arguments as for the H_2^+ process, reactions (A.5 - A.6), to show that reactions (A.8) fail to give the required rate by at least 3 orders of magnitude. However, the observed CH^+ abundance in the ISM is at least 2 orders of magnitude larger than is predicted by models. This is the well-known "CH^+ problem" described by Black (1989). For an observed abundance of $n_{CH^+}/n_H \sim 5 \times 10^{-9}$ (van Dishoeck and Black 1986) the effective rate coefficient to form H_2 is $k_{H_2} \sim 8 \times 10^{-19}$ cm^3 s^{-1}, very nearly the required value. However, the exponetial factor in the rate coefficient for the second of

reactions (A.8) quickly makes this process too slow for temperatures much less than 100 K. The net result is that none of these gas phase processes are fast enough to maintain the observed molecular hydrogen abundance throughout the ISM.

The rate coefficient for molecule formation on a grain surface is approximately given by

$$k_g = \frac{1}{2}\pi \langle r_g \rangle^2 \langle v \rangle \xi \quad \mathrm{cm}^3\ \mathrm{s}^{-1}, \tag{A.9}$$

where ξ is the probability of the reaction taking place, $\langle r_g \rangle$ is the mean grain radius, and $\langle v \rangle$ is the mean thermal velocity (Hollenbach, Werner, and Salpeter 1971). The formation rate is then $R_g = k_g n_g n_{\mathrm{H}}$ $\mathrm{cm}^{-3}\ \mathrm{s}^{-1}$. In order to compare rates, we must have an expression similar to the left side of equation (A.1). Thus, we will write

$$\begin{aligned} R_g &= k_g n_{\mathrm{H}} n \epsilon \\ &= \frac{1}{2}\left(\frac{\pi \langle r_g \rangle^2 n_g}{n}\right) v \xi n_{\mathrm{H}} n \\ &= \frac{1}{2}\eta \langle v \rangle \xi n_{\mathrm{H}} n \\ &= k_{\mathrm{H}_2} n_{\mathrm{H}} n \\ &\approx k_{\mathrm{H}_2} n_{\mathrm{H}}^2 \quad \mathrm{cm}^{-3}\ \mathrm{s}^{-1}, \end{aligned} \tag{A.10}$$

where ϵ $(= \frac{n_g}{n})$ is the dust to gas ratio, η is the surface area due to dust per H atom, and $k_{\mathrm{H}_2} = \frac{1}{2}\eta \langle v \rangle \xi$. We can determine η through the empirical relationship (Bohlin, Savage, and Drake 1978)

$$\left\langle \frac{N(\mathrm{H} + \mathrm{H}_2)}{E(\mathrm{B}-\mathrm{V})} \right\rangle = 5.8 \times 10^{21} \quad \mathrm{cm}^{-2}\ \mathrm{mag}^{-1}, \tag{A.11}$$

and by employing the standard expressions

$$\tau_V = Q_{ext}\pi \langle r_g \rangle^2 n_g L,$$
$$A_V = 1.086\tau_V, \qquad \text{(A.12)}$$
$$A_V = 3.0E(B-V),$$

and $Q_{ext} \approx 2$ (Spitzer 1978), with $\langle A_V/L \rangle \approx 1.89$ mag kpc^{-1} (Münch 1952). Thus, $\eta = 2.4 \times 10^{-22}$ cm^2. With $\langle v \rangle = 10^5$ cm s^{-1}, we find $k_{H_2} = 1.2 \times 10^{-17}\xi$ cm^3 s^{-1}. For this process to be rapid enough, we only require $\xi \approx 0.1$.

While the argument presented here has has not been a rigorous proof, it should be clear that grain surface formation of H_2 in interstellar dust clouds is the dominant and required process to maintain the observed equilibrium abundance. Gas phase reactions can (for order of magnitude calculations) be neglected. Grain surface processes of heavier elements and molecules may be much more complicated. Indeed, in dark clouds, cold grains may act as sinks for gas phase molecules (see, *e.g.*, Prasad *et al.* 1987; Watson and Salpeter 1972). Spectroscopic signatures of solid CO (presumably frozen out of the gas onto grain surfaces) have been observed in several interstellar clouds (Lacy *et al.* 1984; Larson *et al.* 1985). A great deal of chemical processing can take place in the accreted material. Sputtering of grains in shocks or destruction by chemical processes may return appreciable molecular abundances into the interstellar medium (Seab 1987). Thus, the presence of grains can both enrich the environment in chemical species, and rob it of them.

APPENDIX B

TABLES OF CHEMICAL REACTIONS

In this appendix, tables of the chemical reactions and rates which were used in the models discussed in Chapters 3 and 4 are presented. Table III.1 lists the chemistry which may have occurred around the epoch of recombination in the early Universe. The reactions used to describe the chemistry within the expanding envelope of Supernova 1987A can be found in Table IV.1. Brief references for each reaction rate appear at the end of each table. The complete references follow the main reference list at the end of this dissertation.

TABLE III.1

THE CHEMISTRY AT RECOMBINATION

#	Reactants	Products	Rate ($cm^3\ s^{-1}$)	Reference
Reactions involving H				
1	$H + h\nu$	$H^+ + e$	see text	
2	$H + H^-$	$H_2 + e$	2.0×10^{-9}	21
3	$H + H_2^+$	$H_2 + H^+$	6.4×10^{-10}	9
4	$H + H_2$	$H + H + H$	$6.5 \times 10^{-7} \exp(-52000/T_{mat}) T_{mat}^{-1/2}$ $\times[1 - \exp(-6000/T_{mat})]$	20
5	$H + H^+$	$H_2^+ + h\nu$	a	1,2
6	H(n=2) + H(n=1)	$H_2 + h\nu$	1.0×10^{-13}	1
7	$H + HeH^+$	$H_2^+ + He$	9.1×10^{-10}	9
8	$H + e$	$H^- + h\nu$	b	17
9	$H + HD$	$H + H + D$	same as reaction 4	
10	$H + HD^+$	$HD + H^+$	6.4×10^{-10}	9
11	$H + D$	$HD + h\nu$	1.0×10^{-25}	3
12	$H + D^+$	$HD^+ + h\nu$	same as reaction 5	
		$H^+ + D$	2.0×10^{-9}	4
Reactions involving H^+				
13	$H^+ + H^-$	$H + H$	$4.0 \times 10^{-6} T_{mat}^{-1/2}$	5,6

TABLE III.1 - *Continued*

14	$H^+ + He$	$HeH^+ + h\nu$	$2.24 \times 10^{-17} T_{mat}^{-0.7825} \exp(908/T_{mat})$	18
			$7.9 \times 10^{-18} T_{mat}^{-1/2} \quad T_{mat} \leq 1000$	
15	$H^+ + HD$	$H_2 + D^+$	$8.0 \times 10^{-10} \exp(-405/T_{mat})$	7
16	$H^+ + D$	$HD^+ + h\nu$	same as reaction 5	
		$H + D^+$	$2.0 \times 10^{-9} \exp(-43/T_{mat})$	4
17	$H^+ + e$	$H + h\nu$	see text	15
Reactions involving H_2^+				
18	$H_2^+ + e$	$H + H$	$3.65 \times 10^{-7} T_{mat}^{-0.37}$	16
19	$H_2^+ + h\nu$	$H + H^+$	c	22
20	$H_2^+(v > 3) + He$	$HeH^+ + H$	$3.0 \times 10^{-10} \exp(-6717/T_{mat})$	18
21	$H_2^+ + H^-$	$H + H + H$	$4.0 \times 10^{-6} T_{mat}^{-1/2}$	5,6
		$H + H_2$		
22	$H_2^+ + H_2$	$H_3^+ + H$	2.1×10^{-9}	8
Reactions involving H_2				
23	$H_2 + h\nu$	$H + H$	d	23
24	$H_2 + e$	$H + H + H$	$6.4 \times 10^{-12} T_{mat}^{1/2} \exp(-139000/T_{mat})$	23
25	$H_2 + D^+$	$HD + H^+$	8.0×10^{-10}	7
26	$H_2 + He^+$	$He + H + H^+$	1.0×10^{-13}	19
27	$H_2 + HeH^+$	$H_3^+ + He$	1.26×10^{-9}	10
Reactions involving H^-				
28	$H^- + h\nu$	$H + e$	by detailed balance with reaction 8	17

TABLE III.1 – *Continued*

29	$H^- + He^+$	$He + H$	$4.0 \times 10^{-6} T_{mat}^{-1/2}$	5,6
30	$H^- + D$	$HD + e$	2.0×10^{-9}	9
Reactions involving HeH^+				
31	$HeH^+ + e$	$He + H + h\nu$	1.0×10^{-11}	18
32	$HeH^+ + h\nu$	$He^+ + H$	$2.62 \times 10^7 \exp(-133210/T_{rad})$ s^{-1}	18
33	$HeH^+ + D$	$HD^+ + He$	9.1×10^{-10}	9
Reactions involving HD				
34	$HD + h\nu$	$H + D$	same as reaction 23	
35	$HD + He^+$	$He + H^+ + D$ $He + H + D^+$	1.0×10^{-13}	19
36	$HD + e$	$H + D + e$	same as reaction 24	
Reactions involving HD^+				
37	$HD^+ + e$	$H + D$	$3.65 \times 10^{-7} T_{mat}^{-0.37}$	16
38	$HD^+ + h\nu$	$H + D^+$ $H^+ + D$	same as reaction 19	
39	$HD^+(v > 3) + He$	$HeH^+ + D$	$3.0 \times 10^{-10} \exp(-6717/T_{mat})$	18
Reactions involving H_3^+				
40	$H_3^+ + e$	$H_2 + H$	$1.9 \times 10^{-6} T_{mat}^{-1/2}$	11
		$H + H + H$	$1.9 \times 10^{-6} T_{mat}^{-1/2}$	11

TABLE III.1 - *Continued*

Reactions involving He_2^+				
41	$He_2^+ + H_2$	$He_2H^+ + H$	5.3×10^{-10}	12
42	$He_2^+ + e$	$He + He$	1.0×10^{-11}	13
43	$He_2^+ + h\nu$	$He^+ + He$	$3.0 \times 10^8 \exp(-133210/T_{rad})$ s^{-1}	14
Reactions involving He, He^+, He^{++}, D, and D^+				
44	$He + h\nu$	$He^+ + e$		23
45	$He + He^+$	$He_2^+ + h\nu$	1.0×10^{-16}	14
46	$He^+ + h\nu$	$He^{++} + e$		23
47	$He^+ + e$	$He + h\nu$	$1.01 \times 10^{-10} T_{mat}^{-0.642}$	23
48	$He^{++} + e$	$He^+ + h\nu$	$2.176 \times 10^{-10} (T_{mat}/4)^{-0.7278}$	23
49	$D + h\nu$	$D^+ + e$	same as reaction 1	
50	$D^+ + e$	$D + h\nu$	same as reaction 17 (see eq. III.11)	

NOTES FOR TABLE III.1

a) $k_5 = 10^{-20}\exp(3.37119 - 2.84341\ln(T_{mat}) + 0.726574[\ln(T_{mat})]^2 - 0.0368664[\ln(T_{mat})]^3)$
$= 10^{-20}(1.50982 - 0.00533637T_{mat} + 0.000804546T_{mat}^2) \quad T_{mat} < 50$

b) $k_8 = 10^{-15}[0.87235471 + 0.37721590(T_{mat}/1000) - 0.011361003(T_{mat}/1000)^2$
$-1.2224447 \times 10^{-4}(T_{mat}/1000)^3] \quad 5000 > T_{mat} > 2500$
$= 10^{-18}T_{mat}(1.0684935 - 2.5771494 \times 10^{-4}T_{mat} + 4.5173269 \times 10^{-8}T_{mat}^2)$
$2500 \geq T_{mat} \geq 10$

c) Calculated for H_2^+ thermally populated at T_{mat} and destroyed by radiation at T_{rad}.

d) $\Gamma_{H_2} = 6.5375 \times 10^9 \exp(-142444/T_{rad})\Psi \ \ s^{-1}$
$\Psi = 0.01[1.42997 + 0.258955(T_{rad}/1000) + 0.0330835(T_{rad}/1000)^2 - 0.00241683(T_{rad}/1000)^3]$

REFERENCES FOR TABLE III.1

1) This work.
2) Bates 1951.
3) Lepp and Shull 1984.
4) Smith 1966.
5) Dalgarno and McCray 1973.
6) Peterson *et al.* 1971.
7) Fehsenfeld *et al.* 1973.
8) Bowers *et al.* 1969.
9) Karpas, Anicich, and Huntress 1979.
10) Orient 1977
11) Prasad and Huntress 1980.
12) Adams, Bohme, and Ferguson 1970.
13) Ferguson, Fehsenfeld, Schmeltekopf 1965.
14) Estimate.
15) Peebles 1968.
16) Auerbach *et al.* 1977.
17) Calculated from cross sections of Wishart 1979.
18) Roberge and Dalgarno 1982.
19) Johnsen and Biondi 1974.
20) Jacobs, Giedt, and Cohen 1967.
21) Browne and Dalgarno 1969 and Bieniek and Dalgarno 1979.
22) Calculated from cross sections of Dunn 1968
23) Black, J. H., private communication.

TABLE VI.1

SUPERNOVA ENVELOPE CHEMISTRY

#	Reactants	Products	Rate ($cm^3\ s^{-1}$)	Reference
Hydrogen Reactions				
1	$H^+ + H$	$H_2^+ + h\nu$	See Table III.1	
2	$C^+ + H$	$CH^+ + h\nu$	$1.11 \times 10^{-16} T^{0.667} \exp\left(-1.14 T^{\frac{1}{4}}\right)$	35
3	$O^+ + H$	$H^+ + O$	$2.283 \times 10^{-10} T^{0.1228}$	37
4	$H_2^+ + H$	$H^+ + H_2$	6.4×10^{-10}	23
5	$CH^+ + H$	$C^+ + H_2$	$1.26 \times 10^{-9} \exp(-208.9/T)$	8
6	$CO^+ + H$	$H^+ + CO$	7.5×10^{-10}	38
7	$H^- + H$	$H_2 + e$	1.3×10^{-9}	39
8	$H + e$	$H^- + h\nu$	See Table III.1	26
9	$H + H + H$	$H_2 + H$	$5.5 \times 10^{-29} T^{-1}$ $cm^6\ s^{-1}$	1
10	$H + C$	$CH + h\nu$	1.0×10^{-17}	2
11	$H(n=2) + H(n=1)$	$H_2 + h\nu$	See Chapter 2	3
12	$H + e$	$H^+ + 2e$	$5.85 \times 10^{-11} T^{\frac{1}{2}} \exp(-157809/T)$	9
13	$H + C.R.$	$H^+ + e$	$0.459 \zeta_o$†	31
14	$H + HCO$	$H_2 + CO$	$1.15 \times 10^{-11} T^{\frac{1}{2}}$	8
15	$HeH^+ + H$	$H_2^+ + He$	9.1×10^{-10}	23
16	$H + H_2O$	$OH + H_2$	$5.49 \times 10^{-17} T^{1.99} \exp(-8990/T)$	4
17	$H + OH$	$O + H_2$	$8.33 \times 10^{-18} T^{1.9} \exp(-2830/T)$	4

TABLE IV.1 – *Continued*

18	$OH^+ + H$	$O^+ + H_2$	$3.7 \times 10^{-10} \exp(-7400/T)$	5
19	$CH_2^+ + H$	$CH^+ + H_2$	$2.4 \times 10^{-9} T^{-0.25} \exp(-1320/T)$	5
20	$H + CH$	$C + H_2$	$6.7 \times 10^{-11} T^{0.5} \exp(-2200/T)$	11
21	$H^+ + e$	$H + h\nu$	See text	24,25
22	$H^+ + O$	$O^+ + H$	$7.514 \times T^{0.1387} \exp(-227/T)$	37
23	$H^+ + OH$	$OH^+ + H$	2.1×10^{-9}	7
24	$H^+ + CH$	$CH^+ + H$	1.9×10^{-9}	7
25	$H^+ + CO$	$CO^+ + H$	$1.3 \times 10^{-10} \exp(-4820/T)$	6
26	$H^+ + H^-$	$H + H$	$4.0 \times 10^{-6} T^{-\frac{1}{2}}$	14,15
27	$H^+ + CO_2$	$HCO^+ + O$	3.0×10^{-9}	7
28	$H^+ + HCO$	$HCO^+ + H$	9.4×10^{-10}	7
		$H_2^+ + CO$	9.4×10^{-10}	7
		$H_2 + CO^+$	9.4×10^{-10}	7
29	$H^+ + He$	$HeH^+ + h\nu$	See Table III.1	22
30	$H^+ + H_2O$	$H_2O^+ + H$	8.2×10^{-9}	7
31	$CO^+ + H_2$	$HCO^+ + H$	1.39×10^{-9}	16
32	$H_2 + O$	$OH + H$	$3.84 \times 10^{-17} T^{1.93} \exp(-3940/T)$	4
33	$H_2 + H$	$H + H + H$	$6.5 \times 10^{-7} T^{-\frac{1}{2}} \exp(-52000/T)$ $\times[1 - \exp(-6000/T)]$	1
34	$CH^+ + H_2$	$CH_2^+ + H$	1.4×10^{-9}	36
35	$OH^+ + H_2$	$H_2O^+ + H$	1.05×10^{-9}	16
36	$C^+ + H_2$	$CH^+ + H$	$2.5 \times 10^{-10} \exp(-3449/T)$	8
37	$O^+ + H_2$	$OH^+ + H$	1.58×10^{-9}	16
38	$H_2^+ + H_2$	$H_3^+ + H$	2.1×10^{-9}	7

TABLE IV.1 - *Continued*

39	$HeH^+ + H_2$	$H_3^+ + He$	1.26×10^{-9}	17
40	$H_2 + OH$	$H_2O + H$	$6.88 \times 10^{-19} T^{2.35} \exp(-1210/T)$	4
41	$H_2O^+ + H_2$	$H_3O^+ + H$	6.1×10^{-10}	7
42	$C^+ + H_2$	$CH_2^+ + h\nu$	6.0×10^{-16}	7
43	$H_2 + C$	$CH + H$	$6.7 \times 10^{-11} T^{\frac{1}{2}} \exp(-14100/T)$	11
44	$CH_2^+ + H_2$	$CH_3^+ + H$	7.2×10^{-10}	7
45	$H_2 + CH$	$CH_2 + H$	$5.0 \times 10^{-13} T^{0.67} \exp(-8820/T)$	11
46	$H_2 + H_2$	$H + H + H_2$	$3.17 \times 10^{-15} \exp\left[-\left(\frac{4060}{T}\right) - \left(\frac{7500}{T}\right)^2\right]$	12
47	H_2 + C.R.	$H^+ + H + e$	$2.2 \times 10^{-2} \zeta_o$†	31
		$H_2^+ + e$	$0.93\zeta_o$	31
		$H + H$	$0.10\zeta_o$	32
		$H^+ + H^-$	$3.0 \times 10^{-4} \zeta_o$	7
48	$H_2^+ + C$	$CH^+ + H$	2.4×10^{-9}	7
49	$H_2^+ + O$	$OH^+ + H$	1.5×10^{-9}	7
50	$H_2^+ + CO$	$HCO^+ + H$	2.16×10^{-9}	40
		$CO^+ + H_2$	6.44×10^{-9}	40
51	$H_2^+ + e$	$H + H$	$8.8 \times 10^{-7} T^{-\frac{1}{2}}$	41
52	$H_2^+ + h\nu$	$H^+ + H$	See Table III.1	
53	$H_2^+(v > 3) + He$	$HeH^+ + H$	$3.0 \times 10^{-10} \exp(-6717/T)$	22
54	$H_2^+ + CO_2$	$CO_2^+ + H_2$	1.4×10^{-9}	7
		$CO^+ + H_2O$	1.4×10^{-9}	7
55	$H^- + CO$	$HCO + e$	5.0×10^{-11}	7
56	$H^- + C$	$CH + e$	1.0×10^{-9}	7
57	$H^- + O$	$OH + e$	1.0×10^{-9}	7

TABLE IV.1 – *Continued*

58	$H^- + h\nu$	$H + e$	a	26
59	$H_3^+ + C$	$CH^+ + H_2$	2.0×10^{-9}	7
60	$H_3^+ + O$	$OH^+ + H_2$	8.0×10^{-10}	7
61	$H_3^+ + CO$	$HCO^+ H_2$	1.7×10^{-9}	7
62	$H_3^+ + OH$	$H_2O^+ + H_2$	1.3×10^{-9}	7
63	$H_3^+ + H_2O$	$H_3O^+ + H_2$	5.9×10^{-9}	7
64	$H_3^+ + CO_2$	$HCO_2^+ + H_2$	1.9×10^{-9}	7
65	$H_3^+ + HCO$	$H_2CO^+ + H_2$	1.7×10^{-9}	7
66	$H_3^+ + e$	$H_2 + H$	$1.9 \times 10^{-6} T^{-\frac{1}{2}}$	7
		$H + H + H$	$1.9 \times 10^{-6} T^{-\frac{1}{2}}$	7
67	$H_3^+ + CH$	$CH_2^+ + H_2$	1.2×10^{-9}	7
68	$HeH^+ + e$	$H + He$	1.0×10^{-10}	22
Carbon Reactions				
69	$C + OH$	$CO + H$	$6.35 \times 10^{-12} T^{\frac{1}{2}}$	7
70	$C + e$	$C^+ + 2e$	$1.448 \times 10^{-10} T^{\frac{1}{2}} \exp(-131125.1/T)$	9
71	C + C.R.	$C^+ + e$	$1.8\zeta_o$†	31
72	$C + CH$	$C_2 + H$	4.0×10^{-11}	42
73	$HCO^+ + C$	$CH^+ + CO$	1.1×10^{-9}	7
74	$C + HCO$	$CH + CO$	1.0×10^{-11}	6
75	$C(^3P, ^1D, ^1S) + h\nu$	$C^+ + e$		20
76	$H_3O^+ + C$	$HCO^+ + H_2$	2.0×10^{-9}	10
77	$H_2O^+ + C$	$CH^+ + OH$	1.1×10^{-9}	7
78	$CH_2^+ + C$	$C_2H^+ + H$	1.2×10^{-9}	7

TABLE IV.1 – *Continued*

79	$HCO_2^+ + C$	$CH^+ + CO_2$	1.0×10^{-9}	7
80	$C^+ + e$	$C + h\nu$	$1.4 \times 10^{-10}T^{-0.607}$	18
81	$C^+ + CH$	$C_2^+ + H$	3.8×10^{-10}	7
		$CH^+ + C$	3.8×10^{-10}	7
82	$C^+ + HCO$	$HCO^+ + C$	4.8×10^{-10}	7
		$CH^+ + CO$	4.8×10^{-10}	7
83	$C^+ + CO_2$	$CO^+ + CO$	1.1×10^{-9}	7
84	$C^+ + OH$	$CO^+ + H$	8.0×10^{-10}	13
		$H^+ + CO$	8.0×10^{-10}	13
85	$C^+ + O$	$CO^+ + h\nu$	See Chapter 2	3
86	$C^+ + H_2O$	$HCO^+ + H$	$9.6 \times 10^{-8}T^{-0.63}$	28
87	$CH^+ + O$	$CO^+ + H$	3.4×10^{-10}	30
		$H^+ + CO$	1.0×10^{-11}	30
88	$CH^+ + e$	$C + H$	$5.0 \times 10^{-10}T^{-\frac{1}{2}}$	43
89	$CH^+ + CO_2$	$HCO^+ + CO$	1.2×10^{-9}	7
90	$CH + O$	$CO + H$	$2.3 \times 10^{-12}T^{\frac{1}{2}}$	7
		$HCO^+ + e$	$1.4 \times 10^{-12}T^{\frac{1}{2}}$	44
91	$HCO^+ + CH$	$CH_2^+ + CO$	6.3×10^{-10}	7
92	$H_3O^+ + CH$	$CH_2^+ + H_2O$	6.8×10^{-10}	7
93	$H_2O^+ + CH$	$CH^+ + H_2O$	3.4×10^{-10}	7
		$CH_2^+ + OH$	3.4×10^{-10}	7
94	$CH_2^+ + CH$	$C_2H_2^+ + H$	7.2×10^{-10}	7
95	$CH_2^+ + e$	$CH + H$	$8.7 \times 10^{-6}T^{-\frac{1}{2}}$	43
96	$CO^+ + e$	$C + O$	$1.1 \times 10^{-5}T^{-\frac{1}{2}}$	41

TABLE IV.1 - *Continued*

97	$CO^+ + H_2O$	$H_2O^+ + CO$	1.7×10^{-9}	34
		$HCO^+ + OH$	8.8×10^{-10}	34
98	$CO^+ + CO_2$	$CO_2^+ + CO$	1.1×10^{-9}	7
99	$CO^+ + O$	$O^+ + CO$	1.4×10^{-10}	7
100	$CO + OH$	$CO_2 + H$	$2.2 \times 10^{-13} \exp(-80/T)$	7
101	CO + C.R.	$CO^+ + e$	$3.0\zeta_o$†	7
102	$HCO_2^+ + CO$	$HCO^+ + CO_2$	7.8×10^{-10}	7
103	$CH_2^+ + CO_2$	$H_2CO^+ + CO$	1.2×10^{-9}	7
104	$O^+ + CO_2$	$O_2^+ + CO$	1.1×10^{-9}	7
105	$OH^+ + CO_2$	$HCO_2^+ + O$	5.4×10^{-9}	7
		$HCO^+ + O_2$	5.4×10^{-9}	7
Oxygen Reactions				
106	O + e	$O^+ + 2e$	$9.949 \times 10^{-11} T^{\frac{1}{2}} \exp(-157809/T)$	9
107	O + C.R.	$O^+ + e$	$2.8\zeta_o$†	31
108	O + HCO	$OH + CO$	$6.9 \times 10^{-12} T^{\frac{1}{2}}$	7
		$H + CO_2$	$5.1 \times 10^{-12} T^{\frac{1}{2}}$	7
109	$O + H_2O$	$OH + OH$	$8.59 \times 10^{-19} T^{2.43} \exp(-7740/T)$	4
110	$H_2O^+ + O$	$O_2^+ + H_2$	7.0×10^{-11}	7
111	$CH_2^+ + O$	$HCO^+ + H$	7.5×10^{-10}	7
112	$O + OH$	$O_2 + H$	$7.5 \times 10^{-10} T^{-\frac{1}{2}} \exp(-30/T)$	4
113	$O^+ + e$	$O + h\nu$	$1.2 \times 10^{-10} T^{-0.626}$	18
114	$O^+ + H_2O$	$H_2O^+ + O$	2.3×10^{-9}	7
115	$OH^+ + e$	$O + H$	$1.42 \times 10^{-6} T^{-\frac{1}{2}}$	45

TABLE IV.1 – *Continued*

116	$HCO^+ + OH$	$HCO_2^+ + H$	1.62×10^{-9}	10
		$H_2O^+ + CO$	6.2×10^{-10}	7
117	$OH + OH$	$H_2O + O$	$2.15 \times 10^{-20} T^{2.61} \exp(958/T)$	4
118	$CH_2^+ + OH$	$H_2CO^+ + H$	7.4×10^{-10}	7
115	$CH_2^+ + HCO$	$C_2H_2O^+ + H$	4.5×10^{-10}	7
		$CH_3^+ + CO$	9.5×10^{-10}	7
119	$HCO^+ + e$	$CO + H$	$1.2 \times 10^{-5} T^{-0.84}$	46
120	$HCO^+ + H_2O$	$H_3O^+ + CO$	2.7×10^{-9}	7
121	$H_2O^+ + e$	$OH + H$	$3.46 \times 10^{-6} T^{-\frac{1}{2}}$	27
		$O + H_2$	$3.46 \times 10^{-6} T^{-\frac{1}{2}}$	27
122	$H_2O^+ + H_2O$	$H_3O^+ + OH$	2.1×10^{-9}	7
123	$CH_2^+ + H_2O$	$H_3CO^+ + H$	5.2×10^{-10}	7
124	$HCO_2^+ + H_2O$	$H_3O^+ + CO_2$	7.8×10^{-10}	7
125	$H_3O^+ + e$	$H_2O + H$	$(0.9)1.2 \times 10^{-5} T^{-\frac{1}{2}}$	45,47
		$OH + H + H$	$(0.1)1.2 \times 10^{-5} T^{-\frac{1}{2}}$	45,47
126	$HCO_2^+ + e$	$H + CO_2$	$4.33 \times 10^{-6} T^{-\frac{1}{2}}$	7,29
		$OH + CO$	$4.33 \times 10^{-6} T^{-\frac{1}{2}}$	7,29
Silicon Reactions				
127	$Si + h\nu$	$Si^+ + e$		21
128	$Si + OH$	$SiO + H$	$1.15 \times 10^{-11} T^{\frac{1}{2}}$	7
129	$Si^+ + e$	$Si + h\nu$	$1.44 \times 10^{-10} T^{-0.617}$	33
130	$Si^+ + OH$	$SiO^+ + H$	6.3×10^{-10}	7
131	$Si^+ + O$	$SiO^+ + h\nu$	1.0×10^{-17}	7

TABLE IV.1 – *Continued*

132	$Si^+ + CH$	$SiC^+ + H$	6.3×10^{-10}	7
133	$Si^+ + H_2O$	$HSiO^+ + H$	8.5×10^{-10}	7
134	$H^+ + SiO$	$SiO^+ + H$	3.3×10^{-9}	7
135	$C^+ + SiO$	$SiO^+ + C$	5.4×10^{-10}	7
		$Si^+ + CO$	5.4×10^{-10}	7
136	$HCO^+ + SiO$	$HSiO^+ + CO$	7.9×10^{-10}	7
137	$H_3^+ + SiO$	$HSiO^+ + H_2$	2.0×10^{-9}	7
138	$SiO^+ + C$	$Si^+ + CO$	1.0×10^{-9}	7
139	$SiO^+ + O$	$Si^+ + O_2$	2.0×10^{-10}	7
140	$SiO^+ + H_2$	$HSiO^+ + H$	1.5×10^{-9}	7
141	$SiO^+ + CH$	$HCO^+ + Si$	5.9×10^{-10}	7
142	$SiO^+ + CO$	$Si^+ + CO_2$	7.9×10^{-10}	7
143	$SiO^+ + HCO$	$HCO^+ + SiO$	6.6×10^{-10}	7
144	$SiO^+ + e$	$Si + O$	$3.5 \times 10^{-6} T^{-\frac{1}{2}}$	7
145	$HSiO^+ + e$	$SiO + H$	$5.2 \times 10^{-6} T^{-\frac{1}{2}}$	7,19
146	$HSiO^+ + CO$	$HCO^+ + SiO$	1.0×10^{-9}	19

† ζ_o is the ionization rate per cm^3 per sec by high energy particles (ISM rate $\approx 5 \times 10^{-17}$ cm^{-3} s^{-1}).

[a] By detailed balance with reaction 8.

REFERENCES FOR TABLE IV.1

1) Jacobs, Giedt, and Cohen 1967.
2) Smith, Liszt, and Lutz 1973.
3) This work.
4) Wagner and Graff 1987.
5) Graff and Dalgarno 1987.
6) Estimate or guess.
7) Prasad and Huntress 1980 (and references therein).
8) Gerlich, Disch, and Scherbarth 1987.
9) Lotz 1967.
10) Herbst and Klemperer 1973.
11) Aannestad 1973.
12) Lepp and Shull 1983.
13) Barsuhn 1977.
14) Dalgarno and McCray 1973.
15) Peterson *et al.* 1971.
16) Kim, Theard, and Huntress 1975.
17) Orient 1977.
18) Weisheit 1973.
19) Turner and Dalgarno 1977.
20) Calculated from cross sections of Henry 1970.
21) Calculated from cross sections of Chapman and Henry 1972.
22) Roberge and Dalgarno 1982.
23) Karpas, Anicich, and Huntress 1979.
24) Osterbrock 1974.
25) McCray 1989.
26) Calculated from cross sections of Wishart 1979.
27) Mitchell and Deveau 1983.
28) Marquette *et al.* 1985.
29) Leung, Herbst, and Huebner 1984.
30) Viggiano *et al.* 1980.
31) Black 1975.
32) Soloman and Werner 1971.
33) Péquignot and Aldrovandi 1986.
34) Prasad, S. S. as referenced by Duley and Williams 1984.
35) Graff, Moseley, and Roueff 1983.

REFERENCES FOR TABLE IV.1 – *Continued*

36) Smith and Adams 1981.
37) Chambaud *et al.* 1980.
38) Federer *et al.* 1984.
39) Browne and Dalgarno 1969 and Bieniek and Dalgarno 1979.
40) Kim and Huntress 1975.
41) Black 1983.
42) Solomon and Klemperer 1972.
43) Mul *et al.* 1981.
44) McGregor and Berry 1973.
45) McGowan *et al.* 1979.
46) Smith and Adams 1984.
47) Branching ratio discussed by van Dishoeck and Black 1989.

LIST OF REFERENCES

R.1 GENERAL

Aaronson, M., Bothun, G., Mould, J., Schommer, R. A., and Cornell, M. E. 1986, *Ap. J.*, **302**, 536.

Aaronson, M., and Mould, J. 1983, *Ap. J.*, **265**, 1.

Aaronson, M., and Mould, J. 1986, *Ap. J.*, **303**, 10.

Aaronson, M., and Olszewski, E. 1988, in IAU Symposium **130**, *Large Scale Structures of the Universe*, ed. J. Audouze, M.-C. Pelletan, and A. Szalay (Dordrecht: Kluwer), p. 409.

Adams, W. S. 1941, *Ap. J.*, **93**, 11.

Adams, W. S. 1943, *Ap. J.*, **97**, 105.

Allen, D. A., Jones, T. J., and Hyland, A. R. 1985, *Ap. J.*, **291**, 280.

Allen, M., and Knapp, G. R. 1978, *Ap. J.*, , **225**, 843.

Allamandola, L. J., Tielens, A. G. G. M., and Barker, J. R. 1985, *Ap. J. (Letters)*, **290**, L25.

Allamandola, L. J., Tielens, A. G. G. M., and Barker, J. R. 1987a, in *Interstellar Processes*, ed. D. J. Hollenbach and H. A. Thronson, Jr. (Dordrecht: Reidel), p. 471.

Allamandola, L. J., Tielens, A. G. G. M., and Barker, J. R. 1987b, in *Polycyclic Aromatic Hydrocarbons in Astrophysics*, ed. A. Léger, L. d'Hendecourt, and N. Boccara (Dordrecht: Reidel), p. 255.

Allamandola, L. J., Tielens, A. G. G. M., and Barker, J. R. 1989, *Ap. J. Suppl.*, in press.

Bachiller, R., Gómez-González, J., Bujarrabal, V., and Martin-Pintado, J. 1988, *Astr. Ap.*, **196**, L5.

Barnard, E. E. 1919, *Ap. J.*, **49**, 1.

Barnard, E. E. 1927, *Atlas of Regions of the Milky Way*, ed. E. B. Frost and M. R. Calvert (Washington: Carnegie Institution).

Bates, D. R. 1951a, *M. N. R. A. S.*, **111**, 303.

Bates, D. R. 1951b, *J. Chem. Phys.*, **19**, 1122.

Bates, D. R. 1953, *Phil. Trans. R. Soc. London A*, **246**, 215.

Beckwith, S., Beck, S. C., and Gatley, I. 1984, *Ap. J.*, **280**, 648.

Betz, A. 1987, in IAU Symposium **120**, *Astrochemistry*, ed. M. S. Vardya and S. P. Tarafdar (Dordrecht: Reidel), p. 327.

Black, J. H. 1988, in *Advances in Atomic and Molecular Physics*, ed. D. R. Bates and B. Bederson (New York: Academic Press), **25**, 477.

Black, J. H., and Dalgarno, A. 1976, *Ap. J.*, **203**, 132.

Black, J. H., and Dalgarno, A. 1977, *Ap. J. Suppl.*, **34**, 405.

Black, J. H., and van Dishoeck, E. F. 1987, *Ap. J.*, **322**, 412.

Blitz, L., and Shu, F. H. 1980, *Ap. J.*, **238**, 148.

Blumenthal, G. R., Faber, S. M., Primack, J. R., and Rees, M. J. 1984, *Nature*, **311**, 517.

Bohlin, R. C., Savage, B. D., Drake, J. F. 1978, *Ap. J.*, **224**, 132.

Bohme, D. K., Wlodek, S., and Wincel, H. 1989, *Ap. J. (Letters)*, **342**, L91.

Bond, H. E. 1989, in IAU Symposium **131**, *Planetary Nebulae*, ed. S. Torres-Peimbert (Dordrecht: Kluwer), p. 251.

Börner, G. 1988, *The Early Universe - Facts and Fiction* (Berlin: Springer-Verlag).

Bouchet, P., Moneti, A., Slezak, E., Le Bertre, T., and Manfroid, J. 1989, *Astr. Ap.*, submitted.

Burbidge, G. R. 1971, *Nature*, **233**, 36.

Burton, M. G., and Geballe, T. R. 1986, *M. N. R. A. S.*, **223**, 13P.

Butler, S. E., and Dalgarno, A. 1980, *Ap. J.*, **241**, 838.

Calvet, N., and Cohen, M. 1978, *M. N. R. A. S.*, **182**, 687.

Calvet, N., and Peimbert, M. 1983, *Rev. Mexicana Astr. Ap.*, **5**, 319.

Carsenty, U., and Solf, J. 1982, *Astr. Ap.*, **106**, 307.

Catchpole, R. M., and Glass, I. S. 1987, *Int. Astr. Union Circ.*, **4457**.

Cernicharo, J., Guélin, M., Martin-Pintado, J., Penalver, J., and Mauersberger, R. 1989, *Astr. Ap. (Letters)*, in press.

Chambaud, G., Launay, J. M., Levy, B., Millie, P., Roueff, E., and Tran Minh, F. 1980, *J. Phys. B*, **13**, 4205.

Chang, E. S., and Temkin, A. 1969, *Phys. Rev. Letters*, **23**, 399.

Charfman, J. J. 1980, in IAU Symposium **87**, *Interstellar Molecules*, ed. B. H. Andrew (Dordrecht: Reidel), p. 645.

Claussen, M. J., Kleinmann, S. G., Joyce, R. R., and Jura, M. 1987, *Ap. J. Suppl.*, **65**, 385.

Cohen, M., 1987, in *Circumstellar Matter*, IAU Symposium 122, I. Appenzeller and C. Jordan, editors, (Dordrecht: Reidel), p. 39.

Cohen, M., and Schmidt, G. D. 1981, *Ap. J.*, **246**, 444.

Coxon, J. A., and Foster, S. C. 1982, *J. Mol. Spectrosc.*, **93**, 117.

Crawford, M. K., Tielens, A. G. G. M., and Allamandola, L. J. 1985, *Ap. J. (Letters)*, **293**, L45.

Crompton, A. W., Gibson, D. K., and McIntosh, A. I. 1969, *Austr. J. Phys.*, **22**, 715.

Crompton, A. W., Gibson, D. K., and Robertson, A. G. 1970, *Phys. Rev. A*, **2**, 1386.

Dalgarno, A., and Lepp, S. 1987, in IAU Symposium **120**, *Astrochemistry*, ed. M. S. Vardya and S. P. Tarafdar (Dordrecht: Reidel), p. 109.

Dalgarno, A., and McCray, R. 1972, *Ann. Rev. Astr. Ap.*, **10**, 375.

Dalgarno, A., and Wright, E. L. 1972, *Ap. J. (Letters)*, **174**, L49.

Dalgarno, A., Du, M. L., and You, J. H. 1989, *Ap. J.*, submitted.

Danziger, I. J., Bouchet, P., Fosbury, R. A. E., Gouffes, C., Lucy, L. B., Moorwood, A. F. M., Oliva, E., and Rufener, F. 1988, in *Supernova 1987A in the Large Magellanic Cloud*, eds. M. Kafatos and A. Michalitsianos (Cambridge: Cambridge University Press), 37.

Dickinson, A. S. 1971, *J. Phys. B*, **4**, L116.

Dinerstein, H. L., Lester, D. F., Carr, J. S., and Harvey, P. M. 1988, *Ap. J. (Letters)*, **327**, L27.

Donn, B. 1968, *Ap. J. (Letters)*, **152**, L129.

Dopita, M. A. *et al.* 1988, *Astr. J.*, **95**, 1717.

Douglas, A. E., and Herzberg, G. 1941, *Ap. J.*, **94**, 381.

Dressler, K., and Wolniewicz, L. 1985, *J. Chem. Phys.*, **82**, 4720.

Draine, B. T., and Salpeter, E. E. 1978, *Nature*, bf 271, 730.

Duley, W. W. 1986, *Quart. J. R. Astr. Soc.*, **27**, 403.

Duley, W. W. 1987, in *Polycyclic Aromatic Hydrocarbons in Astrophysics*, ed. A. Léger, L. d'Hendecourt, and N. Boccara (Dordrecht: Reidel), p. 373.

Duley, W. W., and Williams, D. A. 1981, *M. N. R. A. S.*, **196**, 269.

Duley, W. W., and Williams, D. A. 1984, *Interstellar Chemistry* (London: Academic Press).

Duley, W. W., and Williams, D. A. 1986, *M. N. R. A. S.*, **219**, 859.

Dwek, E. 1989, in IAU Symposium No. 135, *Interstellar Dust*, in press.

Elias, J. H., Gregory, B., Phillips, M. M., Williams, R. E., Graham, J. R., Meikle, W. P. S., Schwartz, R. D., and Wilking, B. 1988, *Ap. J. (Letters)*, **331**, L9.

Ewen, H. I., and Purcell, E. M. 1951, *Nature*, **168**, 356.

Falk, S. W., and Arnett, W. D. 1977, *Ap. J. Suppl.*, **33**, 515.

Federman, S. R. 1987, in IAU Symposium **120**, *Astrochemistry*, ed. M. S. Vardya and S. P. Tarafdar (Dordrecht: Reidel), p. 123.

Field, G. B., Somerville, W. B., and Dressler, K. 1966, *Ann. Rev. Astr. Ap.*, **4**, 207.

Fischel, D., and Sparks, W. M. 1971, *Ap. J.*, **164**, 359.

Ford, A. L., Browne, J. C., Shipsey, E. J., and DeVries, P. 1975, *J. Chem. Phys.*, **63**, 362.

Fransson, C., Cassatella, A., Gilmozzi, R., Kirshner, R. P., Panagia, N., Sonneborn, G., and Wamsteker, W. 1989, *Ap. J.*, in press.

Frenklach, M., and Feigelson, E. D. 1989, *Ap. J.*, **341**, 372 (F&F).

Friedman, A. 1924, *Z. Phys.*, **21**, 326.

Gammie, C. F., Knapp, G. R., Young, K., Phillips, T. G., and Falgarone, E. 1989 *Ap. J. (Letters)*, in press.

Gail, H.-P., and Sedlmayr, E. 1987, in *Physical Processes in Interstellar Clouds*, ed. G. E. Morfill and M. Scholer (Dordrecht: Reidel), p. 275.

Gear, C. W. 1971, *Numerical Initial Value Problems in Ordinary Differential Equations*, Prentice-Hall, Englewood Cliffs, New Jersey.

Ghosh, K. K. 1987, in IAU Symposium **120**, *Astrochemistry*, ed. M. S. Vardya and S. P. Tarafdar (Dordrecht: Reidel), p. 253.

Gibson, D. K. 1970, *Austr. J. Phys.*, **23**, 683.

Giovanardi, C., Natta, A., and Palla, F. 1987, *Astr. Ap. Suppl.*, **70**, 269.

Glassgold, A. E., Mamon, G. A., and Huggins, P. J. 1989, *Ap. J. (Letters)*, **336**, L29.

Goldsmith, P. F. 1987, in *Interstellar Processes*, ed. D. J. Hollenbach and H. A. Thronson, Jr. (Dordrecht: Reidel), p. 51.

Gottlieb, E. W., and Liller, W. 1976, *Ap. J. (Letters)*, **207**, L135.

Grandi, S. A. 1975, *Ap. J.*, **196**, 465.

Harrison, E. R. 1973, *Ann. Rev. Astr. Ap.*, **11**, 155.

Hartmann, J. 1904, *Ap. J.*, **19**, 268.

Herbst, E. 1987, in *Interstellar Processes*, ed. D. J. Hollenbach and H. A. Thronson, Jr. (Dordrecht: Reidel), p. 611.

Henry, R. J. W. 1970, *Phys. Rev. A*, **2**, 1349.

Herschel, W. 1784, *Phil. Trans. R. Soc. London A*, **74**, 437.

Herzberg, G. 1950, *Molecular Spectra and Molecular Structure, I. Spectra of Diatomic Molecules* (Princeton: D. van Nostrand).

Hollenbach, D., and McKee, C. F. 1979, *Ap. J. Suppl.*, **41**, 555.

Hollenbach, D. J., and Salpeter, E. E. 1971, *Ap. J.*, **163**, 155.

Hollenbach, D. J., Werner, M. W., and Salpeter, E. E. 1971, *Ap. J.*, **163**, 165.

Hogan, C. 1989, *Ap. J. (Letters)*, submitted.

Hubble, E. 1929, *Proc. Nat. Acad. Sci.*, **15**, 168.

Hunter, D. A., and Watson, W. D. 1978, *Ap. J.*, **226**, 477.

Irvine, W. M., Goldsmith, P. F., and Hjalmarson, Å 1987, in *Interstellar Processes*, ed. D. J. Hollenbach and H. A. Thronson, Jr. (Dordrecht: Reidel), p. 561.

Jones, B. J. T., and Wyse, R. F. G. 1985, *Astr. Ap.*, **149**, 144.

Jura, M. 1983, *Ap. J.*, **275**, 683.

Jura, M. 1986, *Ap. J.*, **303**, 327.

Jura, M. 1987a, in *Interstellar Processes*, ed. D. J. Hollenbach and H. A. Thronson, Jr. (Dordrecht: Reidel), p. 3.

Jura, M. 1987b, in *Polycyclic Aromatic Hydrocarbons in Astrophysics*, ed. A. Léger, L. d'Hendecourt, and N. Boccara (Dordrecht: Reidel), p. 3.

Jura, M., and Kleinmann, S. G. 1989, *Ap. J.*, **341**, 359.

Jura, M., Joyce, R. R., and Kleinmann, S. G. 1989, *Ap. J.*, **336**, 924.

Karzas, W. J., and Latter, R. 1961, *Ap. J. Suppl.*, **6**, 167.

Keady, J. J., and Hinkle, K. H. 1988, *Ap. J.*, **331**, 539.

Keller, R. 1987 in *Polycyclic Aromatic Hydrocarbons in Astrophysics*, ed. A. Léger, L. d'Hendecourt, and N. Boccara (Dordrecht: Reidel), p. 387.

Kelly, D., *et al.* 1990, in preparation.

Kleinmann, S. G., Sargent, D. G., Moseley, H., Harper, D. A., Loewenstein, R. F., Telesco, C. M., and Thronson, H. A. 1978, *Astr. Ap.*, **65**, 139.

Knapp, G. R., and Morris, M. 1985, *Ap. J.*, **292**, 640.

Knapp, G. R., Gammie, C. F., Young, K., and Phillips, T. G. 1989, in *Submillimetre and Millimetre Astronomy*, ed. A. Webster, in press.

Knapp, G. R., Rauch, K. P., and Wilcots, E. M. 1990, in *The Evolution of the Interstellar Medium*, ed. L. Blitz, in press.

Kołos, W. 1975, *Int. J. Quant. Chem.*, **9**, 133.

Kołos, W. 1976, *J. Mol. Spectrosc.*, **62**, 429.

Kołos, W., and Rychlewski, J. 1976, *J. Mol. Spectrosc.*, **62**, 109.

Kołos, W., and Wolniewicz, L. 1975, *Canadian J. Phys.*, **53**, 2189.

Kołos, W., Szalewicz, K., and Monkhorst, H. J. 1986, *J. Chem. Phys.*, **84**, 3278.

Krolik, J. H. 1989, *Ap. J.*, **338**, 594.

Krupenie, P. H. 1966, NSRDS-NBS 5, *"The Band Spectrum of Carbon Monoxide."*

Kulkarni, S. R., and Heiles, C. 1987, in *Interstellar Processes*, ed. D. J. Hollenbach and H. A. Thronson, Jr. (Dordrecht: Reidel), p. 87.

Kwok, S., and Bignell, R. C. 1984, *Ap. J.*, **276**, 544.

Kwok, S., and Feldman, P. A. 1981, *Ap. J. (Letters)*, **267**, L67.

Kwok, T. L., Dalgarno, A., and Posen, A. 1985, *Phys. Rev. A*, **32**, 646.

Lacy, J. H., Baas, L. J., Allamandolla, L. J., Persson, S. .E., McGregor, P. J., Lonsdale, C. J., Geballe, T. R., and van de Bult, C. E. P. 1984, *Ap. J.*, **276**, 533.

Lafont, S., Lucas, R., and Omont, A. 1982, *Astr. Ap.*, **106**, 201.

Larson, H. P., Davis, D. S., Black, J. H., and Fink, U. 1985, *Ap. J.*, **299**, 873.

Larsson, M. 1983, *Astr. Ap.*, **128**, 291.

Latter, W. B., and Maloney, P. R. 1990, in preparation.

Laurent, C. 1983, in *ESO Workshop on Primordial Helium*, ed. P. A. Shaver, D. Kunth, K. Kjär (Munich: ESO), p. 335.

Layzer, D. 1968, *Ap. Letters*, **1**, 99.

Layzer, D., and Hively, R. 1972, *Ap. J.*, **179**, 361.

Léger, A., and d'Hendecourt, L. 1985, *Astr. Ap.*, **146**, 81.

Léger, A., and d'Hendecourt, L. 1987, in *Polycyclic Aromatic Hydrocarbons in Astrophysics*, ed. A. Léger, L. d'Hendecourt, and N. Boccara (Dordrecht: Reidel), p. 223.

Léger, A., and Puget, J. L. 1984, *Astr. Ap.*, **137**, L5.

Léger, A., d'Hendecourt, L., and Boccara, N. 1987, eds. *Polycyclic Aromatic Hydrocarbons in Astrophysics*, (Dordrecht: Reidel).

Léger, A., d'Hendecourt, L., and Défourneau, D. 1989, *Astr. Ap.*, **216**, 148.

Lemaître, G. 1927, *Ann. Soc. Sci. Brux.*, **47A**, 49.

Leonas, V. B., and Pjarnpuu, A. A. 1981, *Sov. Astr. Letters*, **7**, 19.

Lepp, S., and Dalgarno, A. 1988, *Ap. J.*, **324**, 553.

Lepp, S., Dalgarno, A., McCray, R. 1988, *Bull. A. A. S.*, **20**, 671.

Lepp, S., Dalgarno, A., van Dishoeck, E. F., and Black, J. H. 1988, *Ap. J.*, **329**, 418.

Lepp, S., Dalgarno, A., and McCray, R. 1988, *Bull. A. A. S.*, **20**, 671.

Lepp, S., and Shull, M. 1984, *Ap. J.*, **280**, 465.

Linden, F., and Schmidt, H. 1971, *Z. f. Naturforsch*, **26a**, 1603.

Lo, K. Y., and Bechis, K. P. 1976, *Ap. J. (Letters)*, **205**, L21.

Lucy, L. B., Danziger, I. J., Gouiffes, C., and Bouchet, P. 1990, in IAU Colloquium **120**, *Structure and Dynamics of the Interstellar Medium*,

ed. G. Tenorio-Tagle, M. Moles, and J. Melnick (Berlin: Spinger-Verlag), in press.

Maloney, P. R. 1987, Ph.D. Dissertation; University of Arizona.

Mamon, G. A., Glassgold, A. E., and Huggins, P. J. 1988, *Ap. J.*, **328**, 791.

Margulis, M. S. 1987, Ph.D. Dissertation, University of Arizona.

Martin, P. G. 1978, *Cosmic Dust: Its Impact on Astronomy* (Oxford: Clarendon Press).

McCabe, E. M., Connon Smith, R., and Clegg, R. E. S. 1979, *Nature*, **281**, 263.

McCray, R. 1989, in *Molecular Astrophysics*, ed. T. W. Hartquist (Cambridge University Press), in press.

McCray, R., and Li, H. W. 1989, in *Structure and Evolution of Galaxies*, ed. Fang Li Zhi (Singapore: World Scientific Publishing Co.), in press.

McGregor, P. J., Hyland, A. R., and Hillier, D. J. 1988, *Ap. J.*, **324**, 1071.

McKee, C. F., and Ostriker, J. P. 1977, *Ap. J.*, **196**, 565.

McKellar, A. 1940, *Publ. Astr. Soc. Pacific*, **52**, 187.

Meikle, W. P. S., Allen, D. A., Spyromilio, J., and Varani, G.-F. 1989, *M. N. R. A. S.*, in press.

Merrill, P. W. 1934, *Publ. Astr. Soc. Pacific*, **46**, 206.

Meyer, D. M., and Jura, M. 1985, *Ap. J.*, **297**, 119.

Meyer, D. M., Black, J. H., Chaffee, F. H. Jr., Foltz, C. B., and York, D. G. 1986, *Ap. J. (Letters)*, **308**, L37.

Middleditch, J. *et al.* 1989, *Int. Astr. Union Circ.*, **4735**.

Mihalas, D., and Binney, J. 1981, *Galactic Astronomy: Structure and Kinematics* (San Francisco: W. H. Freeman & Co.).

Morris, M. 1981, *Ap. J.*, **249**, 572.

Münch, G. 1952, *Ap. J.*, **116**, 575.

Myers, P. C. 1987, in *Interstellar Processes*, ed. D. J. Hollenbach and H. A. Thronson, Jr. (Dordrecht: Reidel), p. 71.

Oliva, E., Moorwood, A. F. M., and Danziger, I. J. 1987, *ESO Messenger*, **50**, 18.

Omont, A. 1986, *Astr. Ap.*, **164**, 159.

Osterbrock, D. E. 1974, *Astrophysics of Gaseous Nebulae* (San Francisco: W. H. Freeman & Co.).

Palla, F., and Zinnecker, H. 1987, in XXII *Rencontre de Moriond, Starbursts and Galaxy Evolution*, ed. Trinh Zuan Thuan, T. Montmerle and J. Tran Thanh Van (Gif Sur Yvette: Editions Frontieres), p. 533.

Palla, F., Salpeter, E. E., and Stahler, S. W. 1983, *Ap. J.*, **271**, 632.

Peebles, P. J. E. 1966, *Ap. J.*, **146**, 542.

Peebles, P. J. E. 1968, *Ap. J.*, **153**, 1.

Peebles, P. J. E., and Dicke, R. H. 1968, *Ap. J.*, **164**, 891.

Penzias, A. A., and Wilson, R. W. 1965, *Ap. J.*, **142**, 419.

Petuchowski, S. J., Dwek, E., Allen, J. E., Jr., and Nuth, J. A. 1989, *Ap. J.*, **342**, 406.

Platt, J. R. 1956, *Ap. J.*, **123**, 486.

Prasad, S. S., Tarafdar, S. P., Villere, K. R., and Huntress, W. T. 1987, in *Interstellar Processes*, ed. D. J. Hollenbach and H. A. Thronson, Jr. (Dordrecht: Reidel), p. 631.

Rapp, D., and Francis, W. E. 1962, *J. Chem. Phys.*, **37**, 2631.

Rieke, M. J., Rieke, G. H., and Montgomery, E. F. 1987, in *Infrared Astronomy with Arrays*, C. G. Wynn-Williams and E. E. Becklin, editors, (Honolulu: Institute for Astronomy, University of Hawaii), p. 213.

Rogerson, J., and York, D. G. 1973, *Ap. J.*, **186**, L95.

Rosmus, P., and Werner, H.-J. 1982, *Molec. Phys.*, **47**, 661.

Rowan-Robinson, M., and Harris, S. 1983, *M. N. R. A. S.*, **202**, 797.

Russell, R. W., Soifer, B. T., and Willner, S. P. 1978, *Ap. J.*, **220**, 568.

Saslaw, W. C., and Zipoy, D. 1967, *Nature*, **216**, 976.

Schmidt, W. 1987, in *Polycyclic Aromatic Hydrocarbons in Astrophysics*, ed. A. Léger, L. d'Hendecourt, and N. Boccara (Dordrecht: Reidel), p. 149.

Schmidt, G. D., and Cohen, M. 1981, *Ap. J.*, **246**, 444.

Schmidt, G. D., Cohen, M. and Margon, B. 1980, *Ap. J. (Letters)*, **239**, L133.

Seab, C. G. 1987, in *Interstellar Processes*, ed. D. J. Hollenbach and H. A. Thronson, Jr. (Dordrecht: Reidel), p. 491.

Smith, C., James, S., and Aitken, D. 1988, *Int. Astr. Union Circ.*, **4645**.

Sharp, T. E. 1971, *Atomic Data*, **2**, 119.

Spitzer, L., Jr. 1978, *Physical Processes in the Interstellar Medium* (New York: John Wiley & Sons).

Spyromilio, J., Meikle, W. P. S., Learner, R. C. M., and Allen, D. A. 1988, *Nature*, **334**, 327.

Stephens, T. L., and Dalgarno, A. 1972, *J. Quant. Spectrosc. Rad. Transf.*, **12**, 569.

Stephens, T. L., and Dalgarno, A. 1974, *Mol. Phys.*, **28**, 1049.

Sunyaev, R. A. 1968, *Sov. Phys. - DOKLADY*, **13**, 183.

Thackeray, A. D. 1962, *M. N. R. A. S.*, **124**, 251.

Thompson, R. 1987, *Ap. J.*, **312**, 784.

Thompson, R., and Jannuzi, B. T. 1989, *Ap. J.*, **344**, 799.

Thronson, H. A. 1981, *Ap. J.*, **248**, 984.

Thronson, H. A., and Mozurkewich, D. 1983, *Ap. J.*, **271**, 611.

Thronson, H. A., Latter, W. B., Black, J. H., Bally, J., and Hacking, P. 1987, *Ap. J.*, **322**, 770.

Tielens, A. G. G. M., Allamandola, L. J., Barker, J. R., and Cohen, M. 1987, in *Polycyclic Aromatic Hydrocarbons in Astrophysics*, ed. A. Léger, L. d'Hendecourt, and N. Boccara (Dordrecht: Reidel), p. 273.

Trumpler, R. J. 1930, *Publ. Astr. Soc. Pacific*, **42**, 214.

Ulich, B. L., and Haas, R. W. 1976, *Ap. J. Suppl.*, **30**, 247.

van de Hulst, H. C. 1945, *Neder. Tij. Natuurkunde*, **11**, 201.

van der Zwet, G. 1987, in *Polycyclic Aromatic Hydrocarbons in Astrophysics*, ed. A. Léger, L. d'Hendecourt, and N. Boccara (Dordrecht: Reidel), p. 351.

van der Zwet, G., and Allamandola, L. J. 1985, *Astr. Ap.*, **146**, 76.

van Dishoeck, E. F. 1989a, in *Rate Coefficients in Astrochemistry*, ed. T. J. Millar and D. A. Williams (Dordrecht: Kluwer), p. 49.

van Dishoeck, E. F. 1989b, in *Proceedings of the summer school on: Millimetre and Submillimetre Astronomy*, ed. R. D. Wolstencroft and W. B. Burton (Dordrecht: Kluwer), p. 117.

van Dishoeck, E. F., and Black, J. H. 1986, *Ap. J. Suppl.*, **62**, 109.

van Dishoeck, E. F., and Black, J. H. 1988, *Ap. J.*, **334**, 771.

van Dishoeck, E. F., and Black, J. H. 1989, in *Rate Coefficients in Astrochemistry*, ed. T. J. Millar and D. A. Williams (Dordrecht: Kluwer), p. 209.

Viala, Y. P. 1986, *Astr. Ap. Suppl.*, **64**, 391.

Viala, Y. P., Letzelter, C., Eidelsberg, M., and Rostas, F. 1988, *Astr. Ap.*, **193**, 265.

Vidal-Madjar, A., Laurent, C., Gry, C., Bruston, P., Ferlet, R., and York, D. G. 1983, *Astr. Ap.*, **120**, 58.

Volk, K. M., and Kwok, S. 1989, *Ap. J.*, **342**, 345.

Wagoner, R. V. 1973, *Ap. J.*, **179**, 343.

Wagoner, R. V., Fowler, W. A., and Hoyle, F. 1967, *Ap. J.*, **148**, 3.

Walker, A. R. 1987, *M. N. R. A. S.*, **225**, 627.

Watson, W. D., and Salpeter, E. E. 1972, *Ap. J.*, **174**, 321.

Wdowiak, T. J. 1987, in *Polycyclic Aromatic Hydrocarbons in Astrophysics*, ed. A. Léger, L. d'Hendecourt, and N. Boccara (Dordrecht: Reidel), p. 327.

Weinberg, S. 1972, *Gravitation and Cosmology: Principles and Applications of the General Theory of Relativity* (New York: John Wiley & Sons).

Westbrook, W. E., Becklin, E. E., Merrill, K. M., Neugebauer, G., Schmidt, M., Willner, S. P., and Wynn-Williams, C. G. 1975, *Ap. J.*, **202**, 407.

Weymann, R. 1965, *Phys. Fluids*, **8**, 2112.

Witteborn, F. C., Sandford, S. A., Bregman, J. D., Allamandola, L. J., Cohen, M., Wooden, D. H., and Graps, A. L. 1989, *Ap. J.*, **341**, 270.

Wynn-Williams, C. G. 1977, *M. N. R. A. S.*, **181**, 61P.

Yang, J., Turner, M. S., Steigman, G., Schramm, D. N., and Olive, K. A. 1984, *Ap. J.*, **281**, 493.

Zel'dovich, Ya. B., and Novikov, I. D. 1983, in *Relativistic Astrophysics Vol. 2: The Structure and Evolution of the Universe* (Chicago: University of Chicago Press).

Zel'dovich, Ya. B., Kurt, V. G., Sunyaev, R. A. 1969, *Sov. Phys. JETP*, **28**, 146.

R.2 REFERENCES FOR TABLE III.1

Adams, N. G., Bohme, D. K., and Ferguson, E. E. 1970, *J. Chem. Phys.*, **52**, 5101.

Auerbach, D., Cacak, R., Caudano, R., Gaily, T. D., Keyser, C. J., McGowan, J. W., Mitchell, J. B. A., and Wilk, S. F. J. 1977, *J. Phys. B*, **10**, 3797.

Bates, D. R. 1951, *J. Chem. Phys.*, **19**, 1122.

Bieniek, R. J., and Dalgarno, A. 1979, *Ap. J.*, **228**, 635.

Bowers, M. T., Elleman, D. D., and King, J. 1969, *J. Chem. Phys.*, **50**, 4787.

Browne, J. C., and Dalgarno, A. 1969, *J. Phys. B*, **2**, 885.

Dalgarno, A., and McCray, R. 1973, *Ap. J.*, **181**, 95.

Dunn, G. H. 1968, *Phys. Rev.*, **172**, 1.

Fehsenfeld, F. C., Dunkin, D. B., Ferguson, E. E., and Albritton, D. L. 1973, *Ap. J. (Letters)*, **183**, L25.

Ferguson, E. E., Fehsenfeld, F. C., and Schmeltekopf, A. L. 1965, *Phys. Rev.*, **138**, A381.

Jacobs, T. A., Giedt, R. R., and Cohen, N. 1967, *J. Chem. Phys.*, **47**, 54.

Johnsen, R., and Biondi, M. A. 1974, *Icarus*, **23**, 139.

Karpas, Z., Anicich, V., and Huntress, W. T. 1979, *J. Chem. Phys.*, **73**, 5631.

Lepp, S., and Shull, M. 1984, *Ap. J.*, **280**, 465.

Orient, O. J. 1977, *Chem. Phys. Letters*, **52**, 264.

Peebles, P. J. E. 1968, *Ap. J.*, **153**, 1.

Peterson, J. R., Aberth, W. H., Moseley, J. T., and Sheridan, J. R. 1971, *Phys. Rev. A*, **3**, 1651.

Prasad, S. S., and Huntress, W. T., Jr. 1980, *Ap. J. Suppl.*, **43**, 1.

Roberge, W., and Dalgarno, A. 1982, *Ap. J.*, **255**, 489.

Smith, F. J. 1966, *Planet. Space Sci.*, **14**, 929.

Wishart, A. W. 1979, *M. N. R. A. S.*, **187**, 59P.

R.3 REFERENCES FOR TABLE IV.I

Aannestad, P. A. 1973, *Ap. J. Suppl.*, **25**, 223.

Barsuhn, J. 1977, *Astr. Ap. Suppl.*, **28**, 453.

Bieniek, R. J., and Dalgarno, A. 1979, *Ap. J.*, **228**, 635.

Black, J. H. 1975, Ph.D. Thesis, Harvard University.

Black, J. H. 1983, in IAU Symposium **103**, *Planetary Nebulae*, ed. D. F. Flower (Dordrecht: Riedel), p. 91.

Browne, J. C., and Dalgarno, A. 1969, *J. Phys. B*, **2**, 885.

Chambaud, G., Launay, J. M., Levy, B., Millie, P., Roueff, E., and Tran Minh, F. 1980, *J. Phys. B*, **13**, 4205.

Chapman, R. D., and Henry, R. J. W. 1972, *Ap. J.*, **173**, 243.

Dalgarno, A., and McCray, R. 1973, *Ap. J.*, **181**, 95.

Duley, W. W., and Williams, D. A. 1984, *Interstellar Chemistry*, (London: Academic Press).

Federer, W., Villinger, H., Howorka, F., Lindinger, W., Tosi, P., Bassi, D., and Ferguson, E. 1984, *Phys. Rev. Letters*, **52**, 2084.

Gerlich, D., Disch, R., and Scherbarth, S. 1987, *J. Chem. Phys.*, **87**, 350.

Graff, M. M., and Dalgarno, A. 1987, *Ap. J.*, **317**, 432.

Graff, M. M., Moseley, J. T., and Roueff, E. 1983, *Ap. J.*, **269**, 796.

Henry, R. J. W. 1970, *Ap. J.*, **161**, 1153.

Herbst, E., and Klemperer, W. 1973, *Ap. J.*, **185**, 505.

Jacobs, T. A., Giedt, R. R., and Cohen, N. 1967, *J. Chem. Phys.*, **47**, 54.

Karpas, Z., Anicich, V., and Huntress, W. T. 1979, *J. Chem. Phys.*, **73**, 5631.

Kim, J. K., and Huntress, W. T. 1975, *J. Chem. Phys.*, **62**, 2820.

Kim, J. K., Theard, L. P., and Huntress, W. T. 1975, *J. Chem. Phys.*, **62**, 45.

Lepp, S., and Shull, J. M. 1983, *Ap. J.*, **270**, 578.

Leung, C. M., Herbst, E., and Huebner, W. F. 1984, *Ap. J. Suppl.*, **56**, 231.

Lotz, W. 1967, *Ap. J. Suppl.*, **14**, 207.

Marquette, J. B., Rowe, B. R., Dupeyrat, G., Poissant, G., and Rebrion, C. 1985, *Chem. Phys. Letters*, **122**, 431.

McGregor, M., and Berry, R. S. 1973, *J. Phys. B*, **6**, 181.

McCray, R. 1989, in *Molecular Astrophysics*, T. W. Hartquist, editor, (Cambridge: Cambridge University Press), in press.

McGowan, J. W., Mul, P. M., D'Angelo, V. S., Mitchell, J. B. A., Defrance, P., and Froelich, H. R., 1979, *Phys. Rev. Letters*, **42**, 373.

Mitchell, G. F., and Deveau, T. J. 1983, *Ap. J.*, **266**, 646.

Mul, P. M., Mitchell, J. B. A., D'Angelo, V. S., Defrance, P., McGowan, J. W., and Froelich, H. R. 1981, *J. Phys. B*, **14**, 1353.

Orient, O. J. 1977, *Chem. Phys. Letters*, **52**, 264.

Osterbrock, D. E. 1974, *Astrophysics of Gaseous Nebulae*, (San Francisco: W. H. Freeman).

Péquignot, D., and Aldrovandi, S. M. V. 1986, *Astr. Ap.*, **161**, 169.

Peterson, J. R., Aberth, W. H., Moseley, J. T., and Sheridan, J. R. 1971, *Phys. Rev. A*, **3**, 1651.

Prasad, S. S., and Huntress, W. T., Jr. 1980, *Ap. J. Suppl.*, **43**, 1.

Roberge, W., and Dalgarno, A. 1982, *Ap. J.*, **255**, 489.

Smith, D., and Adams, N. G. 1981, *M. N. R. A. S.*, **197**, 377.

Smith, D., and Adams, N. G. 1984, *Ap. J. (Letters)*, **284**, L13.

Smith, W. H., Liszt, H. S., and Lutz, B. L. 1973, *Ap. J.*, **183**, 69.

Solomon, P. M., and Klemperer, W. 1972, *Ap. J.*,

Solomon, P. M., and Werner, M. W. 1971, *Ap. J.*, **165**, 41.

Turner, J. L., and Dalgarno, A. 1977, *Ap. J.*, **213**, 386.

van Dishoeck, E. F., and Black, J. H. 1989, in *Rate Coefficients in Astrochemistry*, ed. T. J. Millar and D. A. Williams (Dordrecht: Kluwer), p. 209.

Viggiano, A. A., Howorka, F., Albritton, D. L., Fehsenfeld, F. C., Adams, N. G., and Smith, D. 1980, *Ap. J.*, **236**, 492.

Wagner, A. F., and Graff, M. M. 1987, *Ap. J.*, **317**, 423.

Weisheit, J. C. 1973, *Ap. J.*, **185**, 877.

Wishart, A. W. 1979, *M. N. R. A. S.*, **187**, 59P.